Thermal Modelling of a Mark II Container

NWMO-TR-2015-06 April 2015

Ruiping Guo

Nuclear Waste Management Organization

nwmo

NUCLEAR WASTE MANAGEMENT ORGANIZATION

SOCIÉTÉ DE GESTION DES DÉCHETS NUCLÉAIRES

Nuclear Waste Management Organization
22 St. Clair Avenue East, 6th Floor
Toronto, Ontario
M4T 2S3
Canada

Tel: 416-934-9814
Web: www.nwmo.ca

Thermal Modelling of a Mark II Container

NWMO-TR-2015-06

April 2015

Ruiping Guo
Nuclear Waste Management Organization

All copyright and intellectual property rights belong to NWMO.

Document History

Title:	Thermal Modelling of a Mark II Container		
Report Number:	NWMO-TR-2015-06		
Revision:	R000	Date:	April 2015
Nuclear Waste Management Organization			
Authored by:	Ruiping Guo		
Verified by:	Mark Gobien		
Reviewed by:	Neale Hunt, Frank Garisto, Dimitrie Marinceu and Mark Gobien		
Approved by:	Paul Gierszewski		

ABSTRACT

Title: **Thermal Modelling of a Mark II Container**
Report No.: **NWMO-TR-2015-06**
Author(s): Ruiping Guo
Company: Nuclear Waste Management Organization
Date: April 2015

Abstract
This technical report describes the analysis methods, assumptions and results obtained in calculations performed to assess fuel temperatures inside a Mark II container, which holds 48 used fuel bundles, assuming the fuel bundles have a decay period of 30 years with a discharge burnup of 220 MWh/(kgU). A variety of external boundary conditions is considered:

- Mark II container in air,
- Mark II container inside the buffer box in air,
- Mark II container inside the buffer box in the backfilled sedimentary rock repository, and
- Mark II container inside the buffer box in the backfilled crystalline rock repository.

The effect of filling the container with fuel of mixed age (10 years and 30 years) is also studied.

Sensitivity cases investigate the importance of the following:

- dividing the physical heat transfer systems into different levels of models,
- the small space between the container and the bentonite material in the buffer box,
- connections between bundle tubes and the inside surface of the container,
- water entering the container via an assumed container defect,
- radiation heat transfer between bundle tubes and between bundle tubes and the inside surface of the container,
- radiation heat transfer between fuel elements and between fuel elements and the inside surface of the bundle tube,
- heat transfer coefficient used for the convective heat transfer from the container surface to air, and
- higher burnup of the used fuel bundles.

All cases assume 37-element fuel bundles; however, the results are also generally applicable to 28-element fuel bundles.

The overall conclusion is that the maximum fuel temperature for the fuel with a burnup of 220 MWh/(kgU) will be less than 58°C during handling of the container, about 73°C during handling of buffer box during placement, and about 123°C after placement in sedimentary or crystalline rock repository.

TABLE OF CONTENTS

Page

ABSTRACT ..... **iii**

1. INTRODUCTION **1**

2. BACKGROUND **1**

3. MODEL GEOMETRY, BOUNDARY CONDITIONS AND MATERIAL PARAMETERS **4**

3.1 MODEL GEOMETRY **4**
3.1.1 Sedimentary DGR Model and Crystalline DGR Model 4
3.1.2 Buffer Box Model 6
3.1.3 Container Model 9
3.1.4 Bundle Model 10
3.2 INITIAL CONDITIONS **13**
3.3 BOUNDARY CONDITIONS **13**
3.3.1 Boundary Conditions for the DGR Model 13
3.3.2 Boundary Conditions for the Buffer Box Model 14
3.3.3 Boundary Conditions for the Container Model 14
3.3.4 Boundary Conditions for the Bundle Model 16
3.4 MATERIAL PARAMETERS **16**

4. MODELLING RESULTS **18**

4.1 VERIFICATION OF THE COMSOL MODEL **18**
4.2 RESULTS **20**
4.2.1 Container in Air 20
4.2.2 Container inside the Buffer Box in Air 24
4.2.3 Container inside the Buffer Box in the Repository 29
4.2.3.1 Sedimentary Rock Environment: 29
4.2.3.2 Crystalline Rock Environment 35
4.3 CONTAINER WITH MIXED AGE BUNDLES IN A SEDIMENTARY REPOSITORY **41**
4.3.1 Mixed Heat Source Model I 42
4.3.2 Mixed Heat Source Model II 43
4.3.3 Mixed Heat Source Model III 44
4.3.4 Mixed Heat Source Model IV 46
4.4 SENSITIVITY ANALYSIS **47**
4.4.1 Influence of Using a Volumetric Heat Source in the Container Model 47
4.4.2 Combining the Buffer Box Model and Container Model into an Equivalent Buffer / Container Model 50
4.4.3 Influence of the Gap between the Container and the Buffer Box 53
4.4.4 Influence of Connections between Fuel Bundle Tubes and the Inside Container Surface 55
4.4.5 Effect of Water entering the Container via an Assumed Container Defect 58
4.4.6 Influence of Radiation Heat Transfer on Temperature 58
4.4.6.1 Influence of Radiation Heat Transfer on the Container Temperature 59
4.4.6.2 Influence of Radiation Heat Transfer on Fuel Temperature 63
4.4.7 Influence of Heat Transfer Coefficient from the Container Surface to Air 67

4.4.8 Influence of Higher Burnup 67
4.5 Summary of the Modelling Results 68

5 CONCLUSIONS 72

REFERENCES 73

LIST OF TABLES

Page

Table 1: Thermal Properties for the Considered Materials 17
Table 2: Summary of Maximum Temperature Results 69
Table 3: Summary of Sensitivity Analysis Results 70
Table 4: Summary of Modified Maximum Temperature Results 71

LIST OF FIGURES

Page

Figure 1: Mark II Used Fuel Container View 2
Figure 2: Dimensions of and Horizontal Cross Section of a Mark II Container 2
Figure 3: In-Room Concept for Placement of Buffer Boxes 3
Figure 4: Mark II 48-Bundle Container Placement Room Concept 3
Figure 5: Sedimentary and Crystalline DGR Model Geometry 5
Figure 6: Finite Element Discretization of the Central Part of the Unit Cell of the Sedimentary DGR Model for Near-Field Analyses 6
Figure 7: Buffer Box for Mark II Used Fuel Container 7
Figure 8: Buffer Box Model Geometry 8
Figure 9: Buffer Box Model Mesh 8
Figure 10: Container Model Geometry 9
Figure 11: Container Model Mesh 10
Figure 12: 37-Element CANDU Fuel Bundle 11
Figure 13: Bundle Model Geometry 12
Figure 14: Bundle Model Mesh 12
Figure 15: Heat Source per 28-Element Bundle and per 37-Element Bundle for a Discharge Burnup of 220 MWh/(kgU) 13
Figure 16: Buffer Box Model Heat Flux Boundary Conditions 14
Figure 17: Container Model Geometry 15
Figure 18: Bundle Model Geometry 16
Figure 19: Maximum Temperatures in the Sedimentary Rock DGR Model obtained using ANSYS and COMSOL 19
Figure 20: Finite Element Discretization of the Central Part of the Unit Cell for Near-Field Analyses for the ANSYS Model 19
Figure 21: Container Temperatures at 8.6 Days for the Container in Air Case 20
Figure 22: Container Temperatures on the x= 0 Plane at 8.6 Days for the Container in Air Case 21
Figure 23: Container Temperatures on the z = 0 Plane (Middle Cross Section of a Container) at 8.6 Days for the Container in Air Case 21
Figure 24: Fuel Temperatures at 8.6 Days for the Container in Air Case 22
Figure 25: Fuel Temperatures on the y = 0 Plane at 8.6 Days for the Container in Air Case 23
Figure 26: Temperatures as a Function of Time for the Container in Air Case 23
Figure 27: Buffer Box Temperature at 20 Days for the Container inside the Buffer Box in Air Case 24
Figure 28: Buffer Box Temperature on the y = 0 Plane at 20 Days for the Container inside the Buffer Box in Air Case 25
Figure 29: Container Temperature at 20 Days for the Container inside the Buffer Box in Air Case 26

Figure 30: Container Temperature on the x = 0 Plane at 20 Days for the Container inside the Buffer Box in Air Case 26
Figure 31: Container Temperatures on the z = 0 Place (Middle Cross Section of a Container) at 20 Days for the Container inside the Buffer Box in Air Case 27
Figure 32: Fuel Temperature at 20 Days for the Container inside the Buffer Box in Air Case.... 28
Figure 33: Fuel Temperature on the y = 0 Plane at 20 Days for the Container inside the Buffer Box in Air Case 28
Figure 34: Temperatures as a Function of Time for the Container inside the Buffer Box in Air Case 29
Figure 35: Rock Temperature at 40 Years for the Container inside the Buffer Box in the Sedimentary Repository Case 30
Figure 36: Rock Temperature at the Repository Level at 40 Years for the Container inside the Buffer Box in the Sedimentary Repository Case..... 31
Figure 37: Container Temperature at 14.7 Years for the Container inside the Buffer Box in the Sedimentary Repository Case 32
Figure 38: Temperature on the x= 0 Plane at 14.7 Years for the Container inside the Buffer Box in a Sedimentary Repository Case 32
Figure 39: Temperature Distribution on the z = 0 Plane (Middle Cross Section of a Container) at 14.7 Years for the Container inside the Buffer Box in a Sedimentary Repository Case 33
Figure 40: Fuel Temperature in the Bundle Model at 14.7 Years for the Container inside the Buffer Box in a Sedimentary Repository Case..... 34
Figure 41: Fuel Temperature on the y = 0 Plane at 14.7 Years for the Container inside the Buffer Box in a Sedimentary Repository Case..... 34
Figure 42: Temperatures as a Function of Time for the Container inside the Buffer Box in a Sedimentary Repository Case 35
Figure 43: Rock Temperature at 34.8 Years for the Container inside the Buffer Box in the Crystalline Repository Case 36
Figure 44: Rock Temperature at the Repository Level at 34.8 Years for the Container inside the Buffer Box in the Crystalline Repository Case 37
Figure 45: Container Temperature at 14.7 Years for the Container inside the Buffer Box in the Crystalline Repository Case 38
Figure 46: Temperature on the x = 0 Plane at 14.7 Years for the Container inside the Buffer Box in the Crystalline Repository Case 38
Figure 47: Temperature on the z = 0 Plane (Middle Cross Section of a Container) at 14.7 Years for the Container inside the Buffer Box in the Crystalline Repository Case 39
Figure 48: Fuel Temperature in the Bundle Model at 14.7 Years for the Container inside the Buffer Box in the Crystalline Repository Case 40
Figure 49: Fuel Temperature on the y = 0 Plane at 14.7 Years for the Container inside the Buffer Box in the Crystalline Repository Case 40
Figure 50: Temperatures for the Container inside the Buffer Box in the Crystalline Repository Case 41
Figure 51: Bundle Distribution in a Mixed Heat Source Model I in a Sedimentary Repository ... 42
Figure 52: Temperatures from Mixed Heat Source Model I in a Sedimentary Repository..... 43
Figure 53: Bundle Distribution in Mixed Heat Source Model II in a Sedimentary Repository 43
Figure 54: Temperatures from Mixed Heat Source Model II in a Sedimentary Repository..... 44
Figure 55: Bundle Distribution in Mixed Heat Source Model III in a Sedimentary Repository 45
Figure 56: Temperatures from Mixed Heat Source Model III in a Sedimentary Repository..... 45
Figure 57: Bundle Distribution in Mixed Heat Source Model IV in a Sedimentary Repository.... 46
Figure 58: Temperatures from Mixed Heat Source Model IV in a Sedimentary Repository 46
Figure 59: Equivalent Bundle Model 47

Figure 60: Fuel Centre Temperature Comparison between the Bundle Model and the Equivalent Bundle Model 48
Figure 61: Fuel Temperature Comparison along Radius (OA) between the Bundle Model and the Equivalent Bundle Model 48
Figure 62: Geometry of the Equivalent Container Model 49
Figure 63: Container Centre Air Temperature Comparison between the Container Model and the Equivalent Container Model 50
Figure 64: Container Temperature Comparison along Line OA at 8.6 Days between the Container Model and the Equivalent Container Model 50
Figure 65: Buffer Box Combination Model Geometry 51
Figure 66: Buffer Box Combination Model Mesh 52
Figure 67: Container Air Temperatures Comparison between the Buffer Box Combination Model and the Separated Models 52
Figure 68: Gap Sensitivity Model Geometry 53
Figure 69: Gap Sensitivity Model Mesh 54
Figure 70: Container Temperature Comparison between Buffer Box Combination Model (BBCM) and Gap Sensitivity Model (GSM) 54
Figure 71: Container Model with All Connections 55
Figure 72: Container Model with Partial Connections (Only connections A, B, C and D are effective) 56
Figure 73: Influence of Connections on the Maximum Container Air Temperature for the Container in Air Case 57
Figure 74: Influence of Connection Width on the Container Central Air Temperatures 57
Figure 75: Effect of Water Entering the Container on Container Centre Temperature for the Container inside the Buffer Box in a Sedimentary Repository Case 58
Figure 76: Radiation Container Model Geometry 59
Figure 77: Radiation Container Model Mesh 60
Figure 78: Container Centre Temperature for the Container inside the Buffer Box in the Sedimentary Repository Case 61
Figure 79: Temperature along Line OA for the Container inside the Buffer Box in the Sedimentary Repository Case 61
Figure 80: Temperatures at 28 Years inside the Container Accounting for Radiation Heat Transfer 62
Figure 81: Temperatures at 14.7 Years inside a Container Not Accounting for Radiation Heat Transfer 62
Figure 82: Influence of Radiation Heat Transfer on Container Air Temperature 63
Figure 83: Radiation Bundle Model Geometry 64
Figure 84: Radiation Bundle Model Mesh 65
Figure 85: Temperatures in the Radiation Bundle Model 65
Figure 86: Temperatures in the Bundle Model (radiation not modelled) 66
Figure 87: Influence of Radiation in a Fuel Tube on Fuel Central Temperature 66
Figure 88: Influence of the Convective Heat Transfer Coefficient on Container Centre Air Temperature 67

1. INTRODUCTION

This technical report describes the analysis methods, assumptions and results obtained in calculations performed to assess fuel temperatures inside a Mark II container assuming the used fuel bundles have a decay period of 30 years with a discharge burnup of 220 MWh/(kgU). A variety of external boundary conditions is considered:

- Mark II container in air.
- Mark II container inside the buffer box in air.
- Mark II container inside the buffer box in the backfilled sedimentary rock repository.
- Mark II container inside the buffer box in the backfilled crystalline rock repository.

Fuel temperatures for a Mark II container in the backfilled sedimentary rock repository with mixed decay age bundles (10 years and 30 years) with a discharge burnup of 220 MWh/(kgU) are studied.

Investigations are also performed to determine the influence of geometric parameters (e.g., the dimensions of the connections between fuel tubes and the inside surface of the container), water entering the container via an assumed container defect, radiation heat transfer, 28-element fuel (as opposed to 37-element fuel), heat transfer coefficient used for the heat convection from the container surface to air and a higher discharge burnup (280 MWh/(kgU)) as opposed to 220 MWh/(kgU).

2. BACKGROUND

The NWMO is designing and assessing the performance of the 12FB-4L – Mark II used fuel container shown in Figure 1. The container consists of an outer copper corrosion-barrier and an inner carbon steel load-bearing shell. The Mark II container has a diameter of 562 mm and a length of 2512 mm with hemispherical heads on each end (all dimensions from drawing: APM-ASSY-04302-0001, REV000A, 2014/4/1). The inner steel layer is 46.23-mm thick at the main cylinder and 30-mm thick at the hemispherical ends. The container is coated with a layer of 3-mm-thick copper (Figure 1). The dimensions of the container are shown in Figure 2. The whole length of the Mark II container is 2512 mm, in which the length of the cylindrical part is 1950 mm. The outside diameter of the container is 562 mm. Each container is loaded with 48 used CANDU fuel bundles arranged in four storage modules, with each module having 12 horizontal bundle tubes.

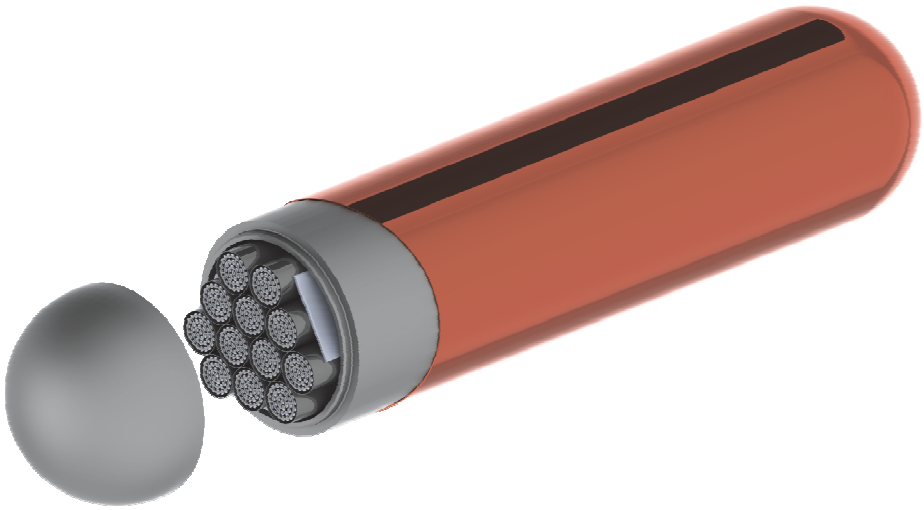

Figure 1: Mark II Used Fuel Container View

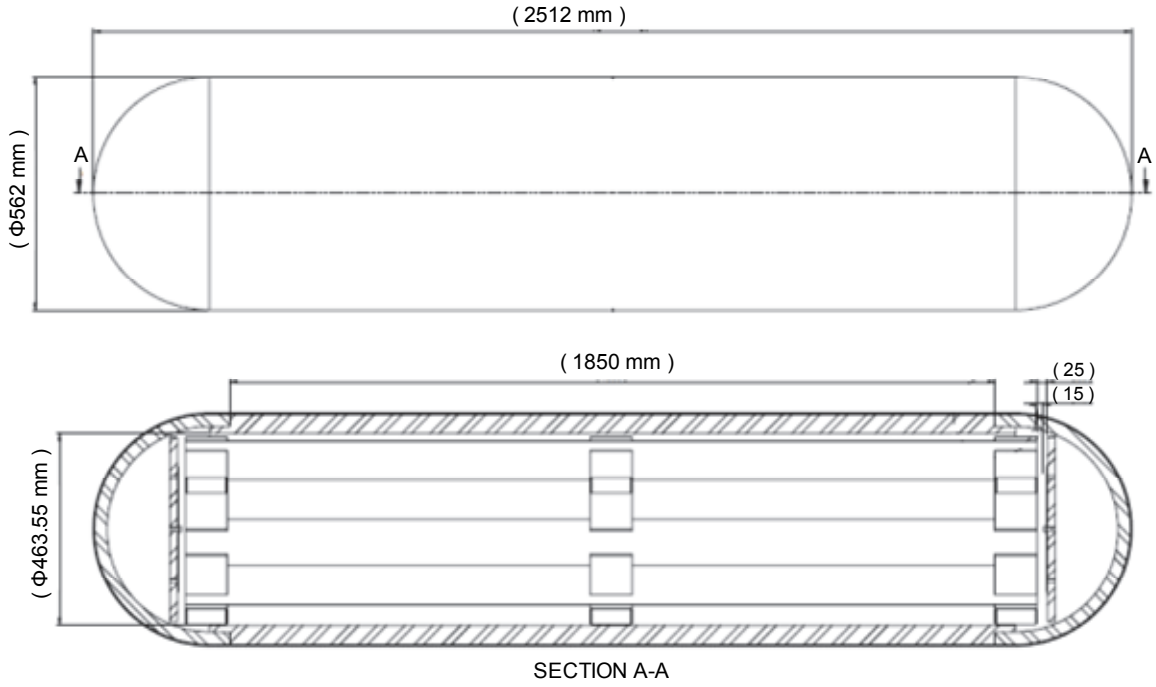

Taken from: DGR NO: APM-ASSY-04302-0001, REV000A, 2014/4/1.

Figure 2: Dimensions of and Horizontal Cross Section of a Mark II Container

The in-room placement concept for the Mark II container is shown in Figure 3. In this concept, the containers are housed in a highly compacted bentonite assembly with a metallic cover (called a “buffer box” in some documents). The buffer boxes are assembled in the Used Fuel Packing Plant, transported underground, and installed in the placement room with the containers perpendicular to the tunnel direction.

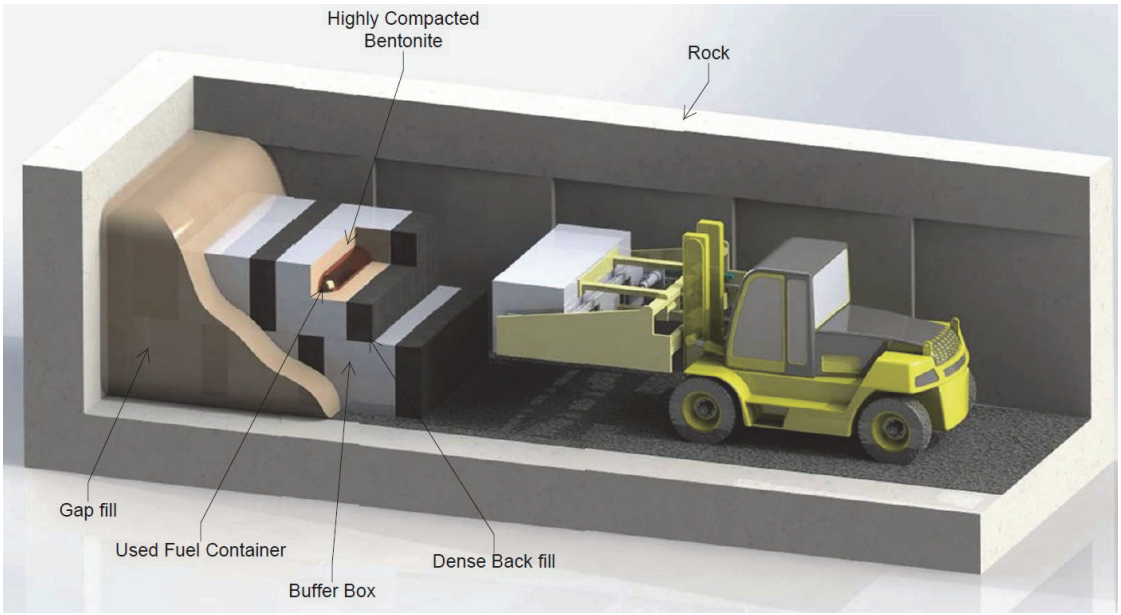

Figure is not to scale and is for illustrative purposes only

Figure 3: In-Room Concept for Placement of Buffer Boxes

The sedimentary and crystalline deep geological repository (DGR) layouts consist of arrays of horizontal, rectangular-shaped placement rooms. The placement rooms are connected by access drifts for the removal of excavated rock and for the transfer of buffer boxes and backfill materials. The assumed depth of the DGR is 500 m. The placement details are shown in Figure 4. The placement rooms are 2.12 m in height and 3.12 m in width with a layer of 100 mm of gap fill (bentonite pellets) placed around the buffer boxes and the dense backfill blocks in the placement rooms. All dimensions of the tunnel cross section are shown in Figure 4.

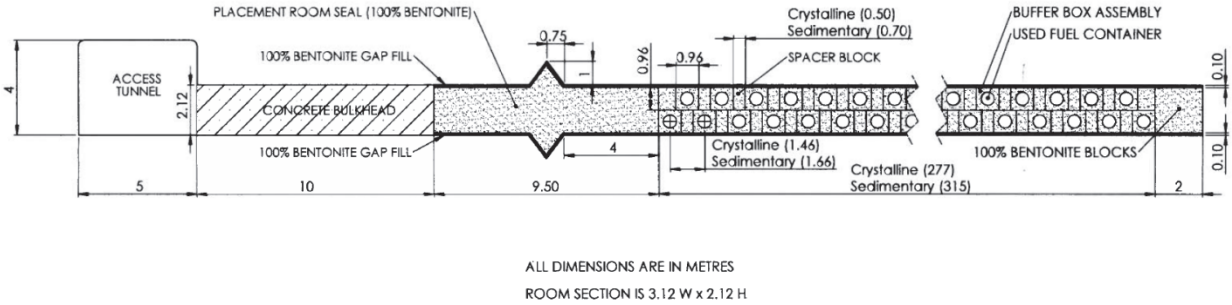

From NWMO draft drawing of Mark II design concept for crystalline and sedimentary host rock (APM-PDD-04000-0003)

Figure 4: Mark II 48-Bundle Container Placement Room Concept

3. MODEL GEOMETRY, BOUNDARY CONDITIONS AND MATERIAL PARAMETERS

COMSOL version 4.3b was used to perform the simulations. COMSOL is a commercial finite element program (COMSOL 2013).

The fuel bundles are assumed to have a decay period of either 10 years or 30 years with a discharge burnup of 220 MWh/(kgU).

Fuel temperatures are calculated for three types of boundary conditions as mentioned in Section 1.

For computational efficiency and ease of modelling, a number of submodels are used, with information passed from one submodel to another via boundary conditions. Specifically:

- For the container in air, a Container Model and a Bundle Model are used. Results from the Container Model are imposed as boundary conditions on the Bundle Model;
- For the container inside the buffer box in air, a Buffer Box Model, a Container Model and a Bundle Model are used. Results from the Buffer Box Model are imposed as boundary conditions on the Container Model and results from the Container Model are imposed as boundary conditions on the Bundle Model;
- For the container inside the buffer box in the backfilled DGR, a DGR Model, a Container Model and a Bundle Model are used. Results from the DGR model are imposed as boundary conditions on the Container Model and results from the Container Model are imposed as boundary conditions on the Bundle Model.

3.1 MODEL GEOMETRY

As discussed above, four models have been created in the course of this work. These are the DGR Model, the Buffer Box Model, the Container Model and the Bundle Model.

Radiation heat transfer is initially ignored in all four models for reasons of computational efficiency. Sensitivity studies are performed later in this document to quantify the effect of including this mechanism.

Each model is described below.

3.1.1 Sedimentary DGR Model and Crystalline DGR Model

The geometry of the Sedimentary DGR Model and Crystalline DGR Model, including dimension information, is shown in Figure 5. There are five kinds of materials: rock (sedimentary or crystalline), buffer box bentonite, spacer blocks (also called backfill blocks), used fuel container and bentonite gap fill.

The horizontal dimensions of a unit cell (Figure 5) are 10 m x 0.73 m for crystalline rock and 10 m x 0.83 m for sedimentary rock based on the criterion that the container surface temperature is less than 100°C. The dimensions of the buffer box are 0.962 m x 0.962 m x 2.912 m for both sedimentary and granite repositories (there are two one-quarters of the buffer box in each model with dimensions of 0.481 m x 0.962 m x 1.456 m). The vertical dimension of

the model unit cell is 1000 m. The bottom of the placement room is 500 m below the top of the model.

The rock should be stratified for the sedimentary repository case; however, for simplicity, rock homogeneity is assumed.

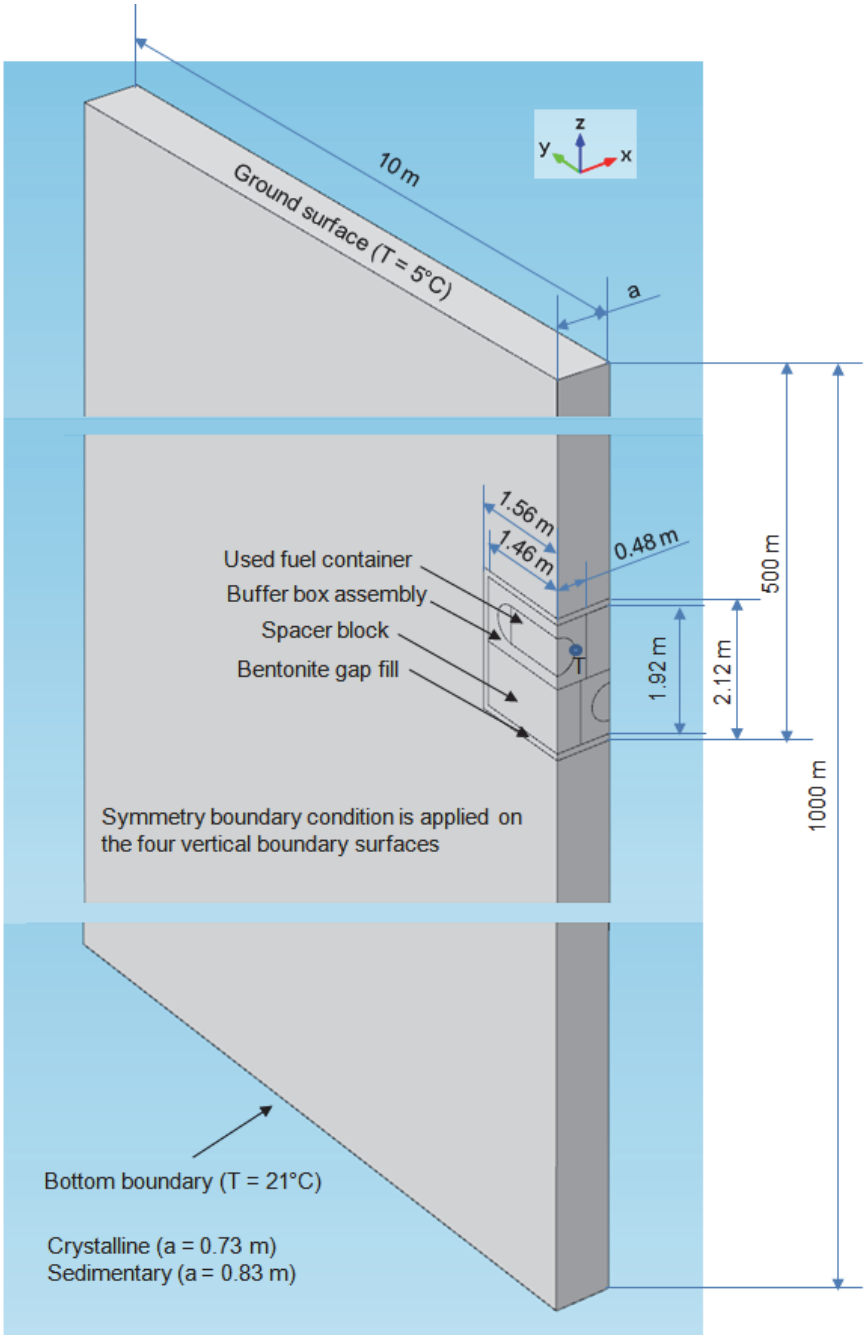

Figure 5: Sedimentary and Crystalline DGR Model Geometry

The finite element discretization for the Sedimentary DGR Model is shown in Figure 6. There are 96,778 tetrahedral elements and 116,067 nodes for the Sedimentary DGR Model. The elements are more densely distributed in the region of interest as shown in Figure 6 (near the placement tunnel room).

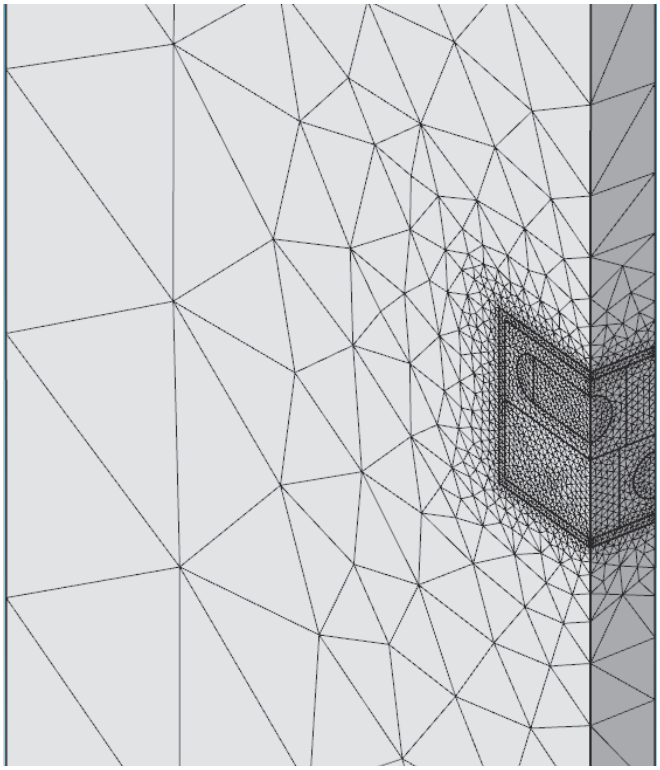

Figure 6: Finite Element Discretization of the Central Part of the Unit Cell of the Sedimentary DGR Model for Near-Field Analyses

The finite element discretization for the Crystalline DGR Model is similar to that for the Sedimentary DGR Model and is not shown. There are 85,049 tetrahedral elements and 101,343 nodes for the Crystalline DGR Model.

3.1.2 Buffer Box Model

The Mark II container is placed within a buffer box as shown in Figure 7. The dimensions of the buffer box are 0.962 m x 0.962 m x 2.912 m.

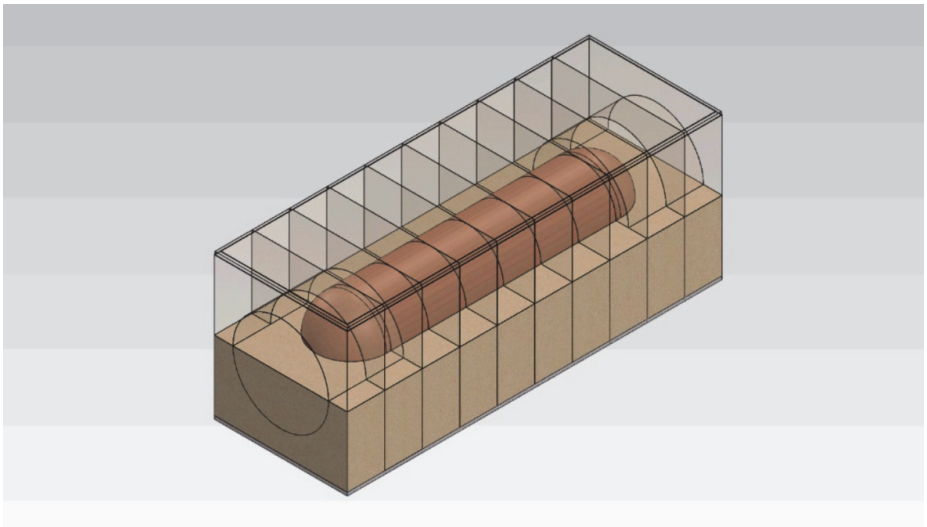

Note: there is no steel sheath shown in this figure.

Figure 7: Buffer Box for Mark II Used Fuel Container

Figure 8 shows the Buffer Box Model geometry. The dimensions of the Buffer Box Model are 0.962 m x0.962 m x 1.456 m. Only one half of the buffer box is modelled because of symmetry. In this Buffer Box Model, there are two kinds of materials. The sheet metal outside of the buffer box is ignored because the sheet metal has holes, which make the temperature on the outside surface of the clay box essentially the same as the temperature on the outside surface of the sheet metal. One of the modelled materials is the bentonite of the buffer box while the other modelled material is a 3-mm-thick layer of copper (on the outside of the used fuel container) that is in contact with the inside portion of the buffer box. In this model, full contact is assumed between the copper layer and the buffer box bentonite. The container is not included in the Buffer Box Model and the total heat source from one half of the container is applied on the inside surface of the copper layer.

Figure 9 shows the mesh of the Buffer Box Model. There are 93,591 tetrahedral elements and 108,352 nodes.

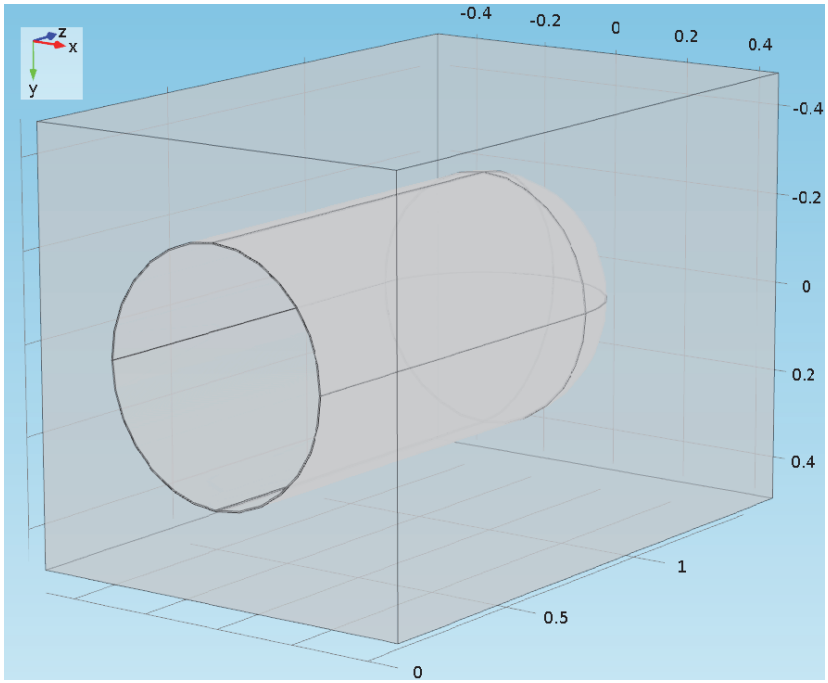

Figure 8: Buffer Box Model Geometry

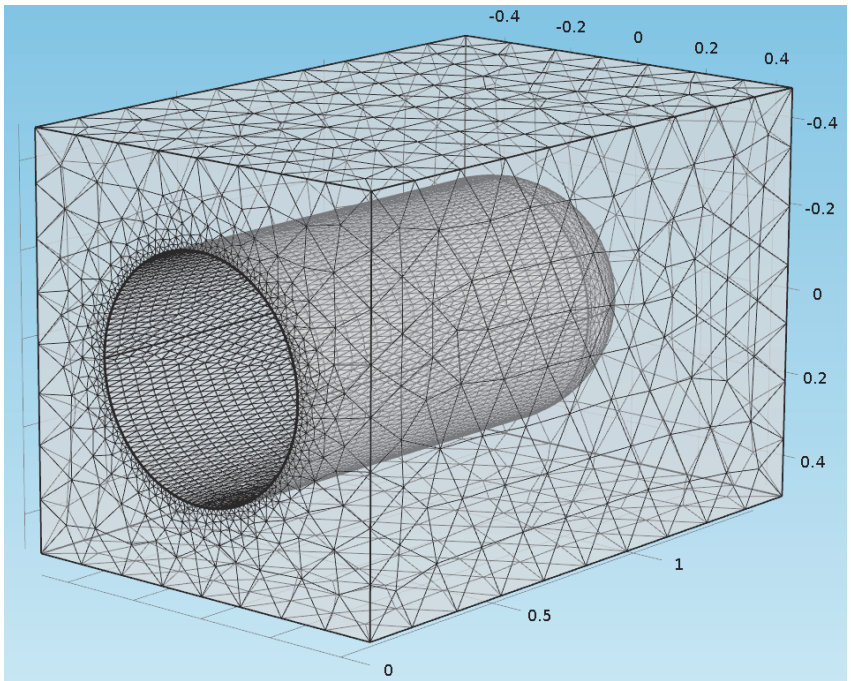

Figure 9: Buffer Box Model Mesh

3.1.3 Container Model

The dimensions of a Mark II container are described in Section 2. Because of symmetry, one half of the container is represented in the Container Model as shown in Figure 10.

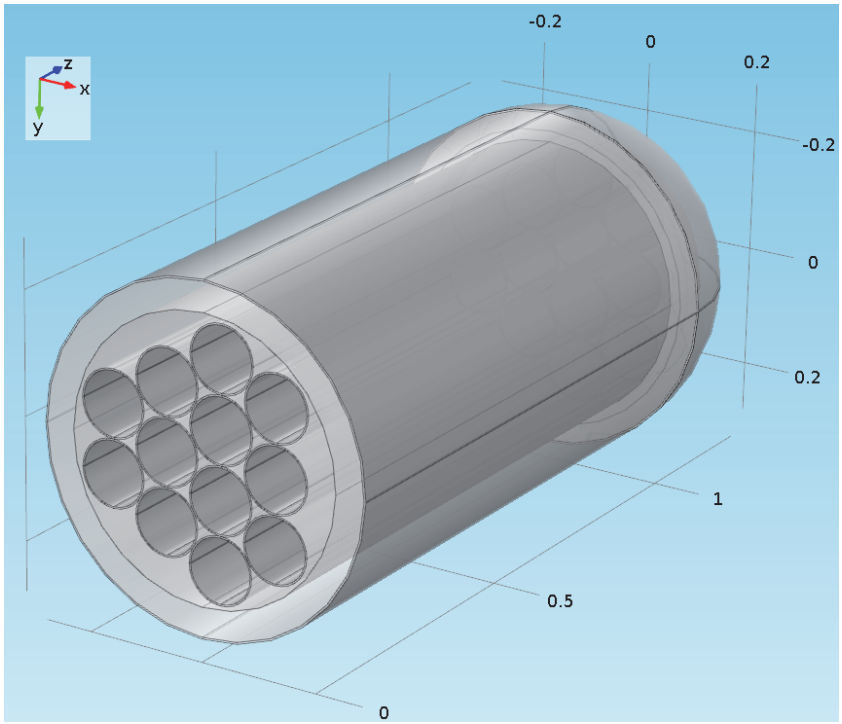

Figure 10: Container Model Geometry

The model includes three kinds of materials: copper, steel and air. The outermost layer of the model is the 3-mm-thick copper coating with an outside diameter of 0.562 m. Inside this layer is a steel layer with a 46.23-mm-thick wall and hemispherical end cap with a thickness of 30 mm. Inside the steel layer are twelve 1.03-m-long steel tubes with a wall thickness of 2.5 mm. It is assumed that there is no physical connection between fuel tubes and the inside surface of the container. The space between the tubes and the steel spherical shell is filled with air. The tubes are empty and the heat source from the fuel will be applied on the inside surface of the tubes. This approximation is expected to be valid (as shown in Section 4.4.1) because the effective thermal conductivity of the material in the tubes is low.

Figure 11 shows the Container Model mesh. There are 740,035 tetrahedral elements and 855,350 nodes.

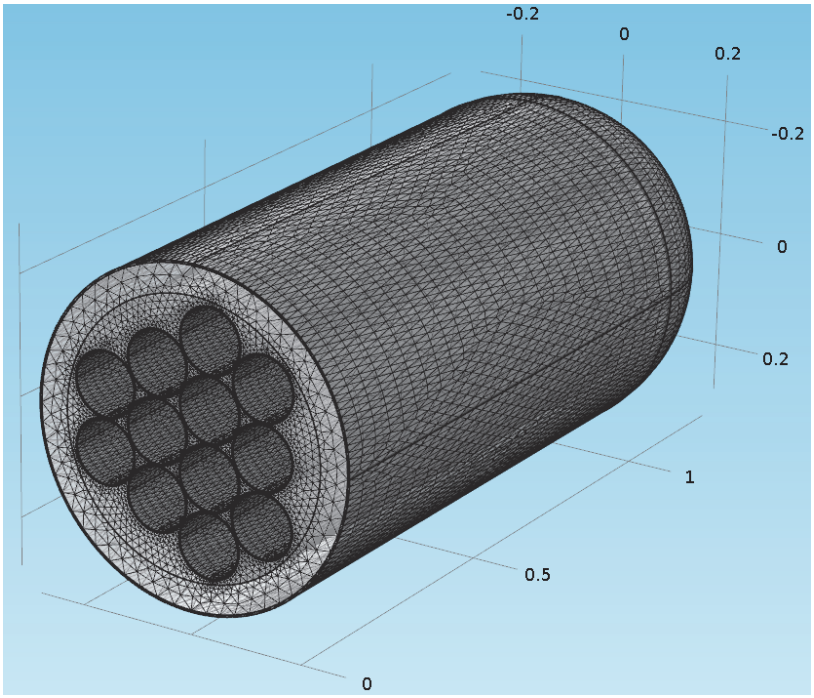

Figure 11: Container Model Mesh

3.1.4 Bundle Model

Inside each container are 48 fuel bundles, with each fuel bundle comprised of either a 37-element or a 28-element fuel bundle. Each fuel element consists of UO_2 pellets and cladding. Since both 28-element and 37-element fuel bundles have similar dimensions and similar mass, the 37-element bundles is used as the representative bundle, as shown in Figure 12.

The outside diameter and the length of a UO_2 fuel pellets in the fuel element are 12.2 mm and 0.493 m, respectively. The average outside diameter of the cladding is 13 mm and the average wall thickness of the cladding is 0.4 mm (Garamszeghy 2013; Tait et al. 2000).

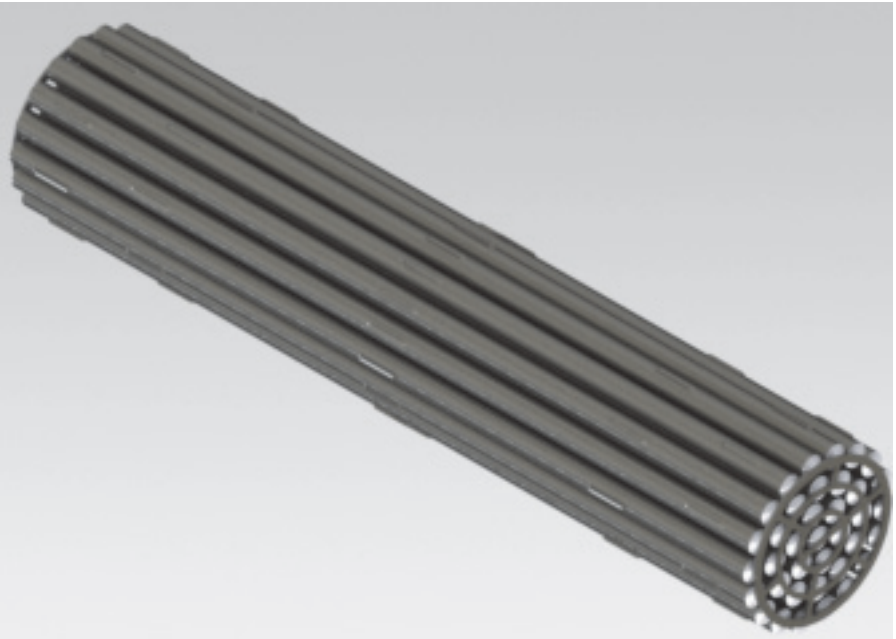

Figure 12: 37-Element CANDU Fuel Bundle

Figure 13 shows the geometry of the Bundle Model. Due to symmetry, the model represents one half of a steel tube in a container with each one-half tube segment holding two fuel bundles. The model components are a steel tube, two fuel bundles and air in the void spaces.

The outside diameter, inside diameter and length of the steel tube are 0.11 m, 0.105 m and 1.03 m, respectively. Inside the steel tube are two 37 Zircaloy-4 fuel sheaths arranged in the form of a CANDU fuel bundle. The fuel sheaths are 1.03 m long tubes with an outside diameter of 13 mm and wall thickness of 0.4 mm. Each fuel sheath is filled with cylindrical-shaped UO_2 fuel pellets. The space between the fuel sheaths and the steel tube is filled with air. The spacers between fuel pins/sheaths and between fuel pins and bundle tubes are not incorporated in the Bundle Model. This simplification is conservative because it results in higher fuel temperatures.

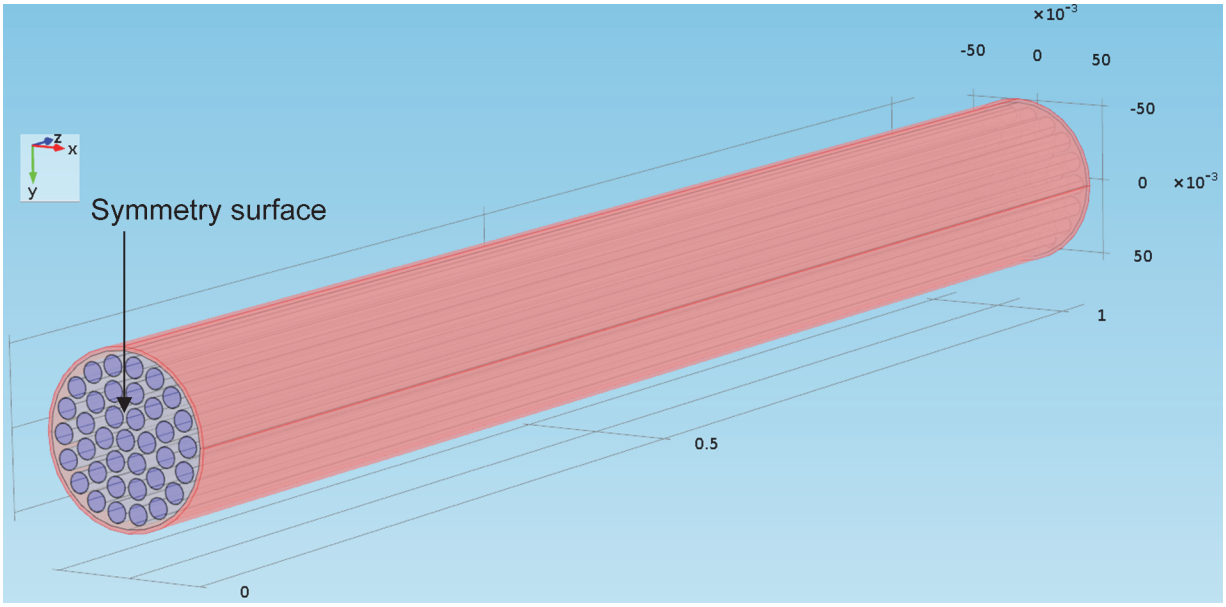

Figure 13: Bundle Model Geometry

The Bundle Model mesh is shown in Figure 14. There are total 641,511 tetrahedral elements and 667,043 nodes.

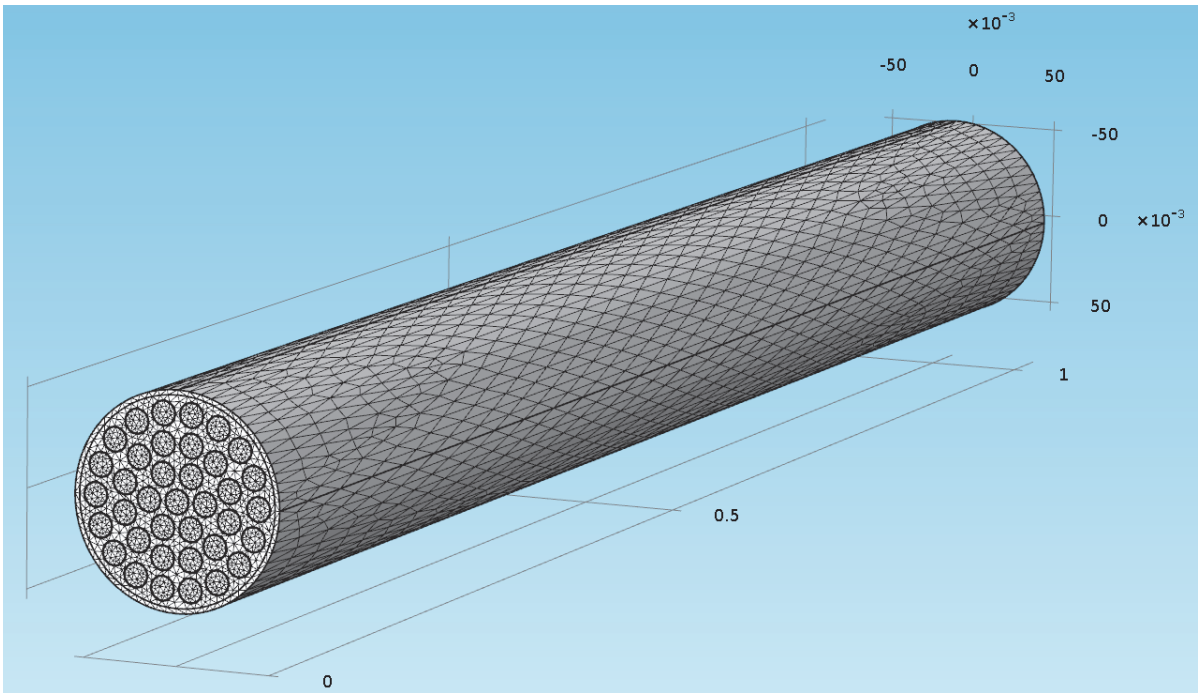

Figure 14: Bundle Model Mesh

3.2 INITIAL CONDITIONS

The initial temperature for all material types in the Bundle Model, the Container Model and the Buffer Box Model is assumed to be ambient (20°C).

The initial temperature for all material types in the DGR Model is a function of depth and is calculated using the following equation (Guo 2010).

$$T_0(z) = 5 + 0.016 \cdot z \quad (1)$$

where T_0(z) is the initial temperature at depth z, °C; z is the depth from the ground surface, m.

3.3 BOUNDARY CONDITIONS

Figure 15 shows the heat source per 28-element CANDU bundle and per 37-element "standard" CANDU bundle, as a function of fuel age, for a bundle with a discharge burnup of 220 MWh/(kgU) (Tait et al. 2000). Because the heat source per 28-element bundle is only 4% higher than that from a 37-element "standard" bundle, the results from simulations performed with 37-element bundles can also be considered representative for 28-element bundles.

Because the Container Model only models one half of the container, the total heat source for a Mark II Container Model is 24 times the heat source of a single bundle.

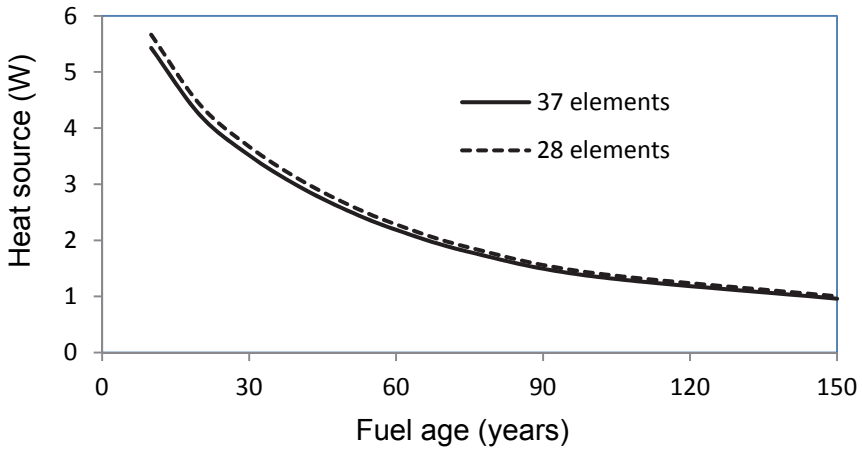

Figure 15: Heat Source per 28-Element Bundle and per 37-Element Bundle for a Discharge Burnup of 220 MWh/(kgU)

3.3.1 Boundary Conditions for the DGR Model

The boundary conditions for the DGR Model are:

- No heat flow on the four vertical outside surfaces.
- The temperature at the ground surface is 5°C.
- The temperature at the bottom of the model is 21°C.

- Twenty-four times the heat source of a single 37-element bundle (as shown in Figure 15) is uniformly applied in the volume of the used fuel container.

3.3.2 Boundary Conditions for the Buffer Box Model

The boundary conditions for the Buffer Box Model are:

- A symmetry boundary condition is applied across the vertical surface ABCD (see Figure 16), i.e., the heat flux across this surface is zero.
- A convective heat flux boundary condition is applied on the outside surfaces AEFB, BFGC, CGHD, DHEA and EHGF (also see Figure 16). The outside ambient room temperature is fixed at 20°C. One half of the total heat source in a used fuel container is uniformly applied as a heat flux on the inside surface of the copper layer.

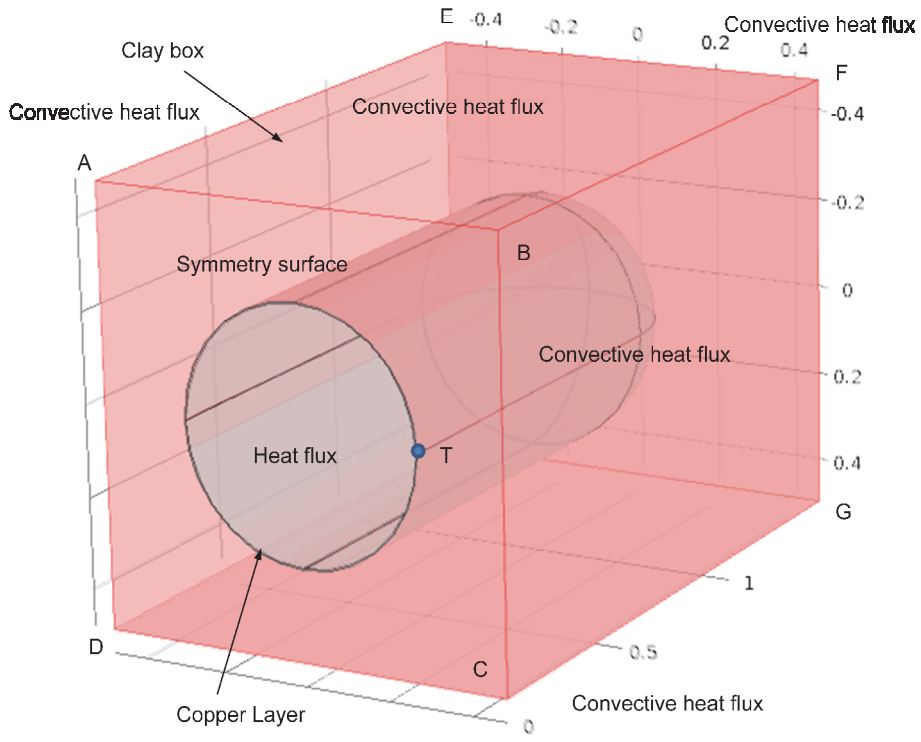

Figure 16: Buffer Box Model Heat Flux Boundary Conditions

3.3.3 Boundary Conditions for the Container Model

The boundary conditions for the Container Model are:

- No heat flow across the symmetry surface (as shown in Figure 17).
- The total heat source inside a single tube, corresponding to the heat from 2 fuel bundles, is uniformly applied as a heat flux on the inside surfaces of each of the 12 tubes.

- Container surface temperature for three different conditions:
    - For the Container inside the Buffer Box in the DGR Model: The temperature at point T on the outside surface of the container (see Figure 5) is applied on the outside surface of the Container Model.
    - For the Container inside the Buffer Box Model: The temperature at point T on the outside surface of the copper (see Figure 16) is applied on the outside surface of the Container Model.
    - For the Container Model in Air: Convective heat flux is applied on the outside surface of the container with the ambient room temperature fixed at 20°C.

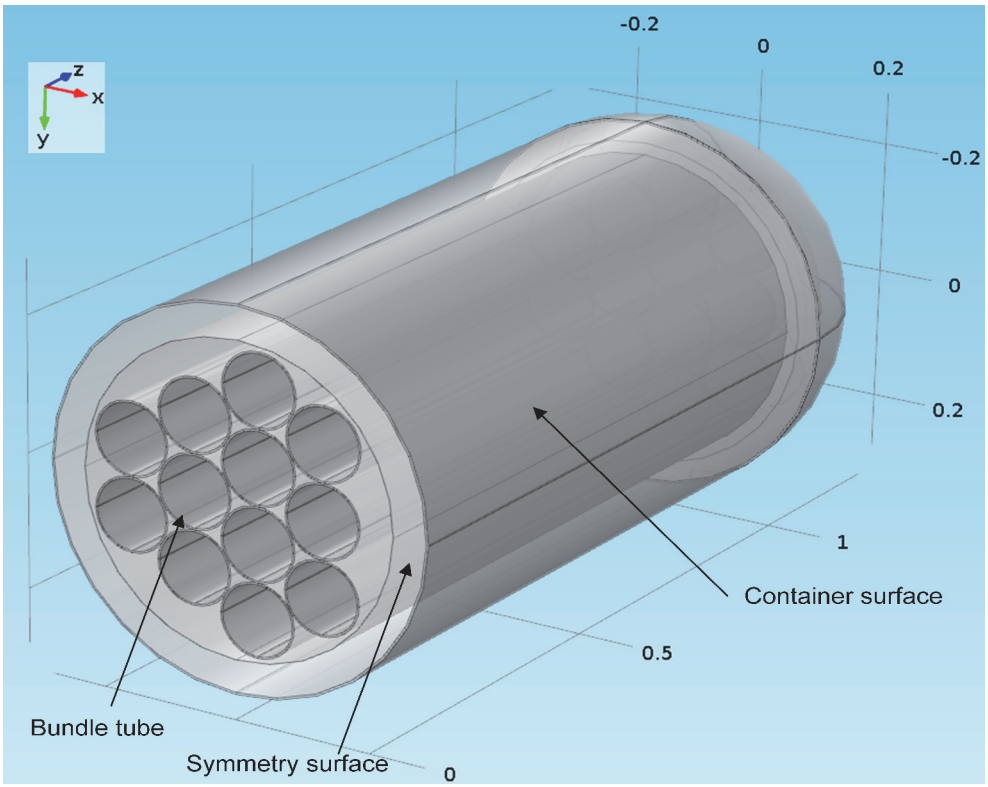

Figure 17: Container Model Geometry

3.3.4 Boundary Conditions for the Bundle Model

The boundary conditions for the Bundle Model are:

- No heat flow across the symmetry surface at z = 0 (as shown in Figure 18).
- The maximum temperature of the air at the center of the container, determined using the Container Model, is applied on the perimetric surface of the Bundle Model and on the end surface at z = 1.03 m.
- The total heat source of two bundles is uniformly applied in the volume of the two 37 UO_2 elements. (There are two 37-element bundles in the Bundle Model).

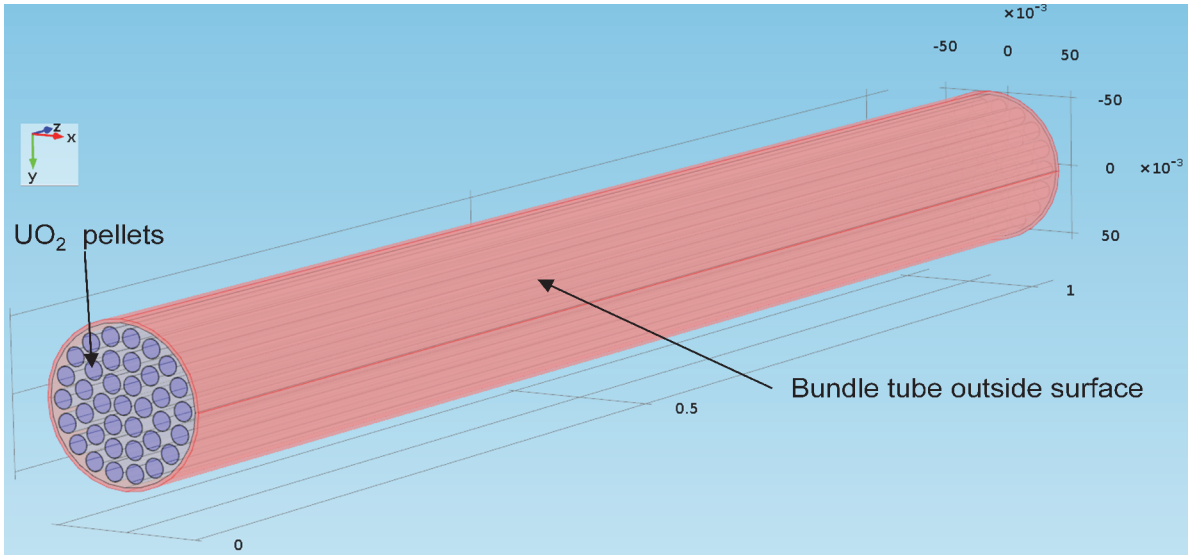

Figure 18: Bundle Model Geometry

3.4 MATERIAL PARAMETERS

The thermal properties of the materials used are shown in Table 1. Thermal conductivity of UO_2 is extrapolated from the thermal conductivity of UO_2 at high temperature (IAEA 2006). The specific heat of Zircaloy-4 cladding is interpolated using the data from IAEA (2006).

Table 1: Thermal Properties for the Considered Materials

Materials	Density [kg/m^3]	Specific Heat [J/kg·°C]	Thermal Conductivity [W/(m·°C)]	Reference
Limestone	2600	830	2.3	Guo 2010
Granite	2700	845	3.0	Guo 2010
Bentonite pellets	1410	920	0.4	Baumgartner 2006
HCB	1700	1440	0.5	Baumgartner 2006
Dense backfill	2120	1100	0.8	Baumgartner 2006
Steel	7870	444	43	The Engineering Toolbox[1]
Copper	8960	385	400	The Engineering Toolbox
UO_2 pellets	10637	235	$6.955-0.009704 \cdot T^*$	IAEA 2006
Zircaloy-4 cladding	6471	$256 + 0.1024 \cdot (T^*+273)$	17.5	IAEA 2006
Water	1000	4187	0.58	The Engineering Toolbox
Air	$-2.8\text{x}10^{-3} \cdot T^* + 1.238$	$2.38\text{x}10^{-7} \cdot T^{*2} + 3.81\text{x}10^{-5} \cdot T^* + 1.0$	$7.21\text{x}10^{-5} \cdot T^* + 0.0242$	The Engineering Toolbox

*T is the temperature, °C.

Convective heat transfer (and hence its coefficient) is difficult to estimate exactly. It depends on the type of media (e.g., gas or liquid), the geometry, the flow properties (such as velocity and viscosity) and other temperature dependent properties. A convective heat transfer coefficient of 13.1 W/(m^2·°C) is applied on the outside container surface for the Container in Air case. This value is taken from "The Engineering Toolbox". For comparison, Lienhard IV and Lienhard V (2011) use a value of 15 W/(m^2·°C) for a copper sphere at a uniform temperature of 40°C suspended in a slow-moving air stream with temperature of 0°C. Compared to the copper sphere case, the value of 13.1 W/(m^2·°C) used here for stationary air with an ambient temperature of 20°C is reasonable.

A convective heat transfer coefficient of 4 W/(m^2·°C) is applied on the buffer box outside surface (Abdel-Ghany and Kozai 2006). No data for the convective heat transfer coefficient for bentonite was found and therefore this value corresponds to that for soil.

[1] Data from website of http://www.engineeringtoolbox.com/thermal-conductivity-d_429.html

The emissivity coefficient for the outside surface of the steel bundle tubes, the inside surface of a container, the outside surface of the Zircaloy-4 claddings and the inside surfaces of the bundle tubes is 0.7 (from “The Engineering Toolbox” online).

Due to lack of information about the emissivity coefficient for the Zircaloy-4 fuel sheath, the emissivity value for steel bundle tubes is applied.

A value of 9654 J/(kg·°C) is used as the specific heat capacity for the copper in the Buffer Box Model to consider the heat consumption for increasing the container temperature. A value of 2951 J/(kg·°C) is used as the specific heat capacity for the bundle tubes in the Container Model to consider heat consumption for increasing the temperature of UO2 and the zircoloy-4 claddings.

4. MODELLING RESULTS

This section presents results for the following cases, all of which are simulated for 30-year old fuel bundles with a discharge burnup of 220 MWh/(kgU):

- Container in Air,
- Container inside the Buffer Box in Air,
- Container inside the Buffer Box in the Sedimentary Rock Repository, and
- Container inside the Buffer Box in the Crystalline Rock Repository.

The following sensitivity cases are also considered:

- Container inside the Buffer Box in the Sedimentary Rock Repository with mixed fuel ages (10 years and 30 years),
- Influence of dividing the buffer box physical system into a buffer box model and a container model,
- Influence of the gap between the container and the buffer box,
- Influence of connections between fuel tube bundle and the inside surface of the container,
- Influence of water entering the container via an assumed container defect,
- Influence of radiation heat transfer between bundle tubes and between bundle tubes and the inside surface of the container,
- Influence of radiation heat transfer between fuel elements and between fuel elements and the inside surface of the bundle tube,
- Influence of heat transfer coefficient used for the heat convection from the container surface to air, and
- Influence of higher burnup of the used fuel bundles.

4.1 VERIFICATION OF THE COMSOL MODEL

To verify the COMSOL model, the maximum temperature obtained using the Sedimentary Rock DGR Model is compared with that obtained using the finite element program ANSYS (personal communication with Dimitrie Marinceu). In this comparison, the COMSOL model geometry is shown in Figure 5. The initial conditions and boundary conditions are as described in Section 3.2 and Section 3.3.1. Parameter values are shown in Table 1.

Figure 19 shows the comparison. There is good agreement; however, the maximum temperature from the ANSYS model is slightly greater than that from the COMSOL model at early times. This is most likely due to the coarser mesh adopted in the ANSYS model (Figure 20) compared to that adopted in the COMSOL model (Figure 6). This difference is not significant in the context of the current study.

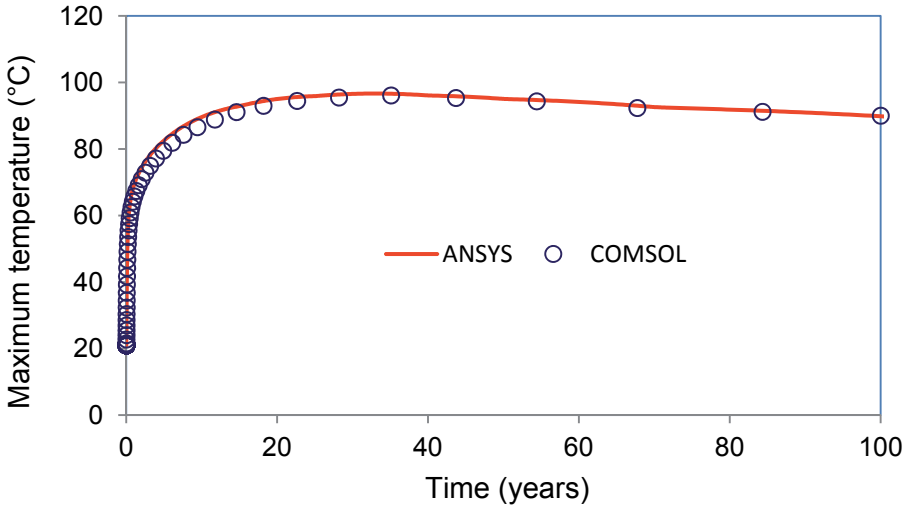

Figure 19: Maximum Temperatures in the Sedimentary Rock DGR Model obtained using ANSYS and COMSOL

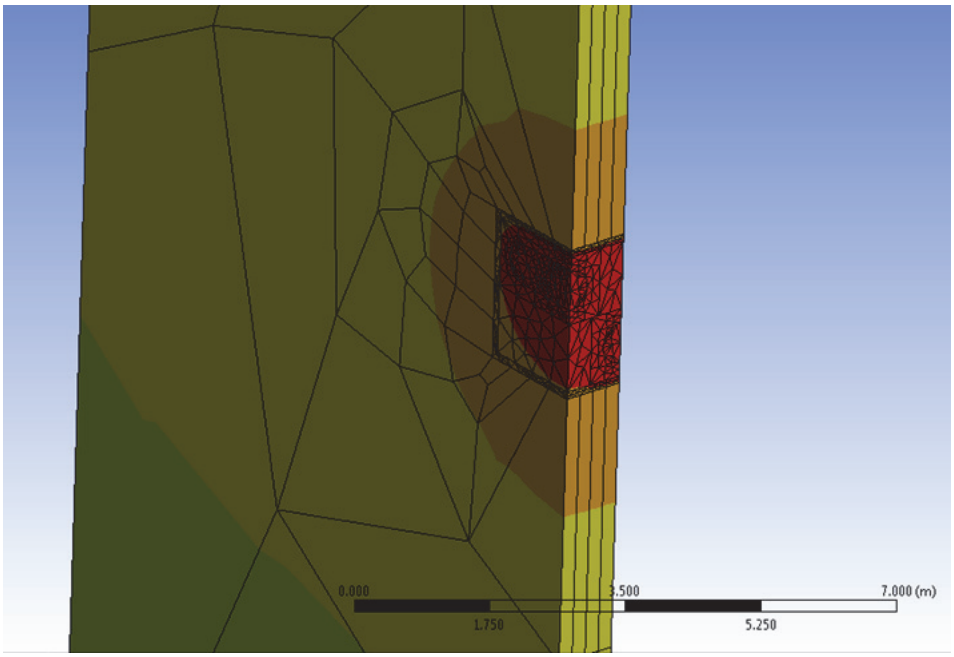

Figure 20: Finite Element Discretization of the Central Part of the Unit Cell for Near-Field Analyses for the ANSYS Model

4.2 RESULTS

This section presents results obtained using the models as described in Section 3. As noted previously, for computational efficiency these models neglect radiation heat transfer and include a number of simplifications. The effects of these simplifications, including radiation heat transfer, are examined in Section 4.4.

4.2.1 Container in Air

This section presents maximum temperature results from the various models for the Container in Air case for fuel with a 30 year decay time. The maximum temperatures occur at 8.6 days.

Container Model:

Figure 21, Figure 22 and Figure 23 show the maximum temperature in the Container Model, on either the transverse cross section through the container axis or the longitudinal cross section through the container center. The highest air temperature is 69°C, occurring at the centre of the container and at 8.6 days. The maximum container surface temperature is 23°C, occurring at 8.6 days.

The air temperature at the centre of the container is used as the boundary condition on the perimetric surface and on the end surface at z = 1.03 m of the Bundle Model.

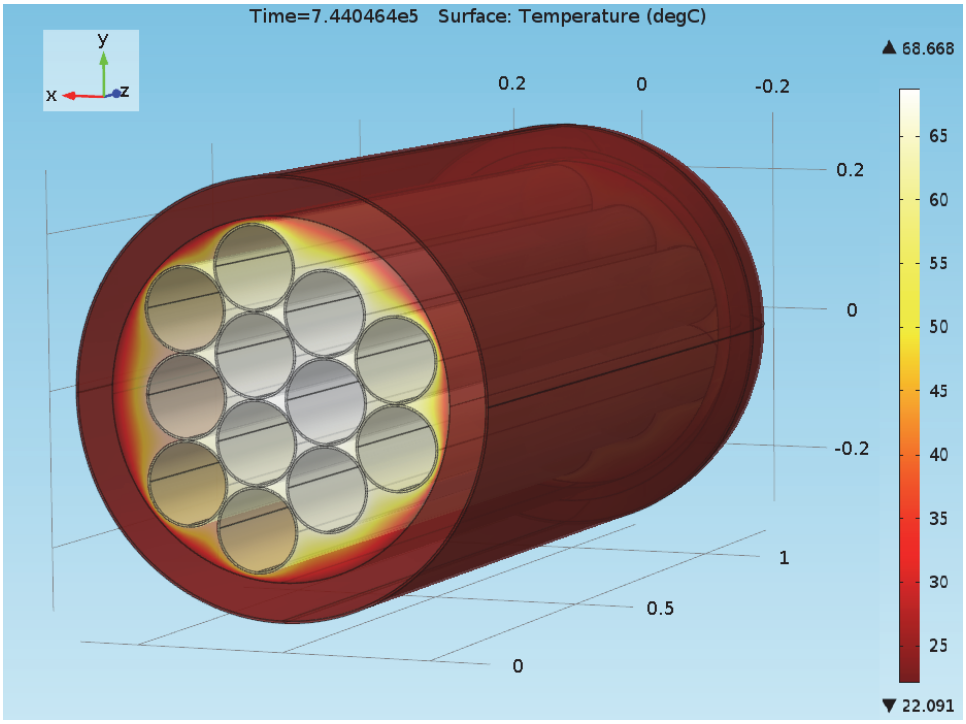

Figure 21: Container Temperatures at 8.6 Days for the Container in Air Case

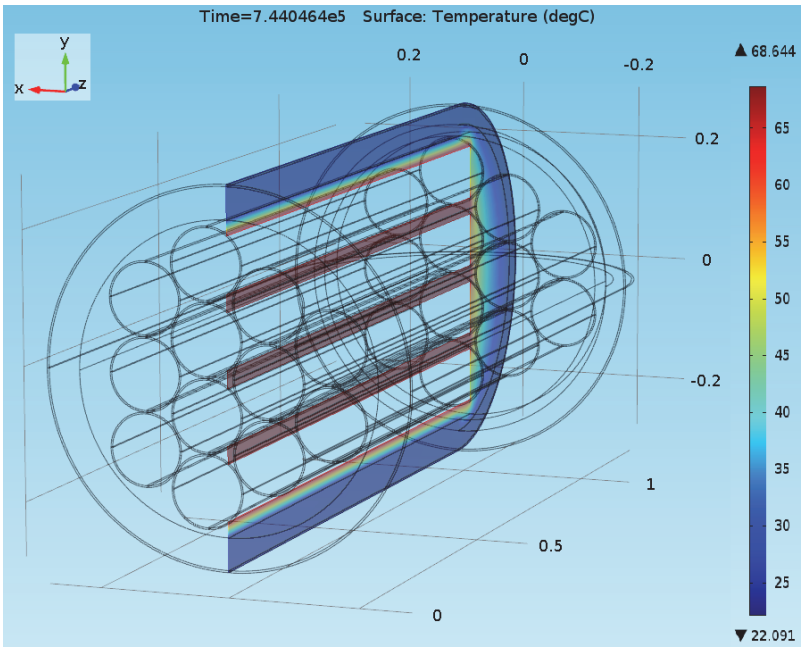

Figure 22: Container Temperatures on the x= 0 Plane at 8.6 Days for the Container in Air Case

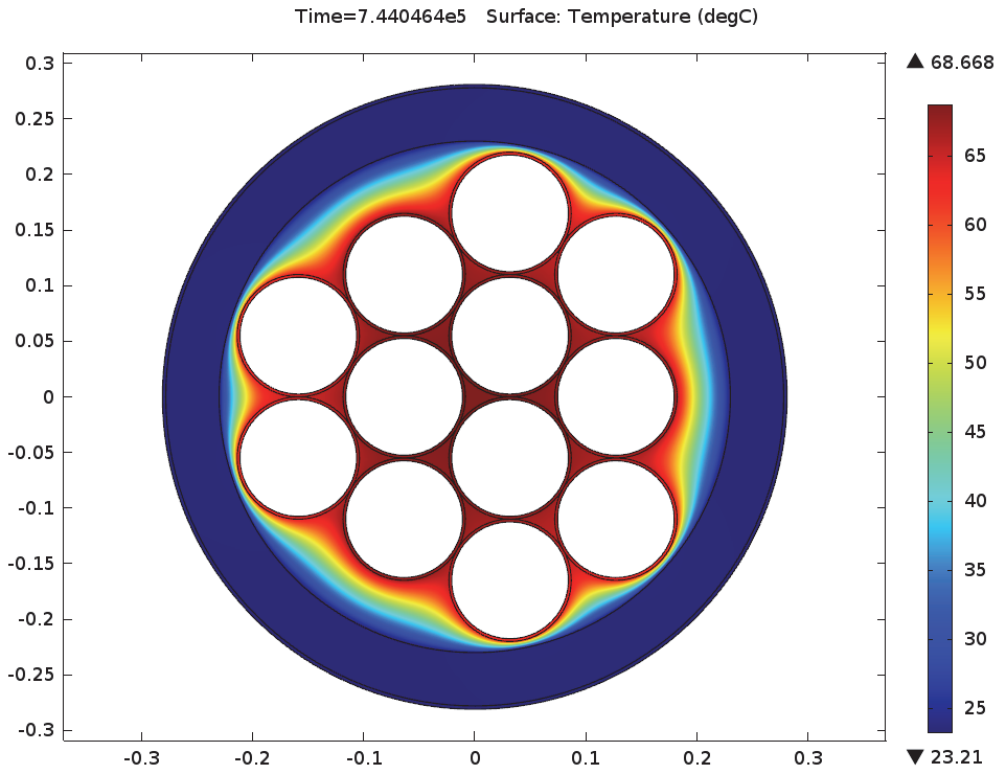

Figure 23: Container Temperatures on the z = 0 Plane (Middle Cross Section of a Container) at 8.6 Days for the Container in Air Case

Bundle Model:

Figure 24 and Figure 25 show the temperatures on the transverse and longitudinal cross sections of the Bundle Model at 8.6 days, at which the fuel centre temperature reaches its maximum value. The highest temperature is 75°C, occurring at the centre of the bundle.

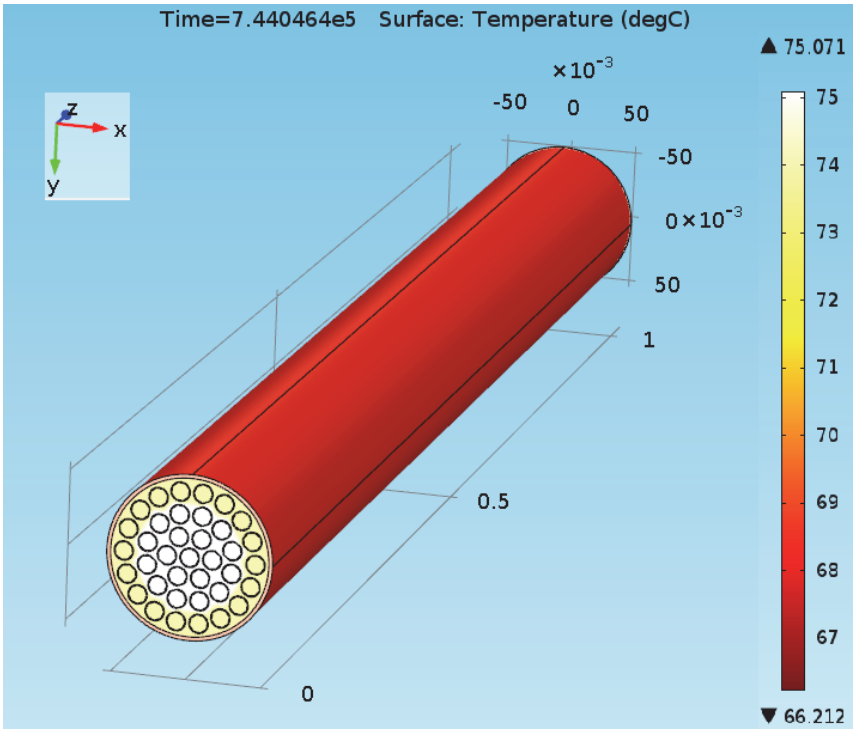

Figure 24: Fuel Temperatures at 8.6 Days for the Container in Air Case

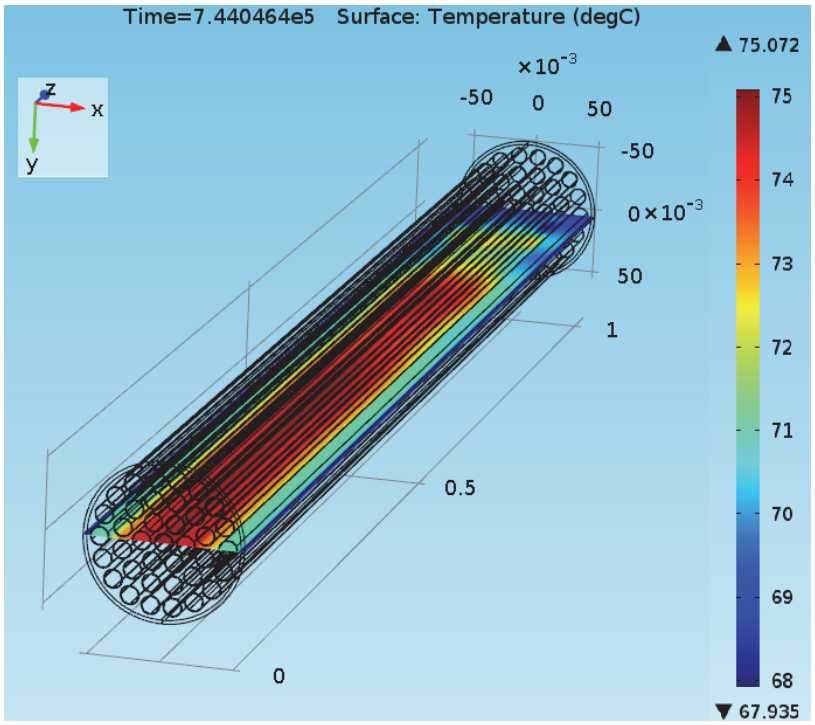

Figure 25: Fuel Temperatures on the y = 0 Plane at 8.6 Days for the Container in Air Case

Figure 26 shows the peak fuel, container central air and the container surface temperatures at the centre of the Container Model as a function of time. The temperatures decrease with time due to the decaying heat source. The difference between the maximum temperature of the fuel (75°C) and the maximum temperature of the air (69°C) is 6°C. The highest container surface temperature is 23°C.

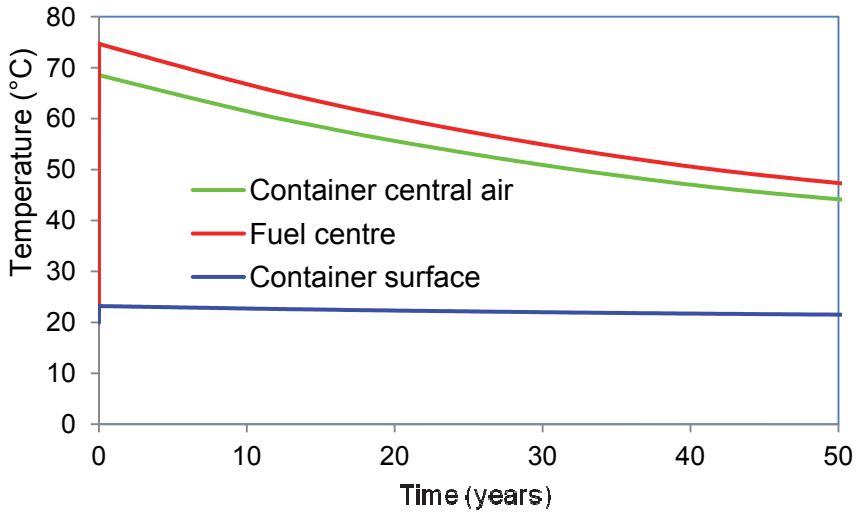

Figure 26: Temperatures as a Function of Time for the Container in Air Case

4.2.2 Container inside the Buffer Box in Air

This section presents maximum temperature results from the various models for the Container inside the Buffer Box in Air Case for fuel with a 30 year decay time.

Buffer Box Model:

Figure 27 and Figure 28 show the maximum temperature in the buffer box and along the transverse and longitudinal cross sections through the container centre. The maximum temperature occurs after 20 days. Due to the high thermal conductivity of copper, the temperature at the inside surface of the bentonite is essentially uniform at 37°C.

The temperature at point T on the outside surface of the copper coating is used as the boundary condition on the outside surface of the Container Model.

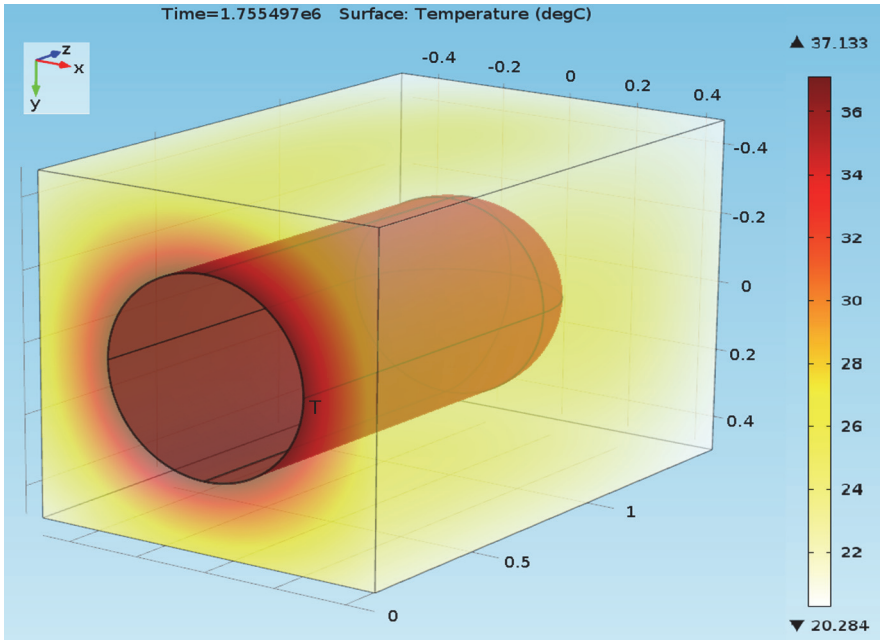

Figure 27: Buffer Box Temperature at 20 Days for the Container inside the Buffer Box in Air Case

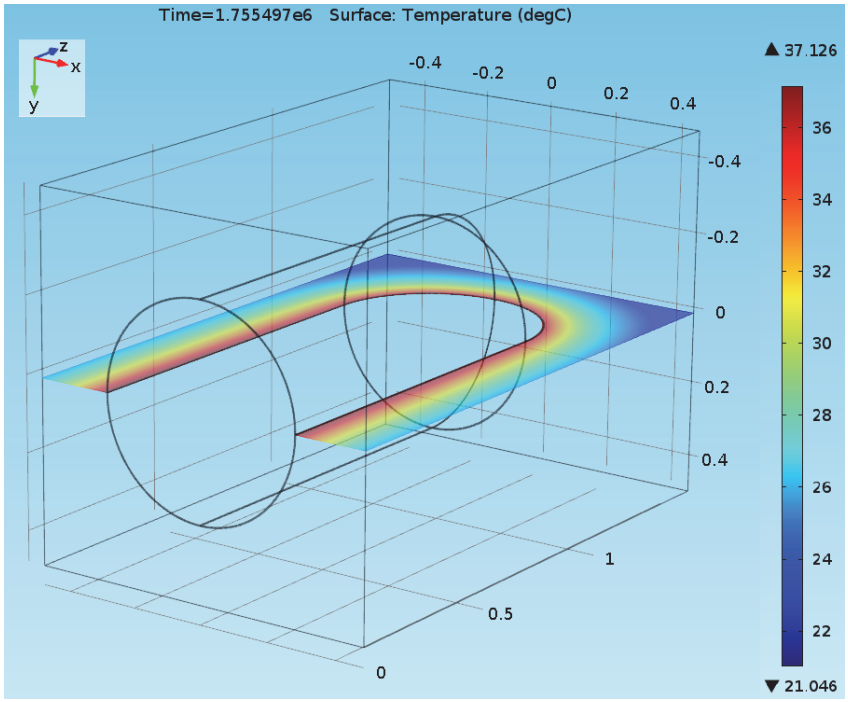

Figure 28: Buffer Box Temperature on the y = 0 Plane at 20 Days for the Container inside the Buffer Box in Air Case

<u>Container Model</u>:

Figure 29, Figure 30 and Figure 31 show the maximum temperature in the Container Model, on the longitudinal cross section through the container axis and on the transverse cross section through the container centre. The maximum temperatures occur after 20 days.

The air temperature at the centre of the container is used as the boundary condition on the perimetric surface and on the end surface at z = 1.03 m of the Bundle Model.

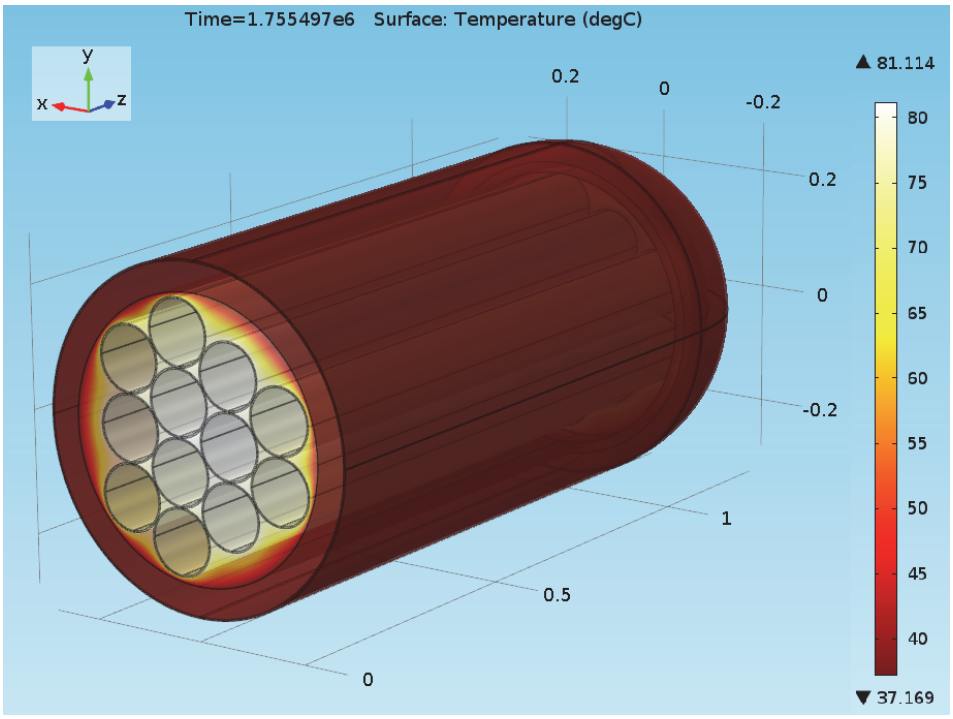

Figure 29: Container Temperature at 20 Days for the Container inside the Buffer Box in Air Case

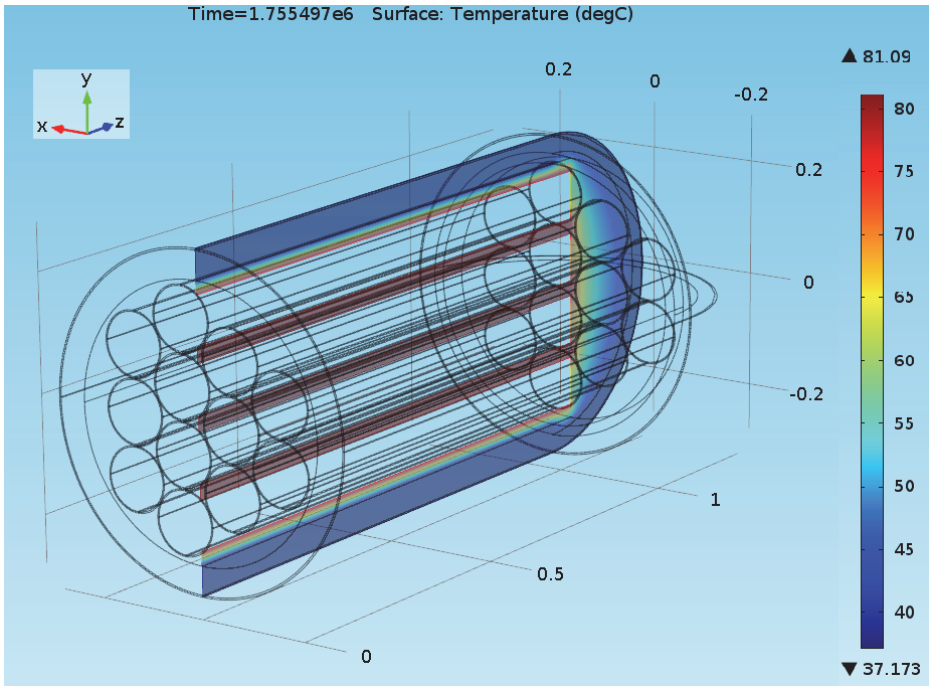

Figure 30: Container Temperature on the x = 0 Plane at 20 Days for the Container inside the Buffer Box in Air Case

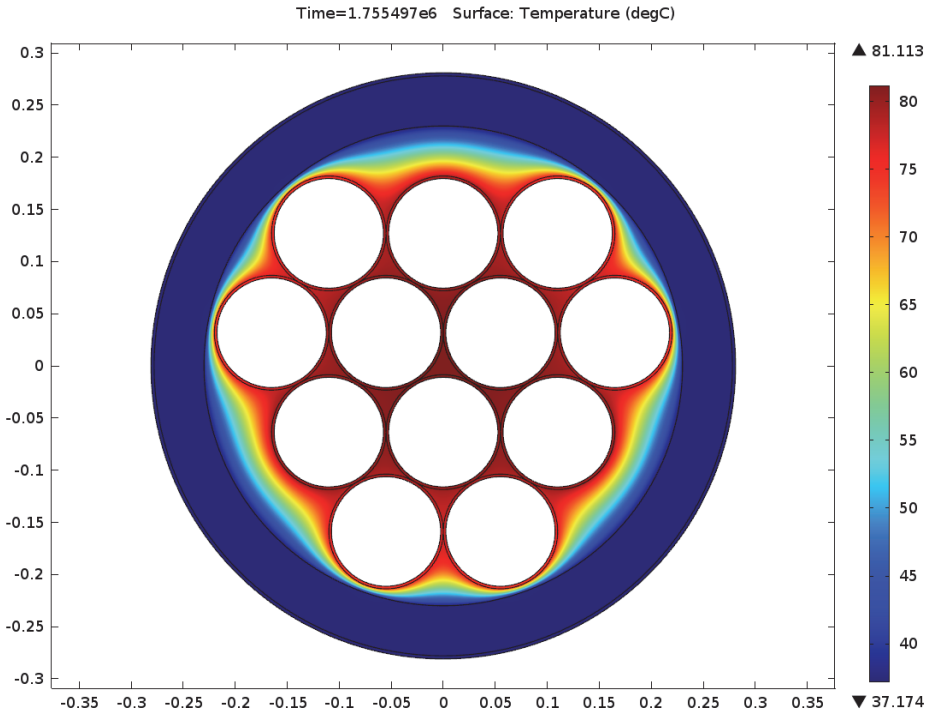

Figure 31: Container Temperatures on the z = 0 Place (Middle Cross Section of a Container) at 20 Days for the Container inside the Buffer Box in Air Case

Bundle Model:

Figure 32 and Figure 33 show the maximum temperature along the transverse cross section and the longitudinal cross section of the Bundle Model. The maximum temperature is reached after 20 days.

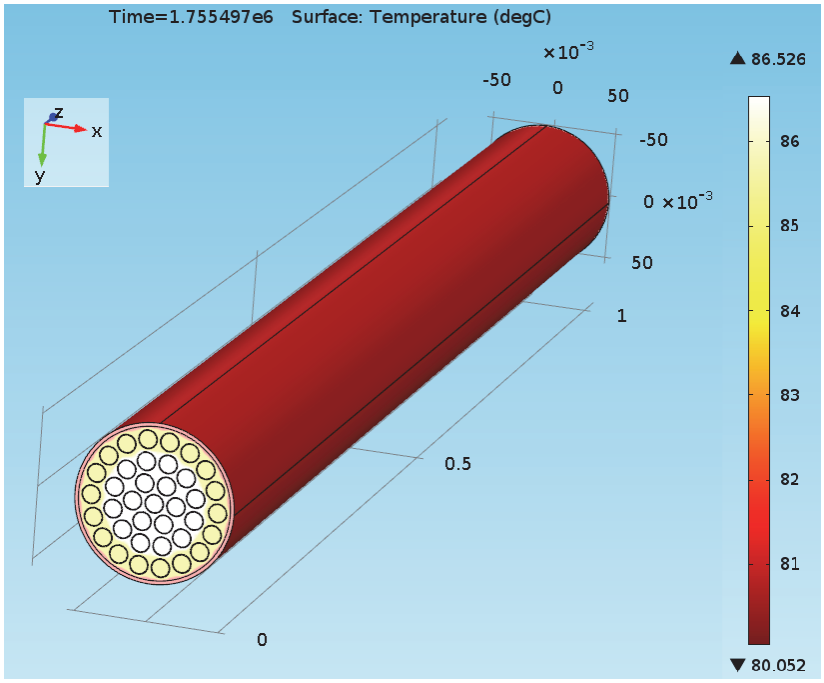

Figure 32: Fuel Temperature at 20 Days for the Container inside the Buffer Box in Air Case

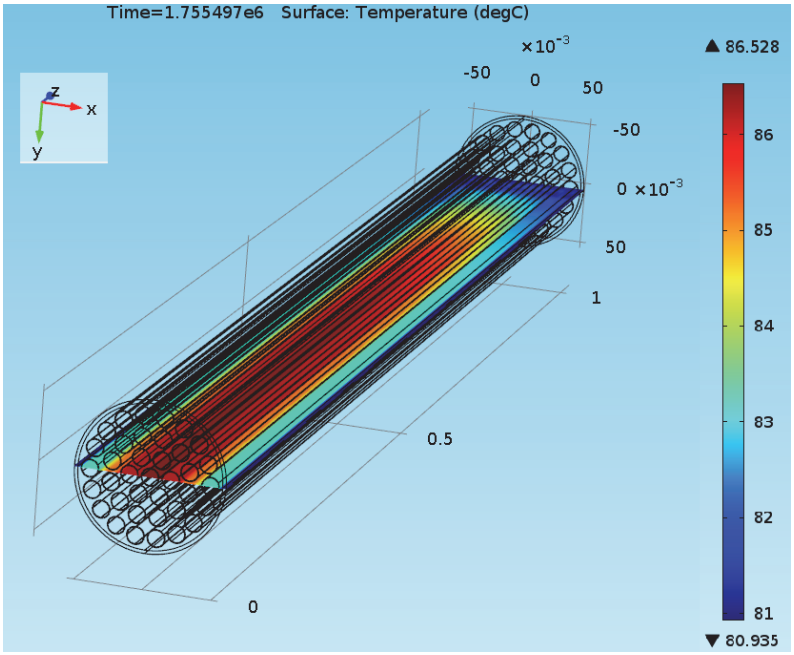

Figure 33: Fuel Temperature on the y = 0 Plane at 20 Days for the Container inside the Buffer Box in Air Case

Figure 34 shows the temperature at the fuel centre, container centre and container surface as a function of time. The maximum fuel temperature reaches a peak value of 86.5°C at 20 days and then decreases. The maximum container temperature reaches the peak value of 81.1°C at 20 days. The maximum container outside surface temperature reaches the peak value of 37.2°C at 20 days. The decrease in temperature is due to the decaying heat source.

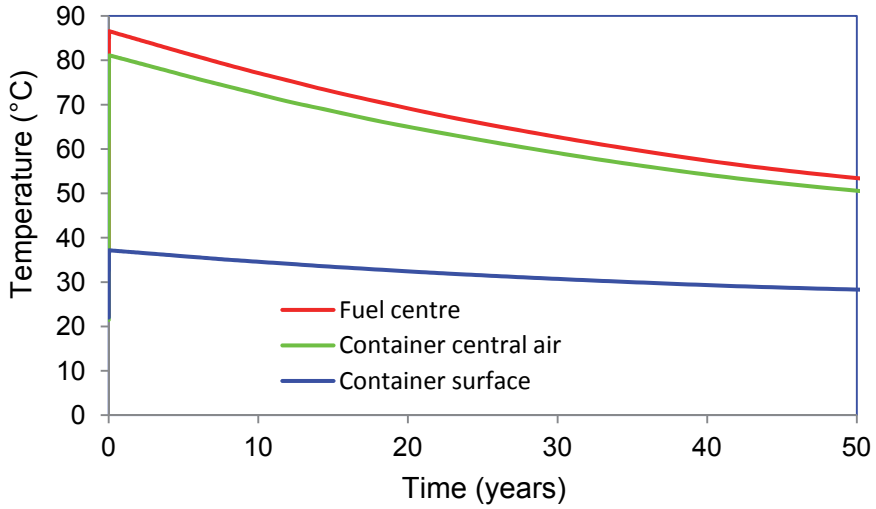

Figure 34: Temperatures as a Function of Time for the Container inside the Buffer Box in Air Case

4.2.3 Container inside the Buffer Box in the Repository

This section presents maximum temperature results from the various models used in the analysis for the Container inside the Buffer Box in the Repository Case for fuel with a 30 year decay time.

Two cases were simulated with the Repository Model. One is for a sedimentary rock site and the other is for a crystalline rock site.

4.2.3.1 Sedimentary Rock Environment:

Repository Model:

Figure 35 shows the temperature in the sedimentary rock and sealing materials at 40 years, which is the time at which the container outside surface temperature reaches its maximum value.

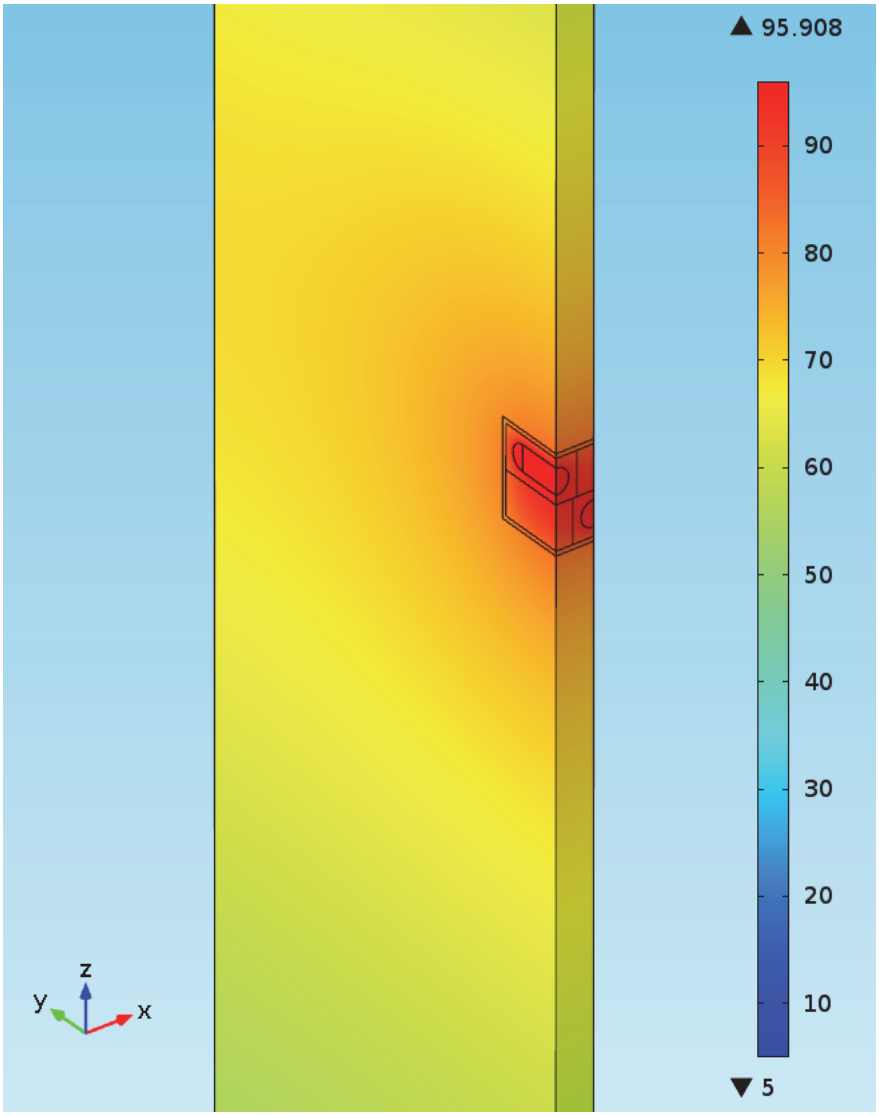

Figure 35: Rock Temperature at 40 Years for the Container inside the Buffer Box in the Sedimentary Repository Case

Figure 36 shows the temperature distribution at the repository level. The maximum container surface temperature is 96°C. The temperature at location T is used as the boundary condition in the Container Model.

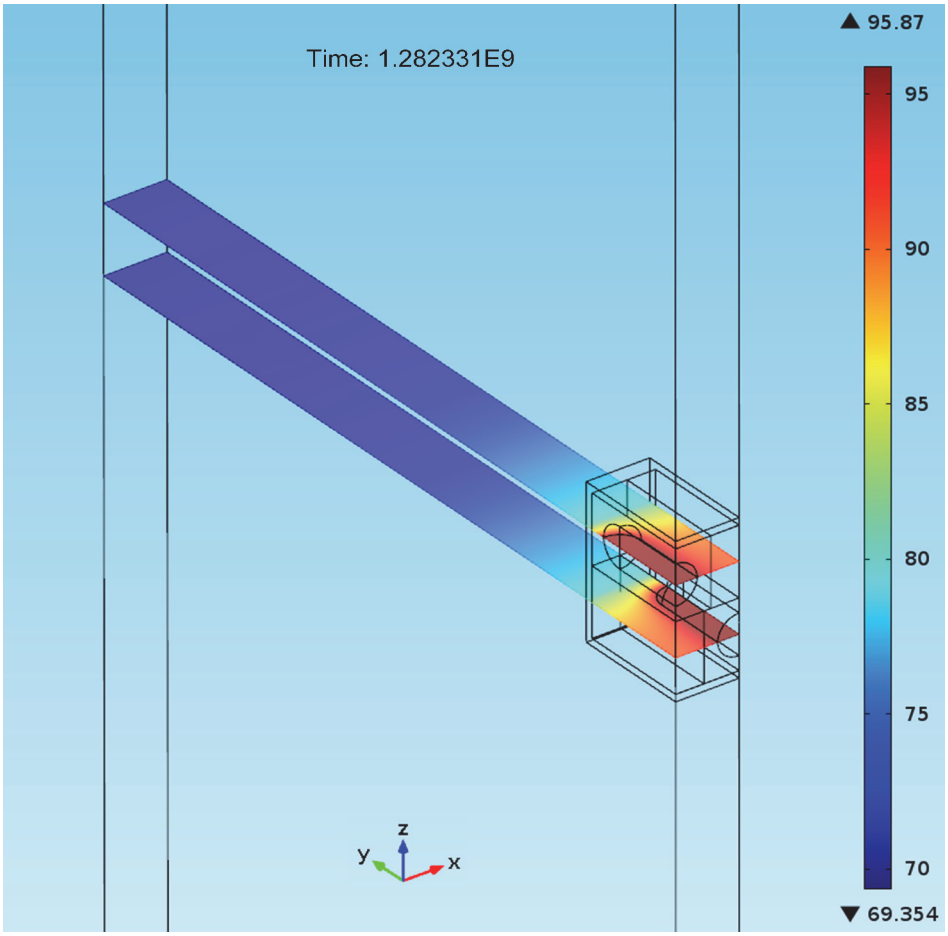

Figure 36: Rock Temperature at the Repository Level at 40 Years for the Container inside the Buffer Box in the Sedimentary Repository Case

<u>Container Model</u>:

Figure 37 shows the maximum temperatures in the container, which are reached after 14.7 years. Figure 38 and Figure 39 show the maximum temperature along a longitudinal cross section through the container axis and along a transverse cross section through the container centre. The maximum temperature of the air in the container is 122°C.

Temperatures from this model are passed to the Bundle Model to be used as boundary conditions.

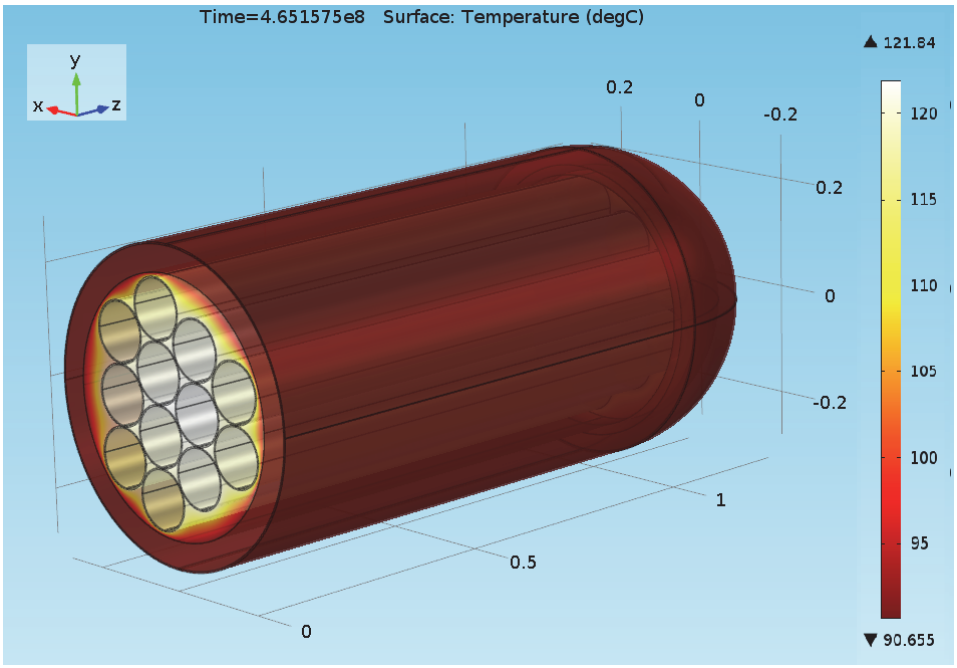

Figure 37: Container Temperature at 14.7 Years for the Container inside the Buffer Box in the Sedimentary Repository Case

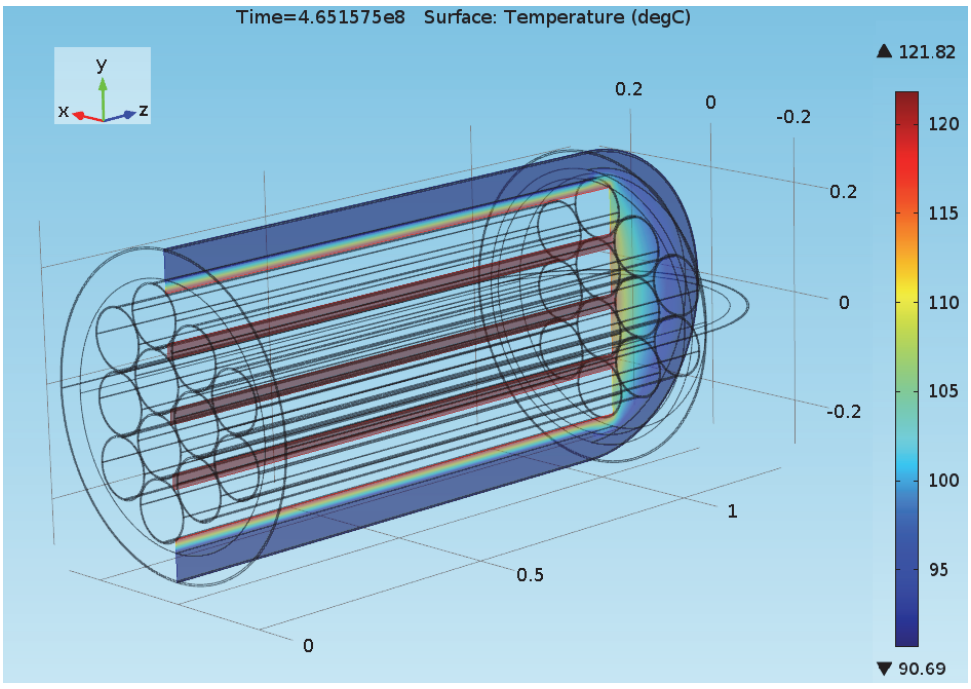

Figure 38: Temperature on the x= 0 Plane at 14.7 Years for the Container inside the Buffer Box in a Sedimentary Repository Case

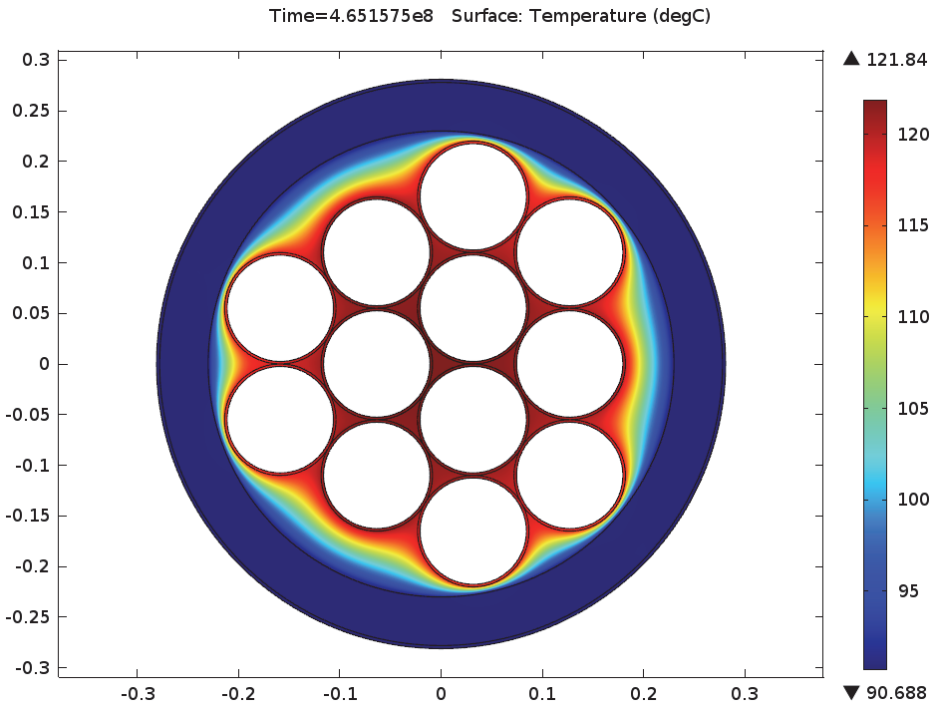

Figure 39: Temperature Distribution on the z = 0 Plane (Middle Cross Section of a Container) at 14.7 Years for the Container inside the Buffer Box in a Sedimentary Repository Case

Bundle Model:

Figure 40 shows the temperature on the transverse cross section and surface of the fuel tube and Figure 41 shows the temperature distribution along the X-Z cross section at 14.7 years (i.e., the time at which the temperature reaches its peak value). The maximum fuel temperature is 126°C occurring at the centre of the fuel bundle located near the centre of the container.

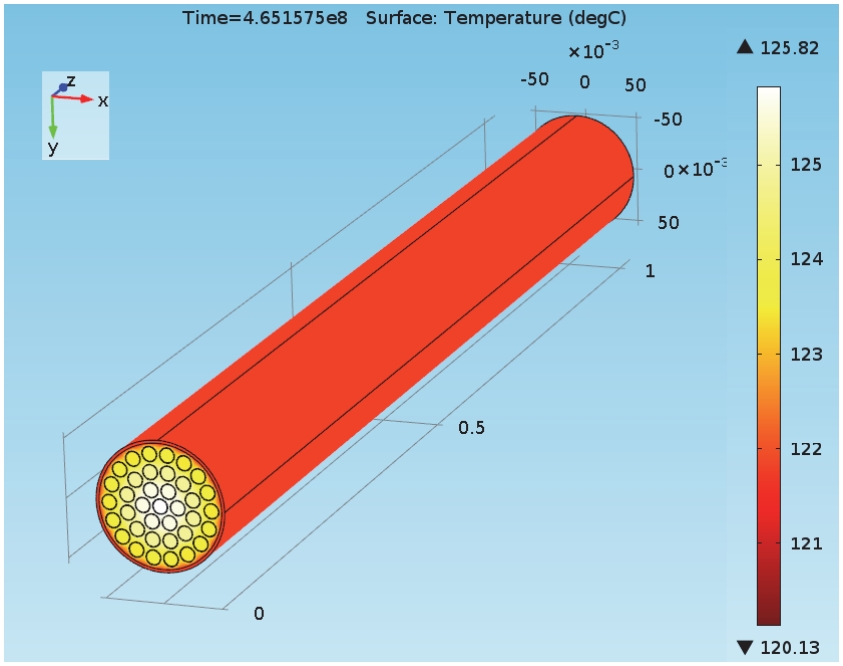

Figure 40: Fuel Temperature in the Bundle Model at 14.7 Years for the Container inside the Buffer Box in a Sedimentary Repository Case

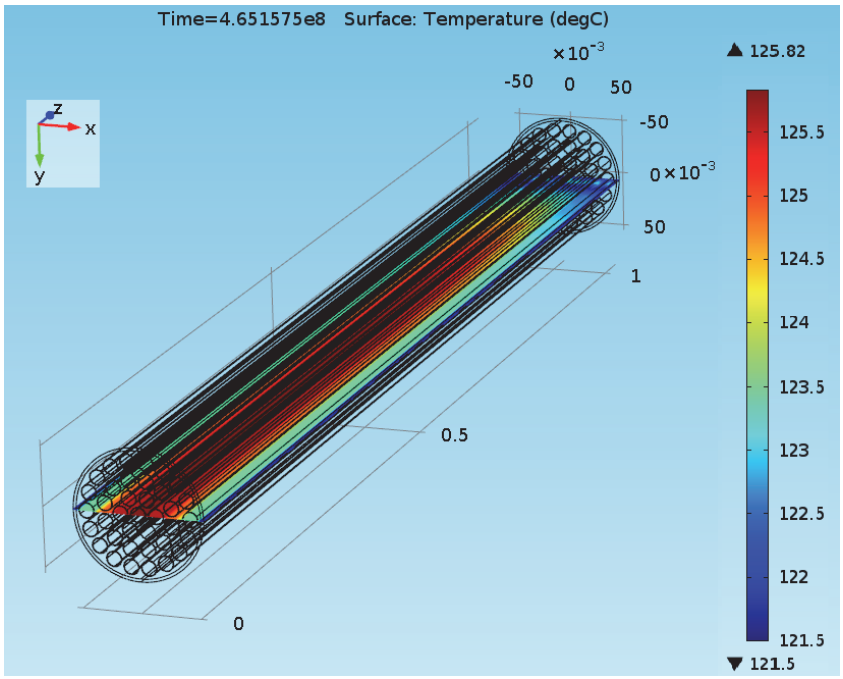

Figure 41: Fuel Temperature on the y = 0 Plane at 14.7 Years for the Container inside the Buffer Box in a Sedimentary Repository Case

Figure 42 shows the time evolution of temperature at the fuel centre, of the air at the container centre and at the container outer surface.

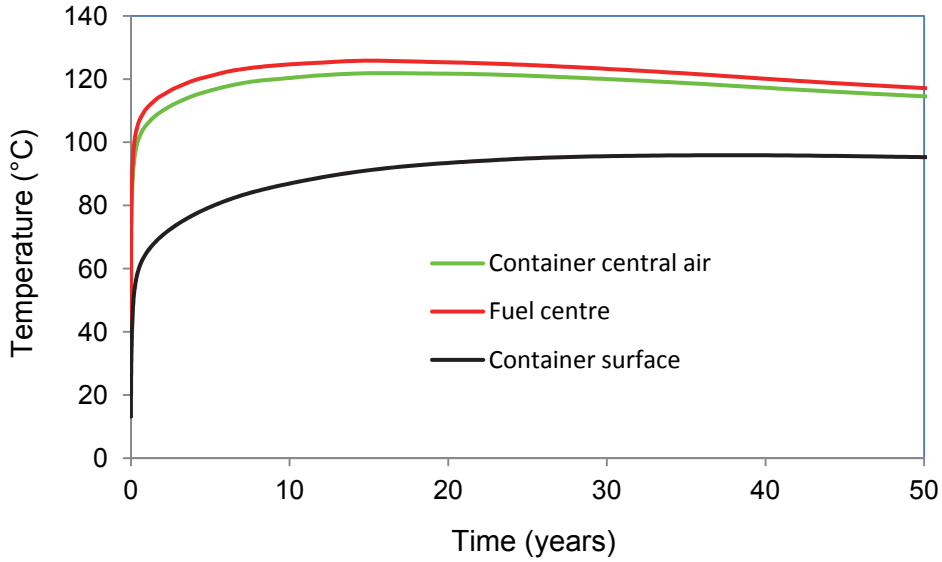

Figure 42: Temperatures as a Function of Time for the Container inside the Buffer Box in a Sedimentary Repository Case

The maximum fuel temperature decreases from a peak value of 126°C at 14.7 years to 116°C at 50 years. The maximum container air temperature decreases from 122°C at 14.7 years to 114°C at 50 years. The maximum container surface temperature decreases from 96°C at 40 years to 95°C at 50 years.

4.2.3.2 Crystalline Rock Environment

Repository Model:

Figure 43 shows the temperature in the crystalline rock and sealing materials at 34.8 years, at which the container outside surface temperature reaches its maximum value. Figure 44 shows the temperature distribution at the repository level. The maximum temperature of the container outside surface is 94°C. The temperature at location T (see Figure 5 for location) is used as the boundary condition in the Container Model.

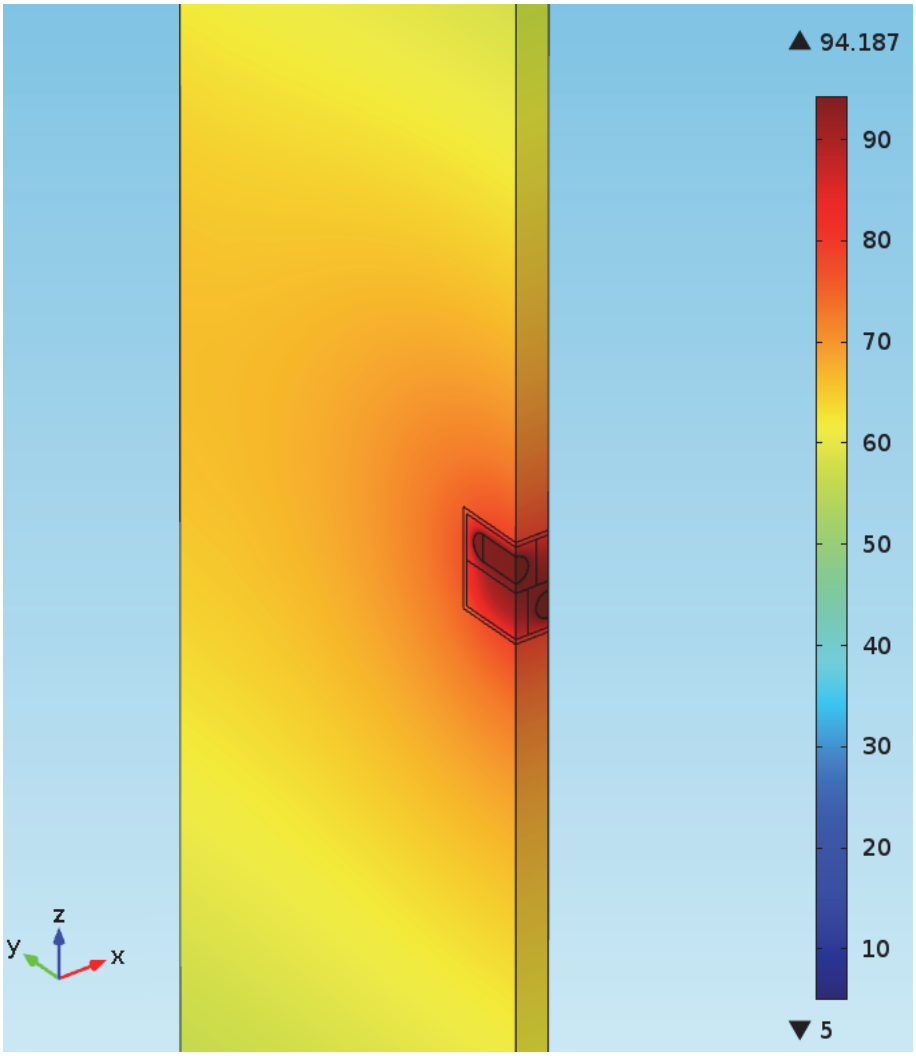

Figure 43: Rock Temperature at 34.8 Years for the Container inside the Buffer Box in the Crystalline Repository Case

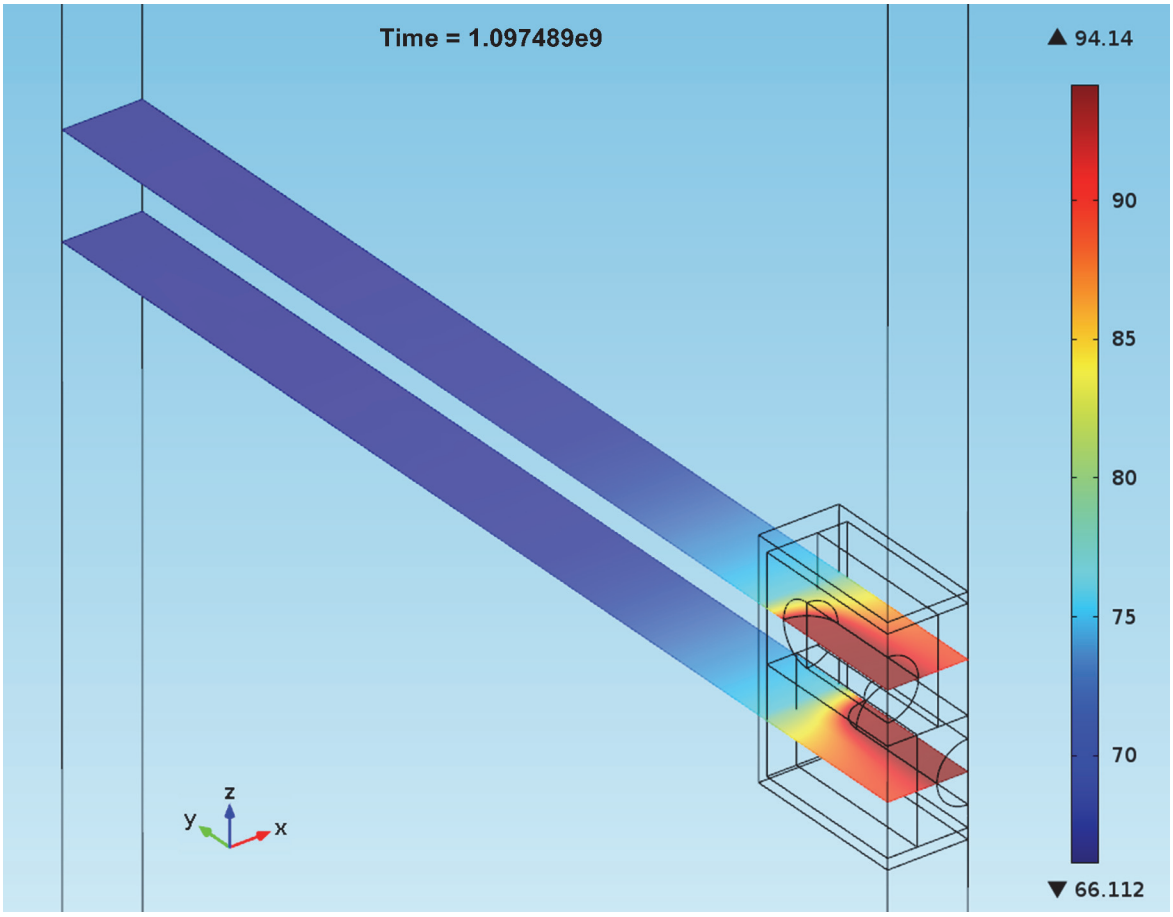

Figure 44: Rock Temperature at the Repository Level at 34.8 Years for the Container inside the Buffer Box in the Crystalline Repository Case

Container Model:

Figure 45 shows the container temperature at 14.7 years, which is the time at which the central air temperature reaches its maximum value. Figure 46 and Figure 47 show the temperature along the longitudinal cross section through the container axis and along the transverse cross section through the container centre at 14.7 years. The maximum air temperature in the container is 121°C.

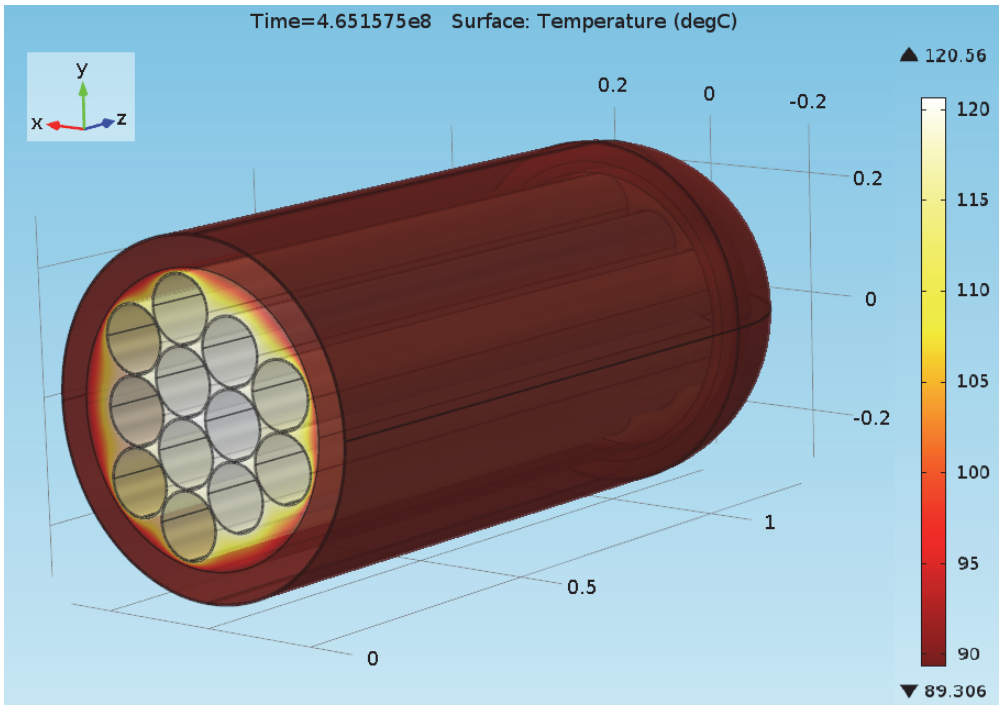

Figure 45: Container Temperature at 14.7 Years for the Container inside the Buffer Box in the Crystalline Repository Case

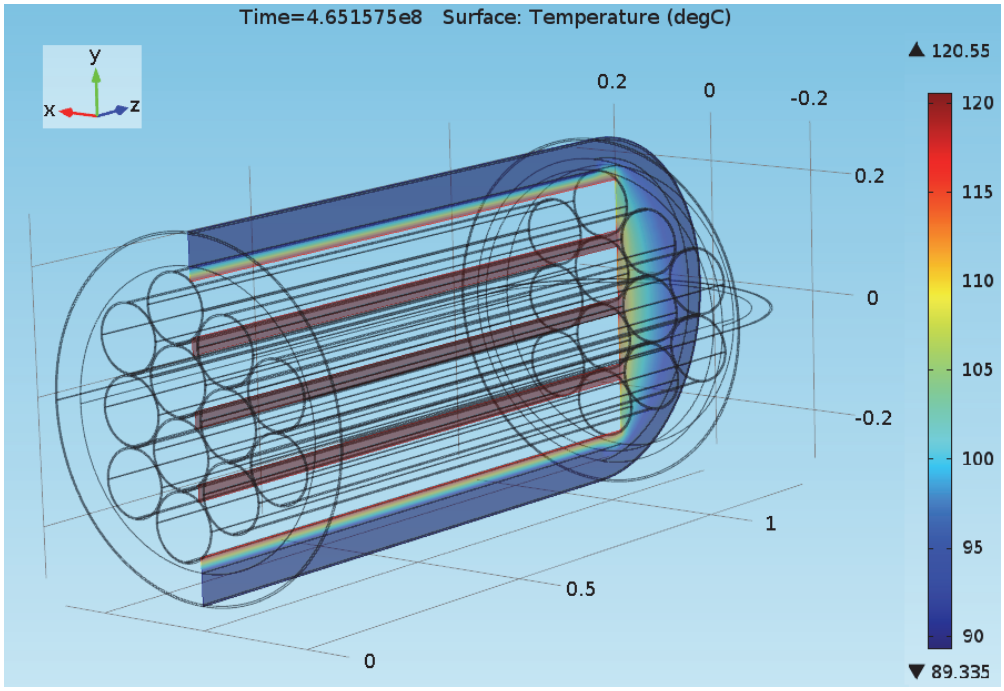

Figure 46: Temperature on the x = 0 Plane at 14.7 Years for the Container inside the Buffer Box in the Crystalline Repository Case

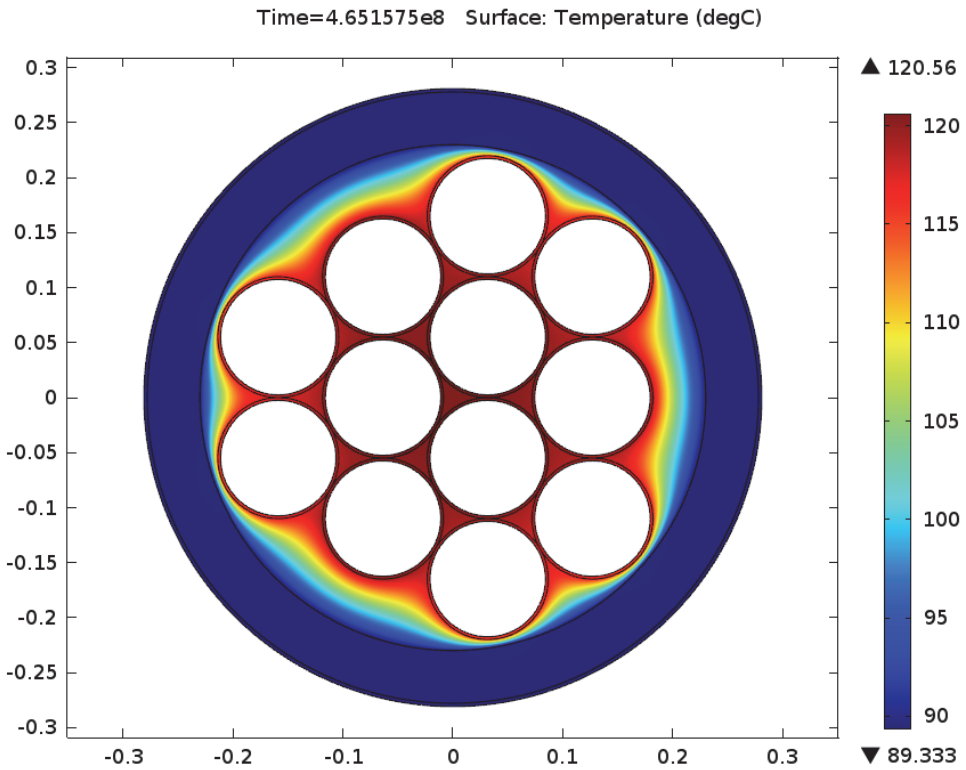

Figure 47: Temperature on the z = 0 Plane (Middle Cross Section of a Container) at 14.7 Years for the Container inside the Buffer Box in the Crystalline Repository Case

Bundle Model:

Figure 48 and Figure 49 show the fuel temperatures in the Bundle Model and along the X-Z cross section at 14.7 years, which is the time at which the central fuel temperature reaches its maximum value. The highest temperature is 125°C at the centre of the fuel located near the centre of the container.

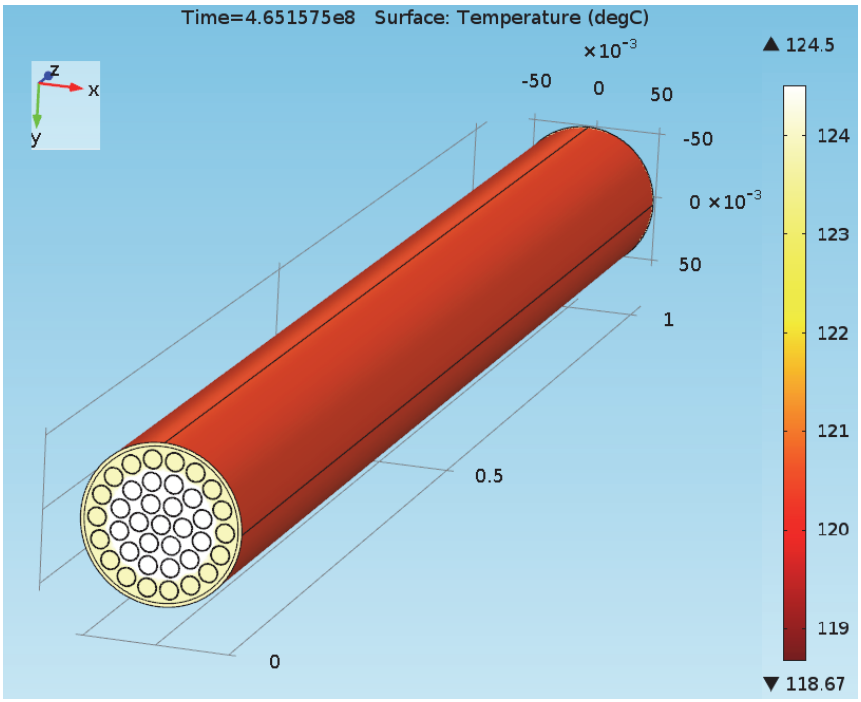

Figure 48: Fuel Temperature in the Bundle Model at 14.7 Years for the Container inside the Buffer Box in the Crystalline Repository Case

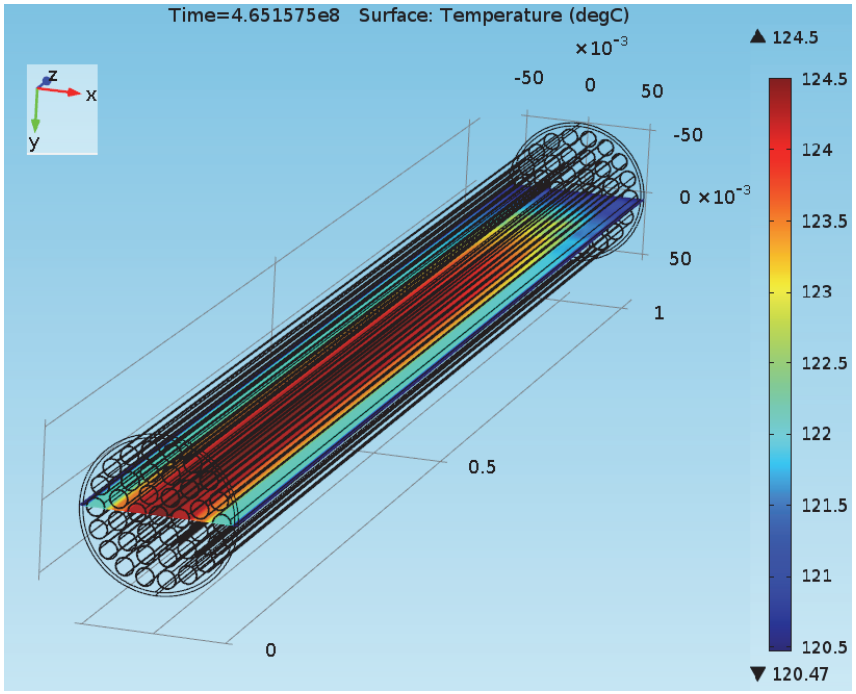

Figure 49: Fuel Temperature on the y = 0 Plane at 14.7 Years for the Container inside the Buffer Box in the Crystalline Repository Case

Figure 50 shows the temperature at the fuel centre, container central air and container surface as a function of time. The fuel temperature decreases from a peak value of 125°C at 14.7 years to 112°C at 50 years. The container centre air temperature decreases from 121°C at 14.7 years days to 110°C at 50 years. The container surface temperature decreases from 94°C at 34.8 years to 93°C at 50 years.

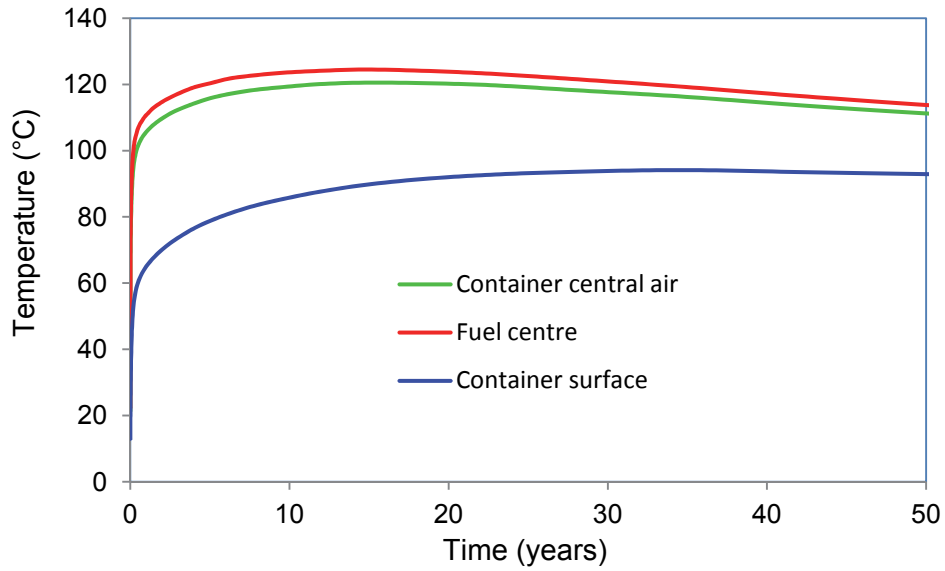

Figure 50: Temperatures for the Container inside the Buffer Box in the Crystalline Repository Case

4.3 CONTAINER WITH MIXED AGE BUNDLES IN A SEDIMENTARY REPOSITORY

The section presents the results of a sensitivity case in which the fuel bundles in the container contain a mix of bundles with 10 year and 30 year decay times. The number of mixed bundles is selected such that the total heat source in a container is not greater than that for a container filled entirely with only 30-year-old bundles. This means that containers with 10-year old fuel hold less than 48 fuel bundles.

The following cases are examined:

- Mixed Heat Source Model I: nine 10-year-old fuel bundles and twelve 30-year-old fuel bundles. This corresponds to the number of bundles in one half of a real container;
- Mixed Heat Source Model II: eighteen 10-year-old fuel bundles;
- Mixed Heat Source Model III: twelve 10-year-old fuel bundles and nine 30-year-old fuel bundles; and
- Mixed Heat Source Model IV: twelve 10-year-old fuel bundles and nine 30-year-old fuel bundles, with a different bundle distribution assumed from that in the Mixed Heat Source Model III case.

4.3.1 Mixed Heat Source Model I

In this model, there are nine 10-year-old fuel bundles and twelve 30-year-old fuel bundles in the Container Model as shown in. The 10-year-old bundles are in the end module of the Container Model Figure 51(a) note: the blue shading represents tubes containing fuel bundles) and the 30-year-old bundles are in the middle module (Figure 51 (b)).

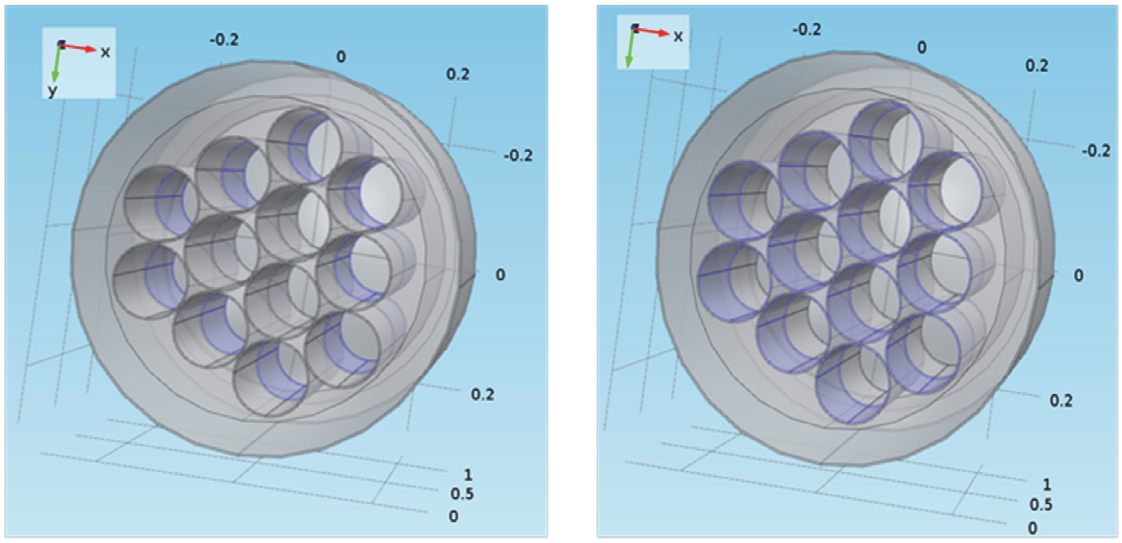

(a) 9 bundles with age of 10 years

(b) 12 bundles with age of 30 years

Note: the blue shading represents tubes containing fuel bundles

Figure 51: Bundle Distribution in a Mixed Heat Source Model I in a Sedimentary Repository

Figure 52 shows fuel temperature, container central air temperature and container surface temperatures as a function of time in the sedimentary repository. The fuel temperature decreases from a peak value of 129°C at 11.9 years to 115°C at 50 years. The container central air temperature decreases from 125°C at 11.9 years to 112°C at 50 years. The container surface temperature decreases from 96°C at 28 years to 94°C at 50 years.

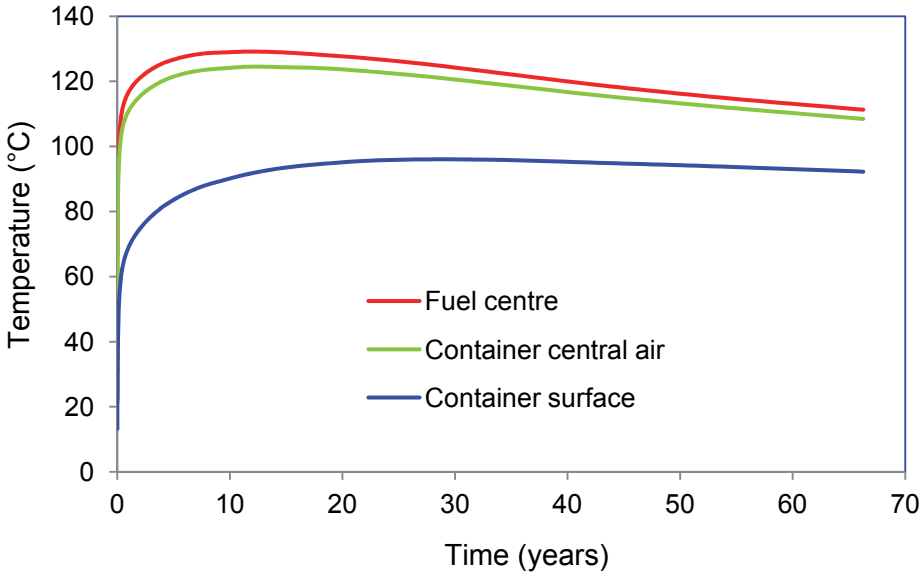

Figure 52: Temperatures from Mixed Heat Source Model I in a Sedimentary Repository

4.3.2 Mixed Heat Source Model II

In this model, there are eighteen 10-year-old fuel bundles as shown in Figure 53. There are nine 10-year-old bundles placed near the container inner surface for each of the two modules in the Container Model.

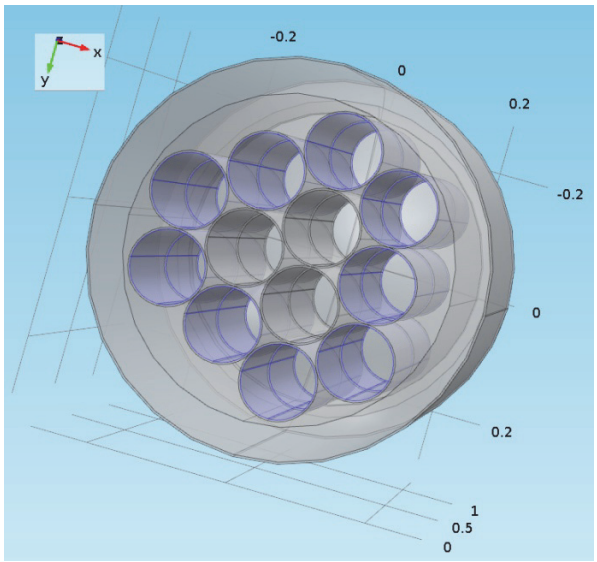

Note: the blue shading represents tubes containing fuel bundles

Figure 53: Bundle Distribution in Mixed Heat Source Model II in a Sedimentary Repository

Figure 54 shows the fuel temperature, container central air temperature and container surface temperature as a function of time in the sedimentary repository. The fuel temperature decreases from a peak value of 133°C at 7.7 years to 114°C at 50 years. The container central air temperature decreases from 128°C at 7.7 years days to 111°C at 50 years. The container surface temperature decreases from 98°C at 22.6 years to 94°C at 50 years.

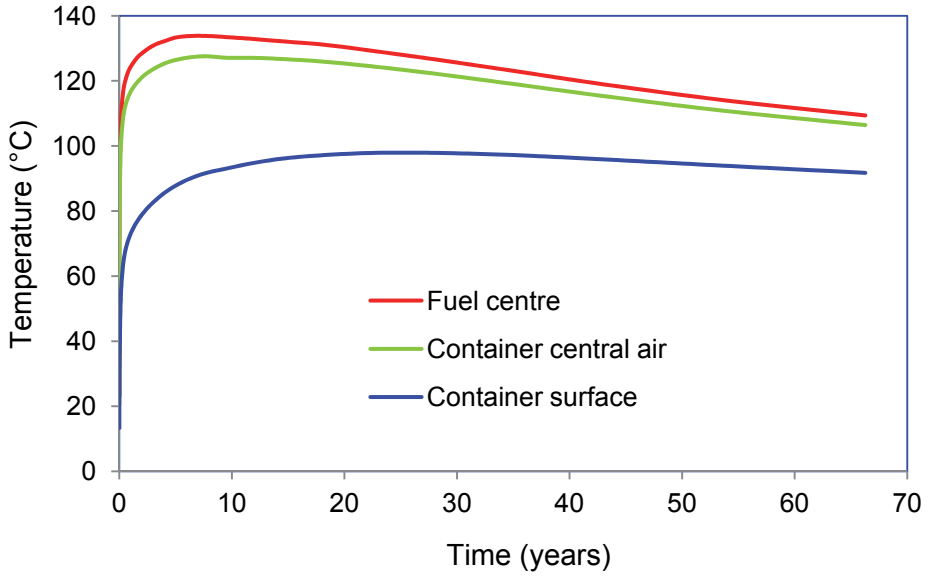

Figure 54: Temperatures from Mixed Heat Source Model II in a Sedimentary Repository

4.3.3 Mixed Heat Source Model III

In this model, there are twelve 10-year-old fuel bundles and nine 30-year-old fuel bundles in the Container Model as shown in Figure 55. In the end module there are twelve 10-year-old bundles as shown in Figure 55 (a) while in the middle module there are nine 30-year-old bundles as shown in Figure 55 (b).

Figure 56 shows the fuel temperature, container central air temperature and container surface temperature as a function of time in the sedimentary repository. The fuel temperature decreases from a peak value of 129°C at 11.9 years to 116°C at 50 years. The container central air temperature decreases from 125°C at 11.9 years days to 113°C at 50 years. The container surface temperature decreases from 100°C at 28 years to 97°C at 50 years.

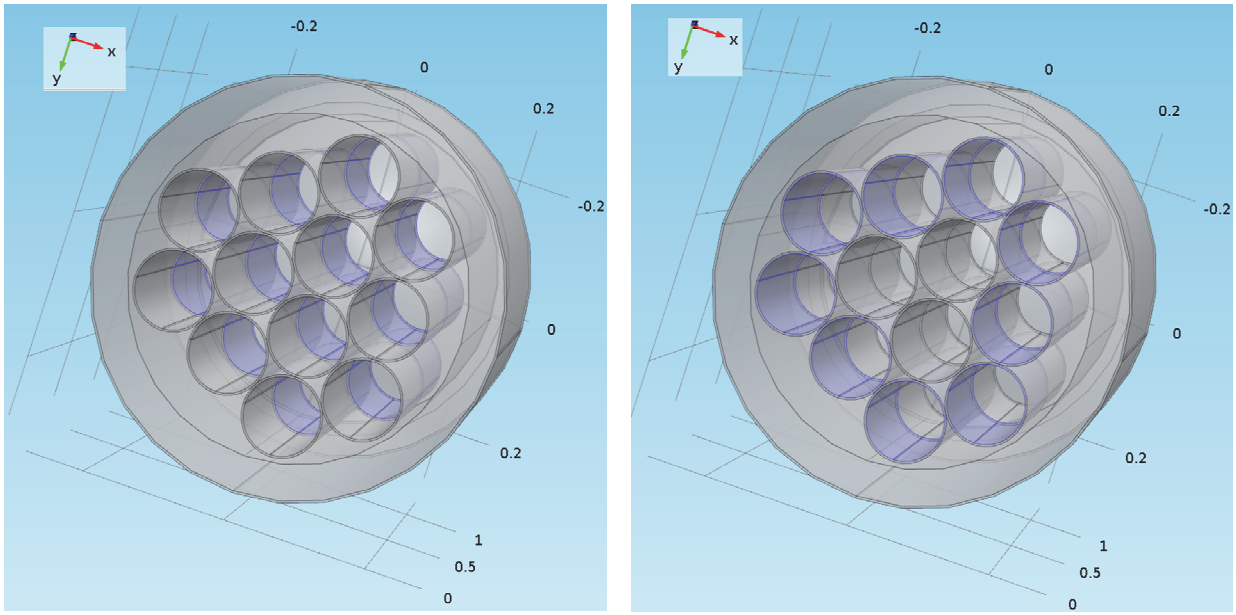

(a) 12 10-year-old bundles (b) 9 30-year-old bundles

Note: the blue shading represents tubes containing fuel bundles

Figure 55: Bundle Distribution in Mixed Heat Source Model III in a Sedimentary Repository

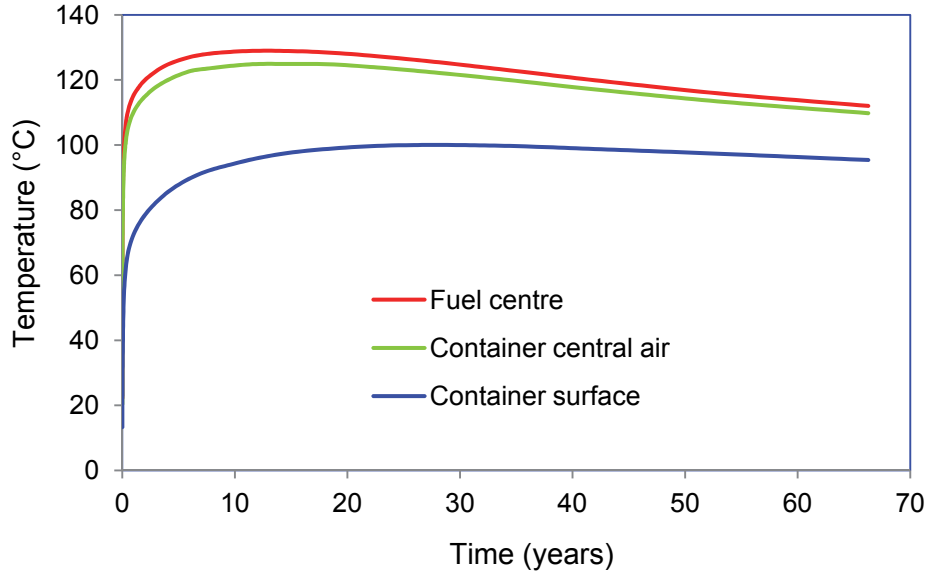

Figure 56: Temperatures from Mixed Heat Source Model III in a Sedimentary Repository

4.3.4 Mixed Heat Source Model IV

In this model, there are twelve 10-year-old fuel bundles and nine 30-year-old fuel bundles in the Container Model as shown in Figure 57. In the end module there are nine 10-year-old bundles as shown in Figure 57 (a). In the middle module there are nine 30-year old bundles as shown in Figure 57 (b) and three 10-year-old bundles as shown in Figure 57 (c).

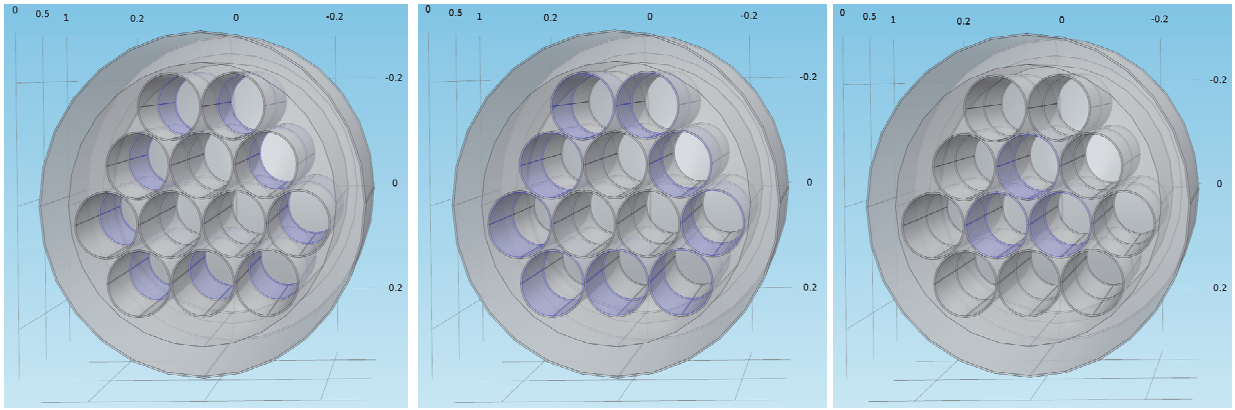

(a) 9 10-year-old bundles (b) 9 30-year-old bundles (c) 3 10-year-old bundles

Note: the blue shading represents tubes containing fuel bundles

Figure 57: Bundle Distribution in Mixed Heat Source Model IV in a Sedimentary Repository

Figure 58 shows the temperature at the fuel centre, container central air temperature and container surface temperature as a function of time in the sedimentary repository. The fuel temperature decreases from a peak value of 137°C at 7.7 years to 120°C at 50 years. The container central air temperature decreases from 131°C at 11.9 years days to 116°C at 50 years. The container surface temperature decreases from 100°C at 28 years to 97°C at 50 years.

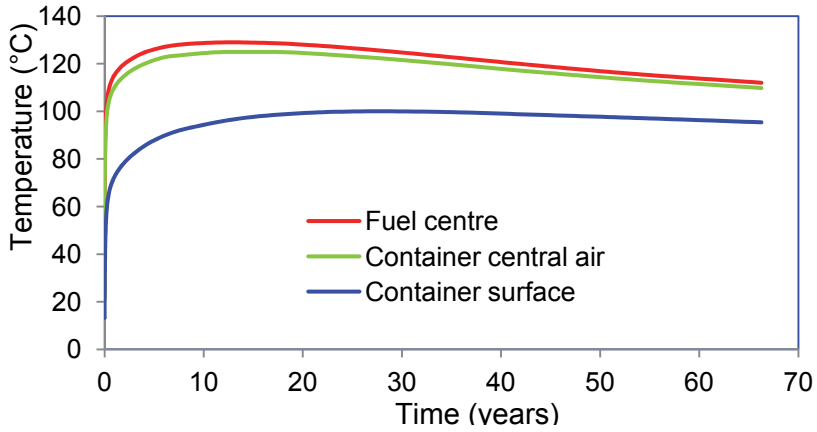

Figure 58: Temperatures from Mixed Heat Source Model IV in a Sedimentary Repository

4.4 SENSITIVITY ANALYSIS

This section examines the influence of adopting a volumetric heat source in the Container Model instead of using a heat flux boundary condition, the effect of dividing the physical system into several levels of submodels, the influence of a gap between a container and a buffer box, the effect of water entering the container via an assumed container defect, and the effect of including radiation heat transfer in the models.

4.4.1 Influence of Using a Volumetric Heat Source in the Container Model

This sensitivity case examines the effect of replacing the heat flux boundary condition applied to the inside of the bundle tubes in the Container Model with an equivalent volumetric heat source.

The parameters used to describe the volumetric heat source are obtained using a variant of the Bundle Model described in Section 3.1.4. In this variant, the 37-element fuel bundle is replaced by an equivalent material having the same heat source, the same heat capacity and the same thermal conductivity. Figure 59 illustrates the resulting Equivalent Bundle Model. This model has two materials (i.e., the steel fuel tube and the equivalent material) with a density and specific heat capacity assigned to the equivalent material of 5751 kg/m^3 and 334 J/(kg·°C).

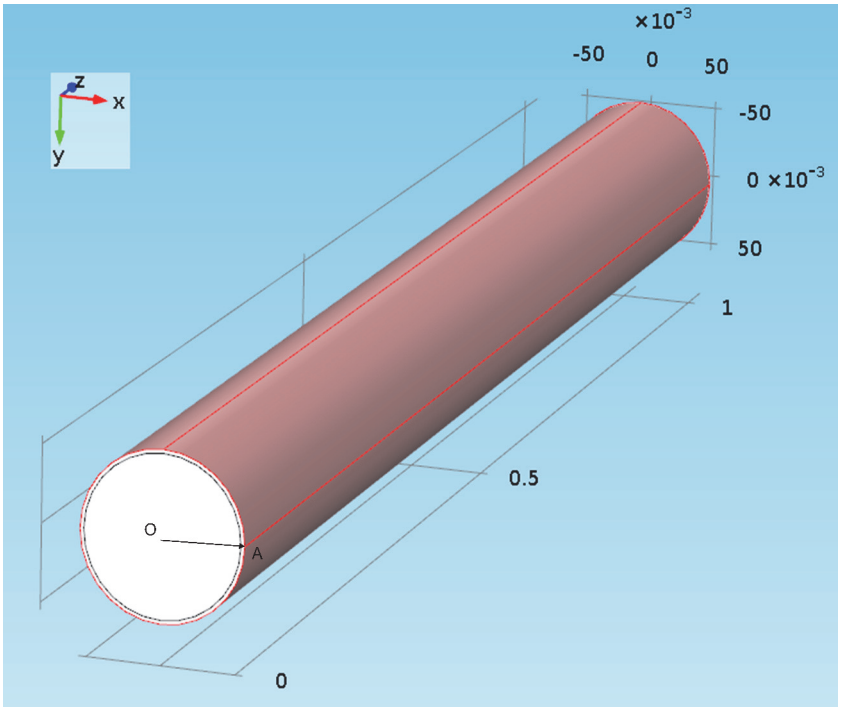

Figure 59: Equivalent Bundle Model

Figure 60 and Figure 61 show temperature comparisons between the Bundle Model and the Equivalent Bundle Model assuming a thermal conductivity for the equivalent material of 0.09 W/(m·°C). Both figures show good agreement, with the small differences in Figure 61 arising due the differences in geometry.

The value of the effective thermal conductivity used in the Equivalent Bundle Model was selected by trial and error so that the temperatures in the radial direction, as calculated by the two models, are in fairly good agreement, as demonstrated in Figure 61. It is the low value of this equivalent thermal conductivity that makes it valid to approximate the fuel bundle heat source in the Container Model by a boundary condition on the inner surface of the bundle tubes.

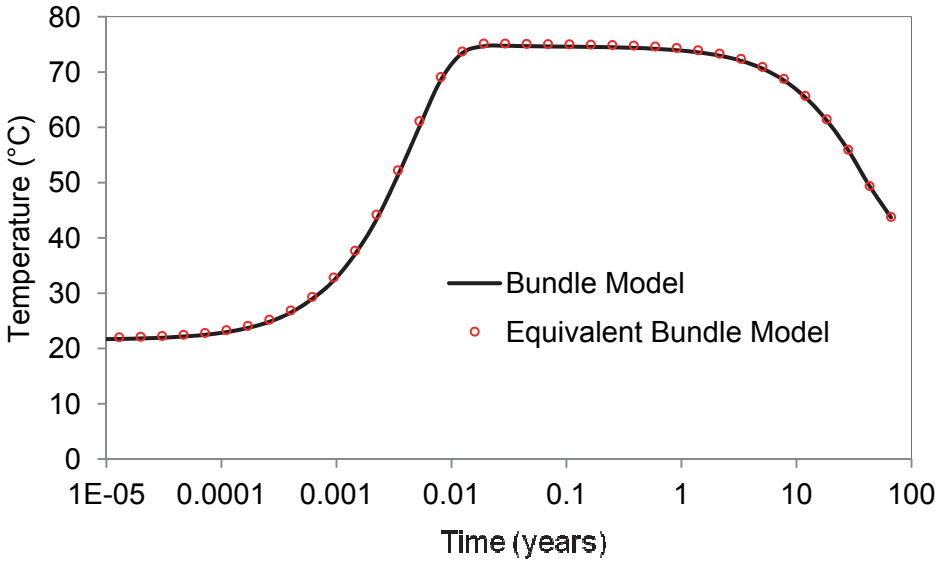

Figure 60: Fuel Centre Temperature Comparison between the Bundle Model and the Equivalent Bundle Model

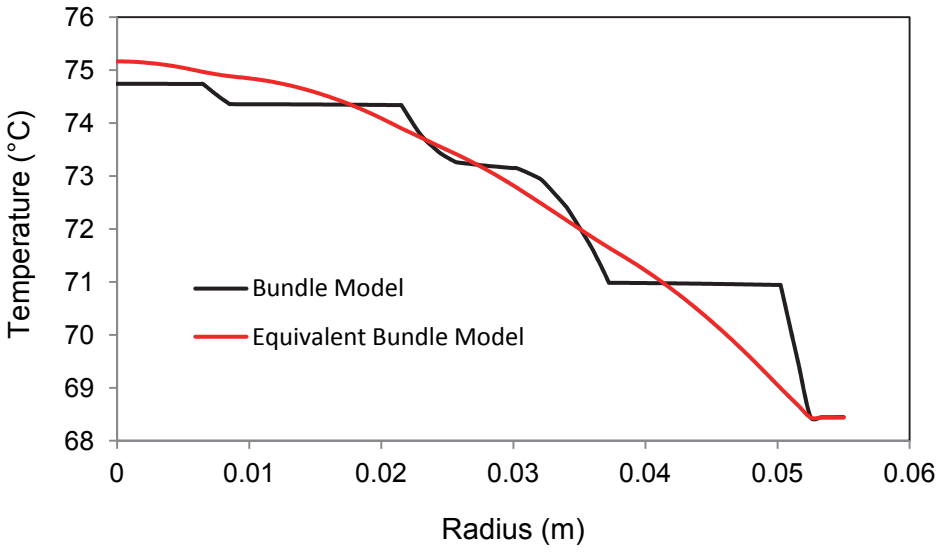

Figure 61: Fuel Temperature Comparison along Radius (OA) between the Bundle Model and the Equivalent Bundle Model

The effect of the volumetric heat source is determined using a variant of the Container Model described in Section 3.1.3. In this variant, the heat flux boundary condition is not used and the fuel tubes are instead assumed filled with the equivalent material described above.

Figure 62 shows the geometry of the Equivalent Container Model. It also shows the locations of Line OA, Line OB and Line OO´, along which temperatures from the Equivalent Container Model are determined.

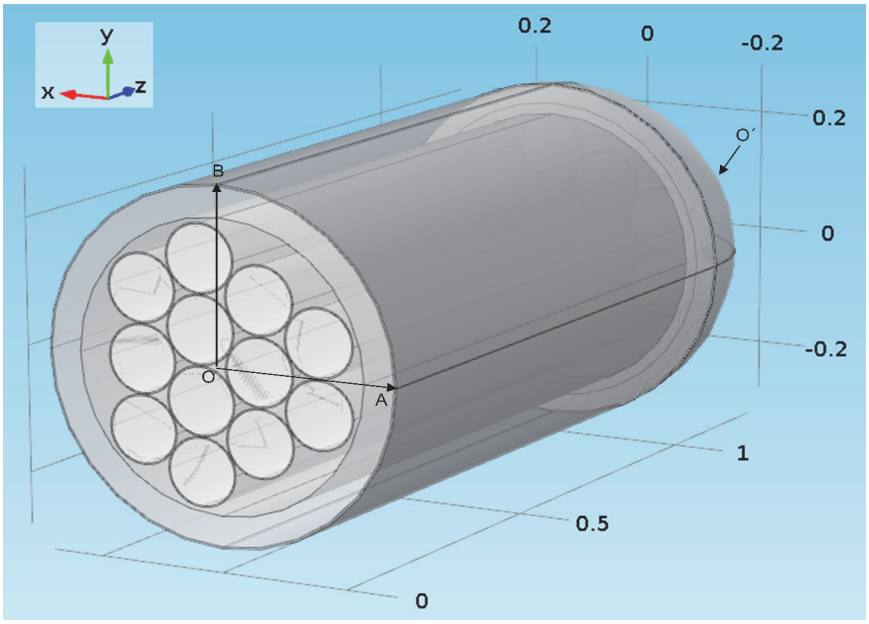

Figure 62: Geometry of the Equivalent Container Model

Figure 63 shows the comparison of the container centre air temperature between from Container Model and the Equivalent Container Model. The results show good agreement.

Figure 64 compares temperatures between the two models along Line OA (see Figure 62) at 8.6 days, which is the time the peak temperature is obtained. The agreement is also very good. The dotted blue line in this figure corresponds to the equivalent material which is only present in the Equivalent Container Model. Similar excellent comparisons have been obtained along Lines OB and OO´; however, these figures are not shown.

These comparisons indicate that the approach adopted in either the Container Model or the Equivalent Container Model is valid for this application.

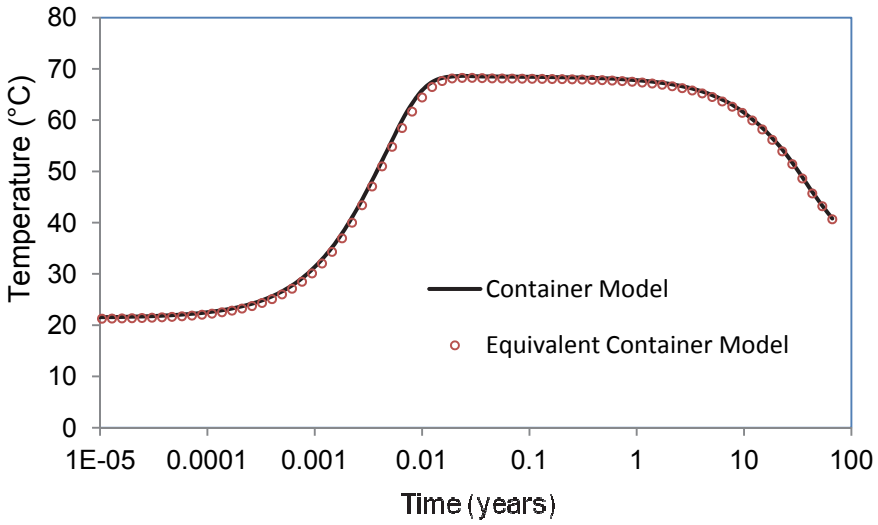

Figure 63: Container Centre Air Temperature Comparison between the Container Model and the Equivalent Container Model

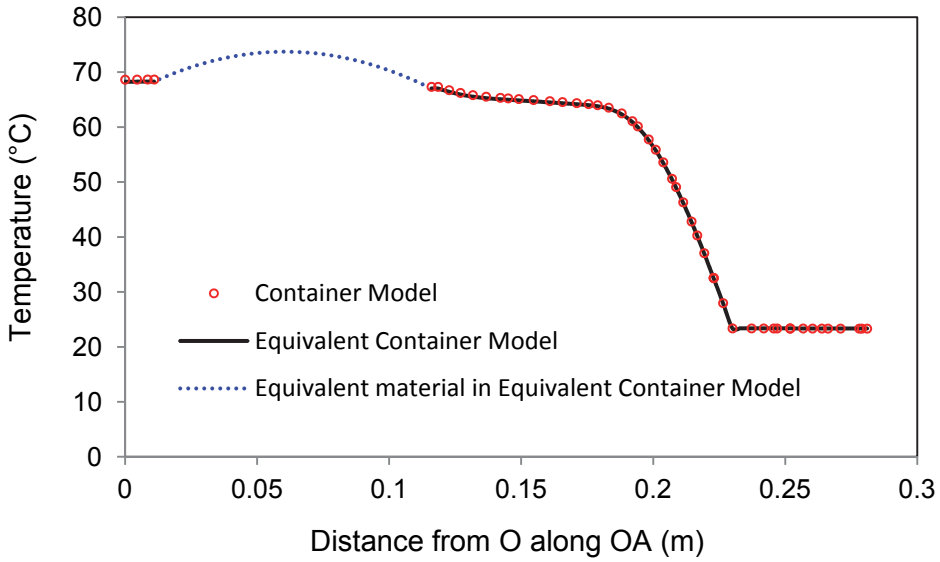

Figure 64: Container Temperature Comparison along Line OA at 8.6 Days between the Container Model and the Equivalent Container Model

4.4.2 Combining the Buffer Box Model and Container Model into an Equivalent Buffer / Container Model

This sensitivity case examines the effect of using a combined model to represent the buffer box and the container.

In Section 4.2.2, the fuel temperature analysis for the Container inside the Buffer Box in Air case includes the following three steps:

- Calculation of the temperatures on the surface of the container using the Buffer Box Model (see Figure 8),
- Calculation of the container central air temperature in the container using results from the Buffer Box Model as the boundary condition in the Container Model, and
- Calculation of the fuel temperature using results from the Container Model as the boundary condition for the Bundle Model.

In this section, a Buffer Box Combination Model including the buffer box and the container is constructed so the temperature of the central air in the container can be directly calculated.

Figure 65 shows the geometry of the Combination Model. There are four kinds of materials: bentonite, the copper coating, the steel container and steel bundle tubes, and the air inside the container.

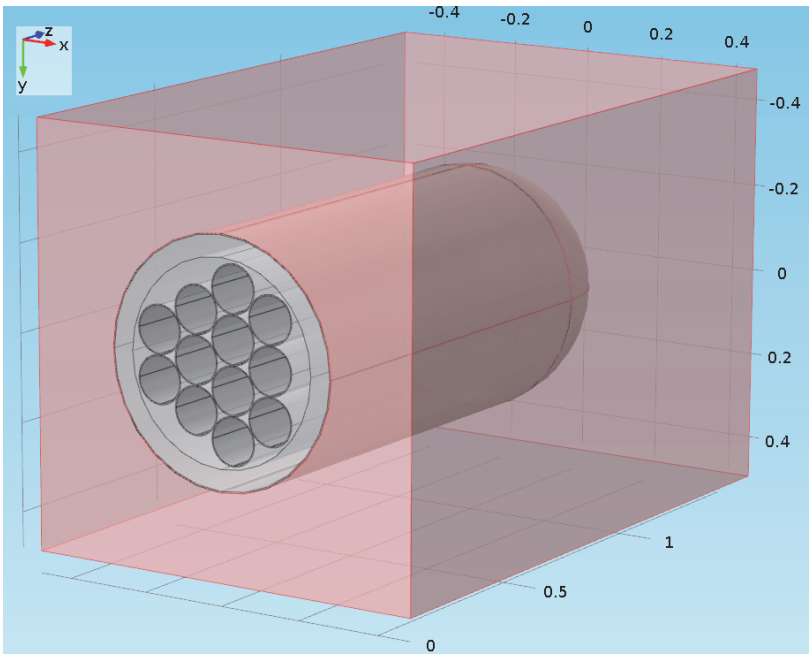

Figure 65: Buffer Box Combination Model Geometry

Figure 66 shows the model mesh. There are 796,663 tetrahedral elements and 1,123,442 nodes.

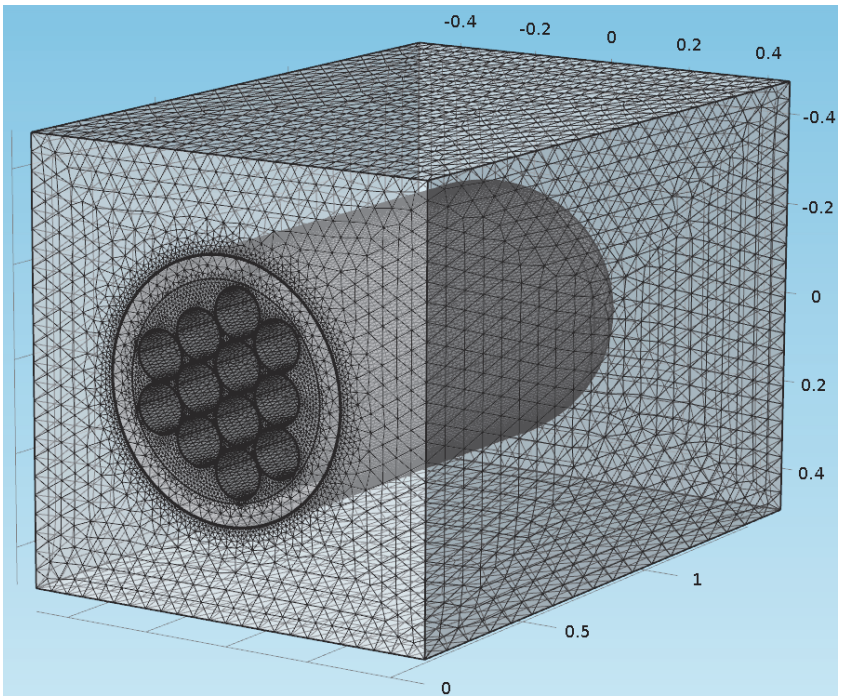

Figure 66: Buffer Box Combination Model Mesh

Figure 67 shows the comparison of the temperature of the central air in the container obtained using the Buffer Box Combination Model with results obtained using the separate models discussed previously. The results show that there is no difference between two methods, thereby indicating that either approach is valid for this application.

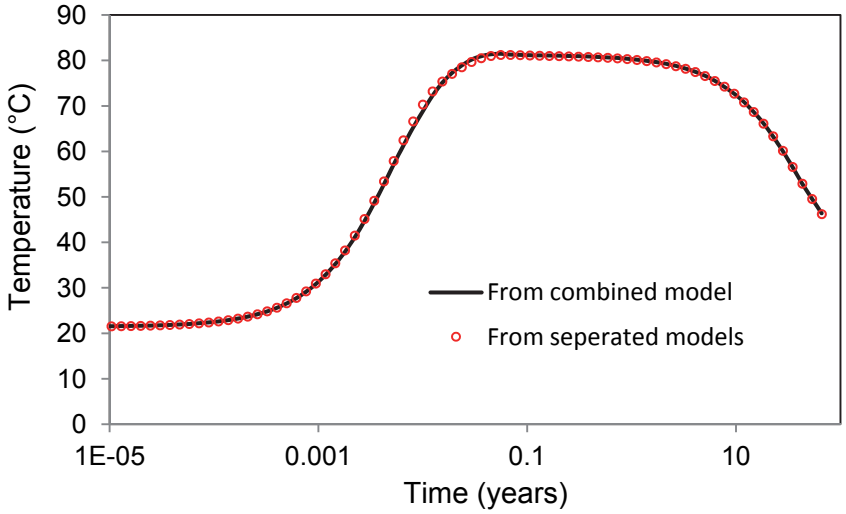

Figure 67: Container Air Temperatures Comparison between the Buffer Box Combination Model and the Separated Models

4.4.3 Influence of the Gap between the Container and the Buffer Box

In Section 3.1.2, it is assumed that there is no gap between a container and its surrounding buffer box. In reality, there may be a gap along some upper part of the container surface when the container is first placed in the buffer box. Over time, the bentonite in the buffer box will saturate and the gap will disappear. The no gap assumption makes the results for the temperature inside the container at early times lower than it would otherwise be. In this section, the influence of a gap between a container and a buffer box is evaluated for the Container inside the Buffer Box in Air case.

Figure 68 shows the geometry of the Gap Sensitivity Model. This model is constructed from the Buffer Box Combined Model described in the previous section. The difference between this model and that shown in Figure 65 is that there is now a 3-mm-thick gap between the container and the buffer box on five sixths of the container surface.

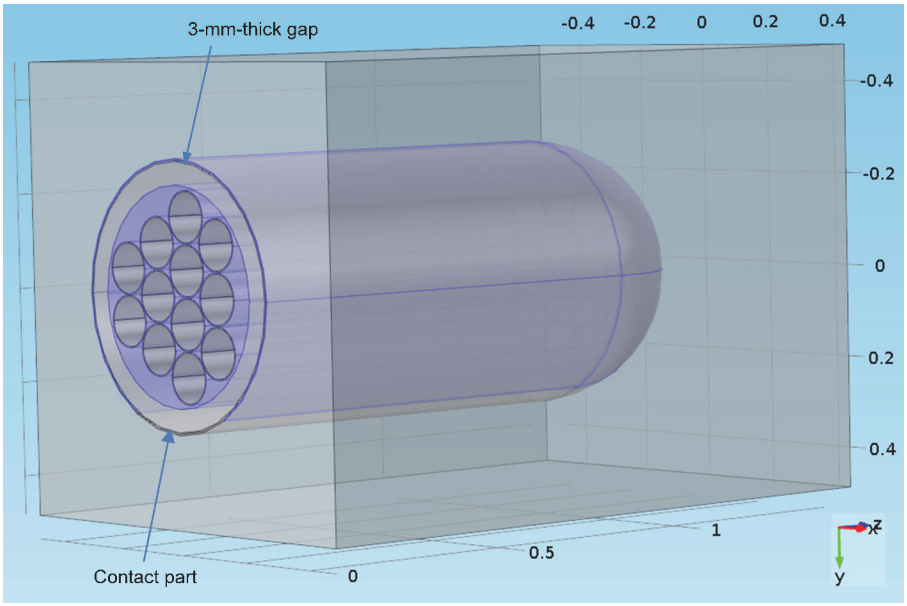

Figure 68: Gap Sensitivity Model Geometry

Figure 69 shows the model mesh. There are 888,778 tetrahedral elements and 1,246,787 nodes.

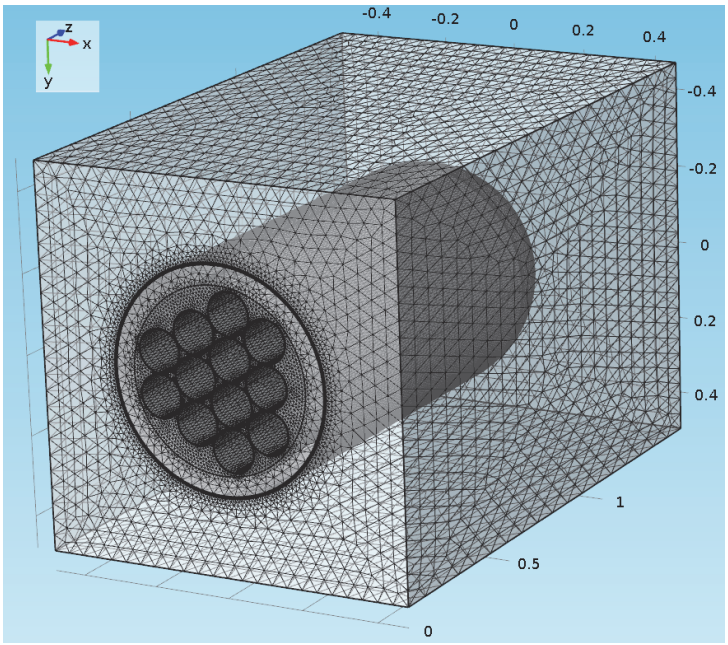

Figure 69: Gap Sensitivity Model Mesh

Figure 70 shows the influence of the assumed gap. Ignoring the gap underestimates the container central air temperature by about 3°C and the container surface temperature by about 3.6°C.

Considering the results from the Bundle Model in Figure 34, the maximum fuel temperature will be 89.5°C.

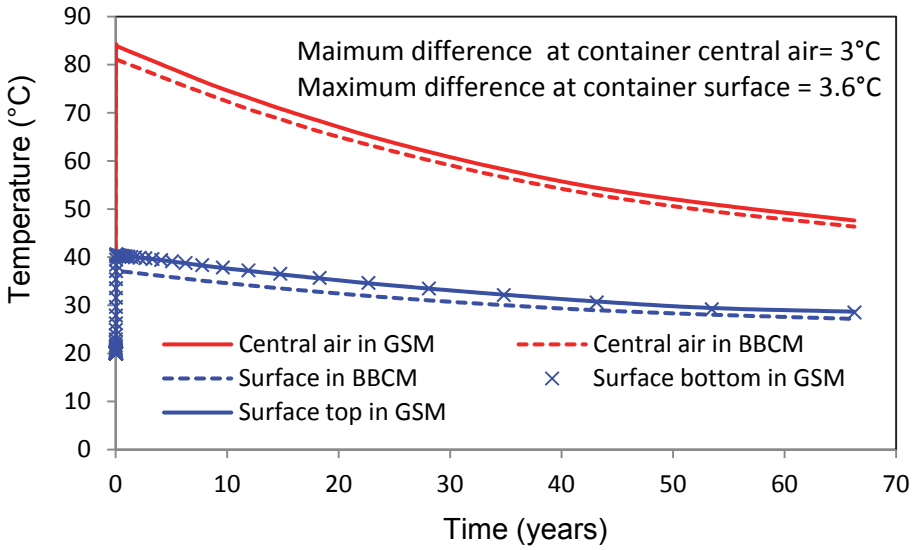

Figure 70: Container Temperature Comparison between Buffer Box Combination Model (BBCM) and Gap Sensitivity Model (GSM)

4.4.4 Influence of Connections between Fuel Bundle Tubes and the Inside Container Surface

All results discussed to this point are based on the assumption that the bundle tubes are not in direct contact with the inside surface of the container. However, in reality there must be some connection between these locations. In this section, the influence of such connections on container temperature is examined for the Container in Air case.

Figure 71 shows the geometry of a Container Model with All Connections in which all outside bundle tubes are connected to the inside surface of the container. The surface dimensions are 5 cm x 1.9 cm for the connections in the middle part of the Container Model and 10 cm x 1.9 cm for the connections near the end of the Container Model.

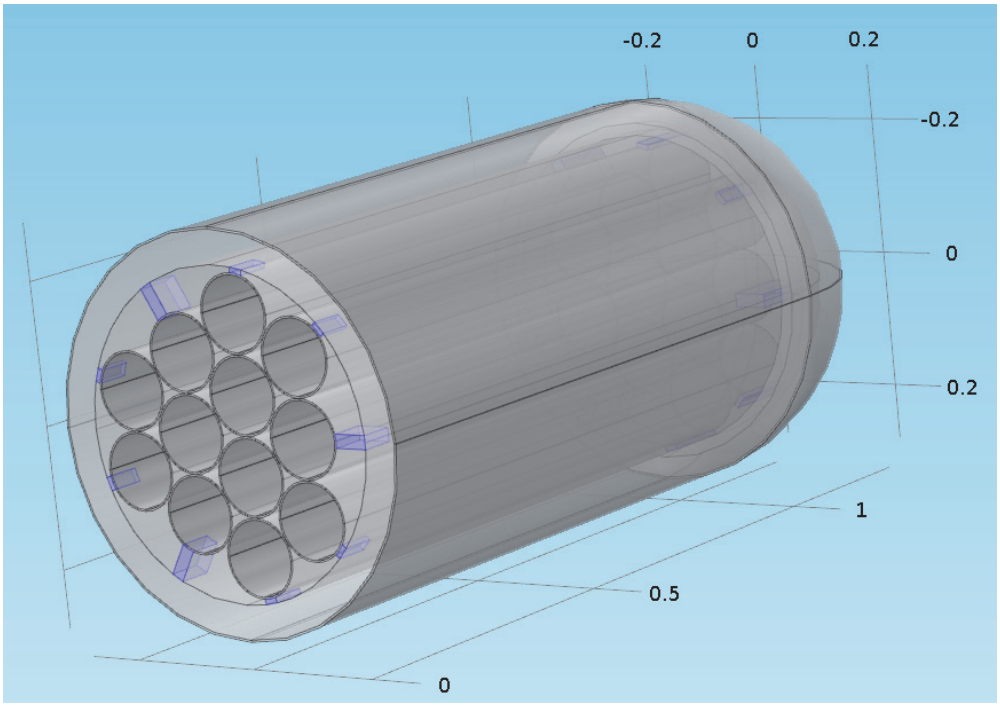

Figure 71: Container Model with All Connections

Figure 72 shows the same geometry of the Container Model with Partial Connections in which only Connections A, B, C and D are effective and all of the others are taken as air. Connections A and B have a cross section with dimensions of 5 cm x 1.9 cm and connections C and D have a cross section with dimensions of 10 cm x 1.9 cm.

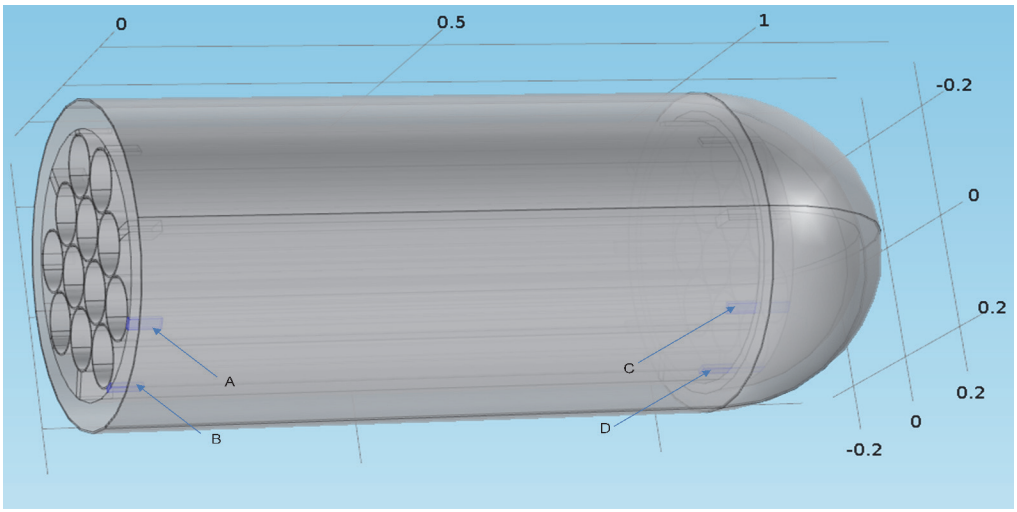

Figure 72: Container Model with Partial Connections (Only connections A, B, C and D are effective)

Figure 73 shows the comparison of the container central air temperature for the reference Container Model (i.e., without any connections), for the container model with all outside bundle tubes connected, and for the container model with only a portion of the outside tubes connected. For the reference Container Model the maximum temperature is 69°C, for the model with all tubes connected the maximum temperature is 41°C, and for the model with some connections the maximum temperature is 59°C.

If all contact points in the Mark II container are welded, the Container Model with All Connections would apply. Otherwise, the temperature in the container would be somewhere between that computed with the Container Model with Partial Connections and the reference Container Model. Thus, for a real case, the container air temperature would likely lie somewhere between 59°C and 69°C.

Considering the results from the Bundle Model in Figure 26, this implies the maximum fuel temperature would be somewhere between 65°C and 75°C.

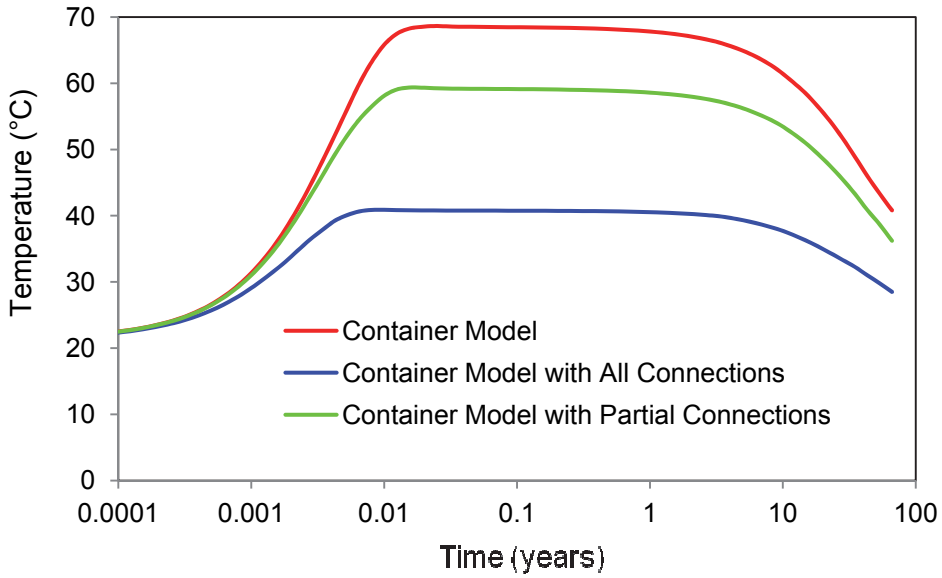

Figure 73: Influence of Connections on the Maximum Container Air Temperature for the Container in Air Case

Figure 74 shows the influence of the width of Connections A, B, C and D on the container central air temperature (from the Container Model with Partial Connections). The peak temperature of the container central air decreases from 63°C for a connection width of 1 mm (in the container tangential direction) to 59°C for a connection width of 19 mm.

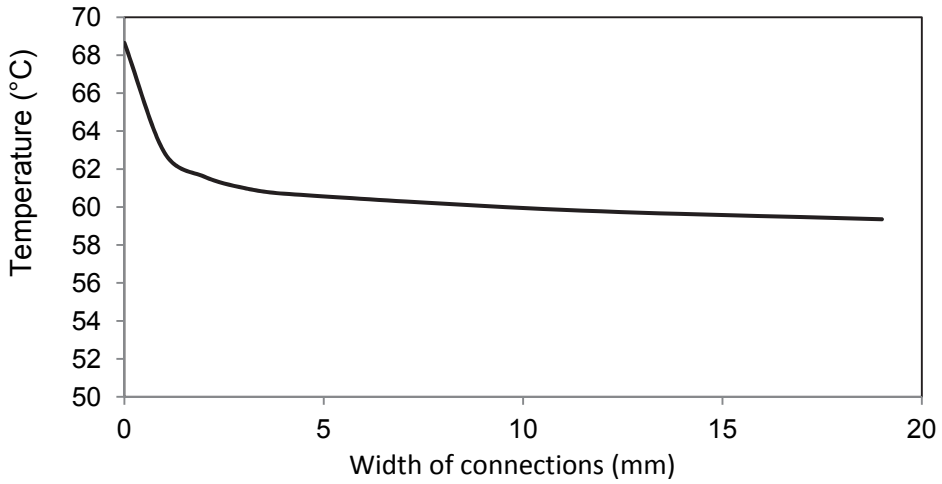

Figure 74: Influence of Connection Width on the Container Central Air Temperatures

4.4.5 Effect of Water entering the Container via an Assumed Container Defect

If a container fails after placement in the repository, water from the surrounding rock can enter, thereby influencing fuel temperatures. This effect is examined in this section.

The case simulated is a variant of the Container in a Sedimentary Repository case. Figure 75 shows the comparison of temperatures at the container centre for cases in which the container is filled and not filled with water. The peak value of the temperature at the container centre can reach 122°C at 14.7 years, if the container is filled with air (see Figure 42); while, if the container is filled with water, the container centre temperature is only 96°C at 14.7 years and reaches a peak value of 99°C at 39 years. Compared with container surface temperature, the container centre temperature when the container is filled with water is only 3.0°C higher. The results also show that temperatures everywhere in the container are essentially the same when container is filled with water. This is due to the fact that water has a much higher thermal conductivity than air.

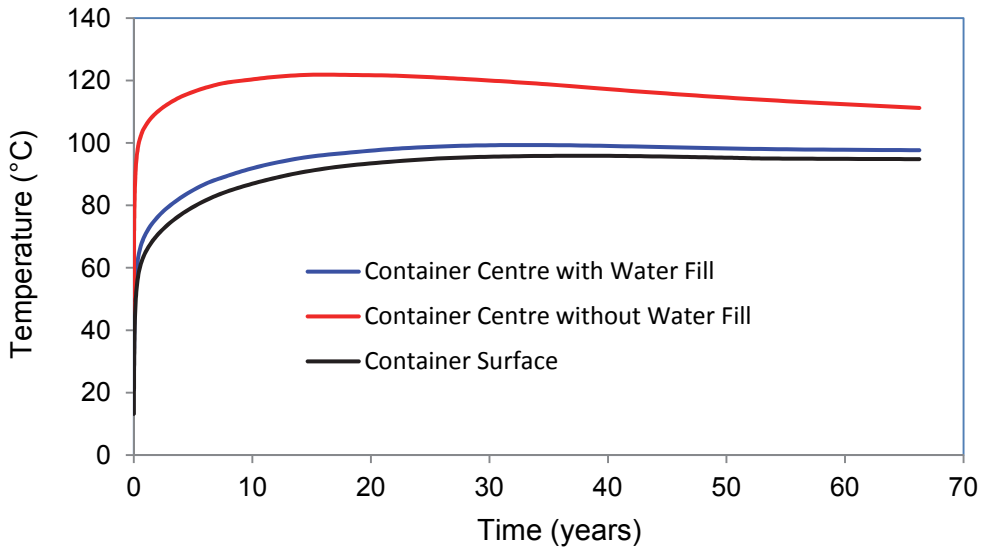

Figure 75: Effect of Water Entering the Container on Container Centre Temperature for the Container inside the Buffer Box in a Sedimentary Repository Case

Because the void spaces are assumed filled with water, the fuel temperature will be essentially the same as the temperature of the container centre.

4.4.6 Influence of Radiation Heat Transfer on Temperature

Radiation heat transfer in a container or in a bundle tube has not been considered in all cases discussed to this point. This section evaluates the influence of radiation heat transfer from the outside surface of the bundle tubes impinging on the inside surface of the container and the influence of radiation emitted from the fuel elements in a fuel tube.

The analysis is based on the Container inside a Buffer Box in a Sedimentary Repository Case with 30-year-old fuel.

4.4.6.1 Influence of Radiation Heat Transfer on the Container Temperature

To analyze the influence of radiation heat transfer, a much smaller model is constructed as shown in Figure 76. This model is one-sixth the size of the Container Model discussed previously. With this smaller model, the COMSOL meshing algorithm had difficulty meshing the extremely small spaces in the regions where the bundle tubes contact each other. To address this, the outside radius of the bundle tubes was reduced from 0.055 m to 0.054 m which resulted in the mesh shown in Figure 77. The mesh includes 80,338 tetrahedral elements and 96,289 nodes.

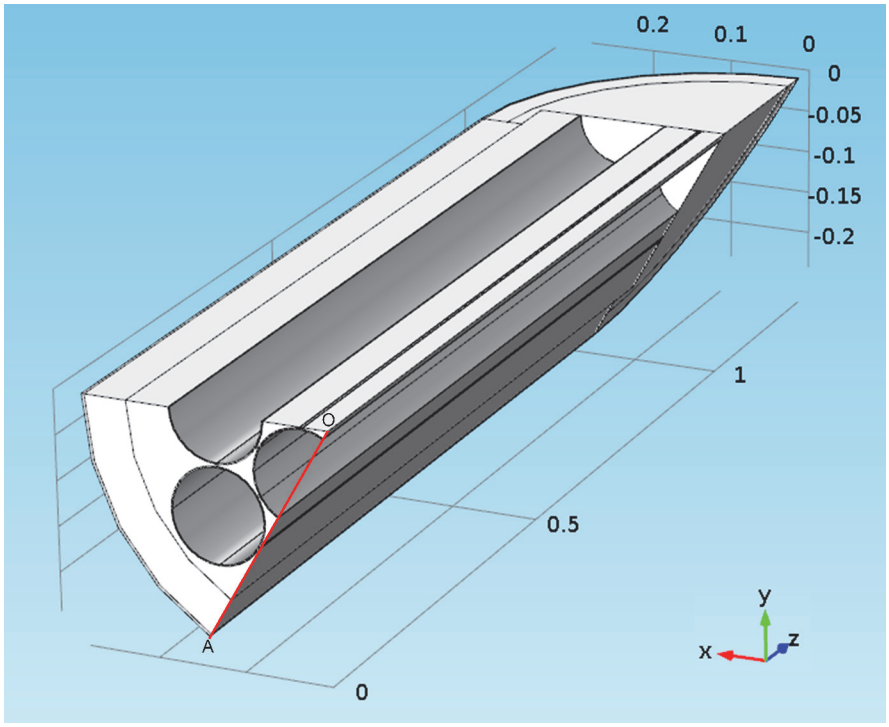

Figure 76: Radiation Container Model Geometry

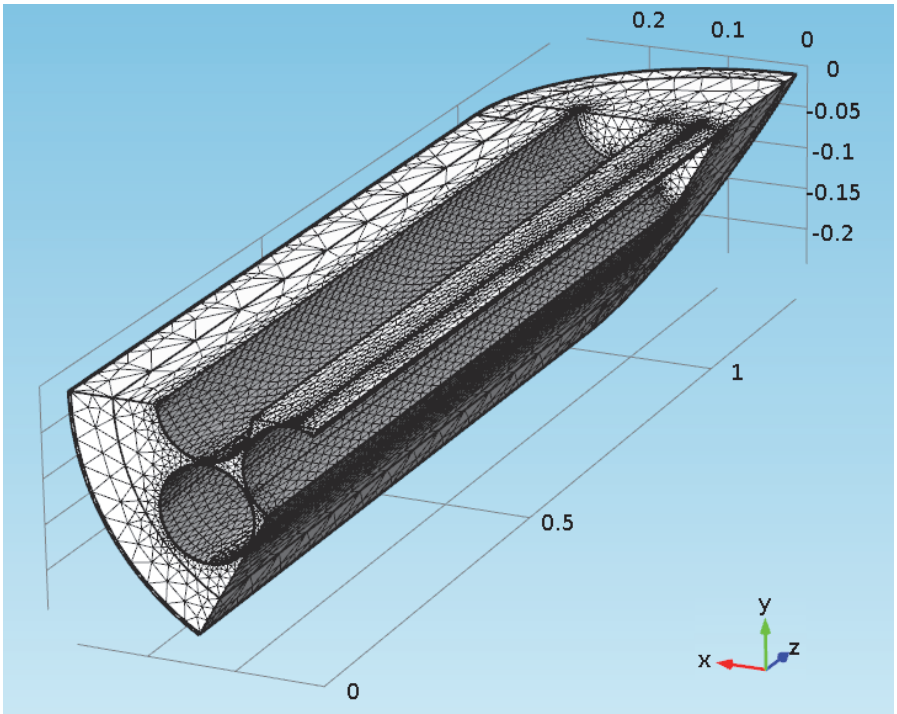

Figure 77: Radiation Container Model Mesh

Three-mm-thick connections between bundle tubes are added wherever the tubes contact each other in the Container Model and the thermal conductivity of air is modified to be 1.21 times the true value to make the temperatures calculated using the small model, but without radiation heat transfer, the same as those calculated using the Container Model. Figure 78 and Figure 79 show the comparison of the container centre temperature and the temperature along Line OA (see Figure 76 for location) between the Container Model and the Radiation Container Model for the Container inside the Buffer Box in a Sedimentary Repository Case. Both figures show that the thermal conduction results from the small Container Model matches those from the Container Model very well.

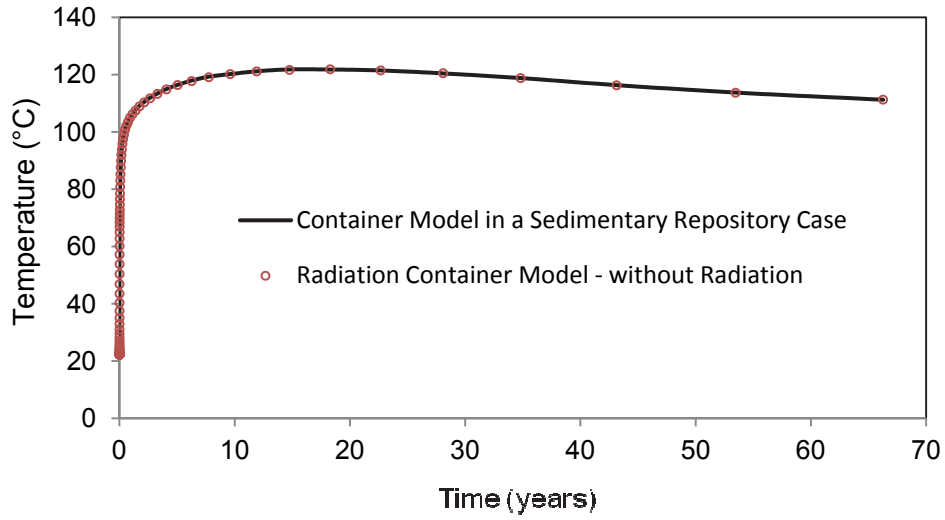

Figure 78: Container Centre Temperature for the Container inside the Buffer Box in the Sedimentary Repository Case

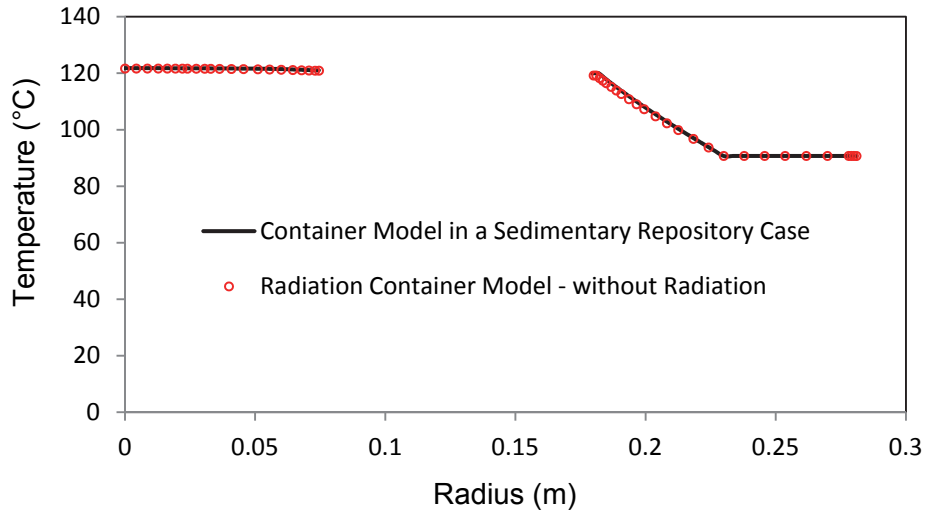

Figure 79: Temperature along Line OA for the Container inside the Buffer Box in the Sedimentary Repository Case

Figure 80 and Figure 81 show the temperatures in the Radiation Container Model both with and without considering radiation heat transfer between the fuel tube surfaces and between the fuel tube surfaces and the inside surface of the container. The highest container centre air temperature is 105°C occurring at 28 years considering radiation and 122°C occurring at 14.7 years without considering radiation heat transfer.

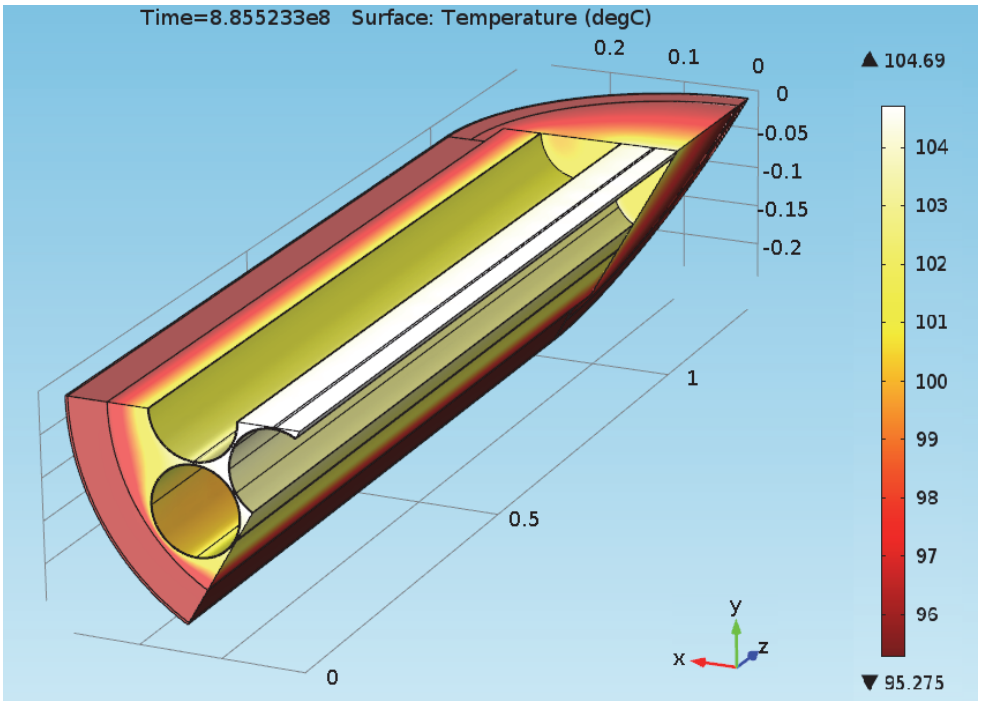

Figure 80: Temperatures at 28 Years inside the Container Accounting for Radiation Heat Transfer

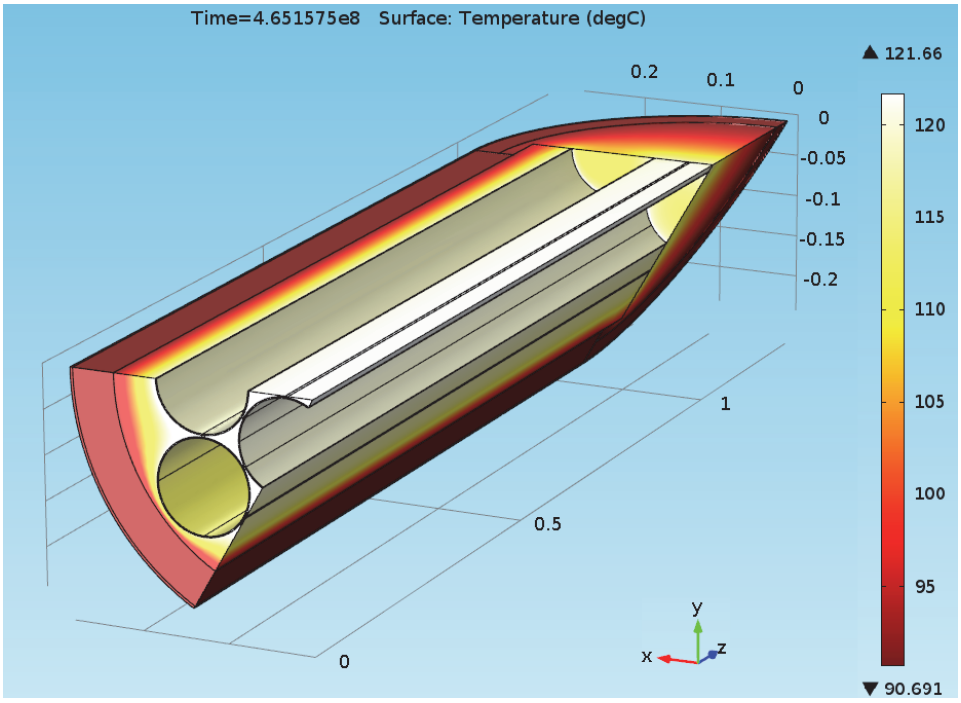

Figure 81: Temperatures at 14.7 Years inside a Container Not Accounting for Radiation Heat Transfer

Figure 82 shows the influence of radiation heat transfer on the container central air temperature. The difference is 17°C at time of maximum air temperature, occurring at 14.7 years. With time, the difference becomes smaller.

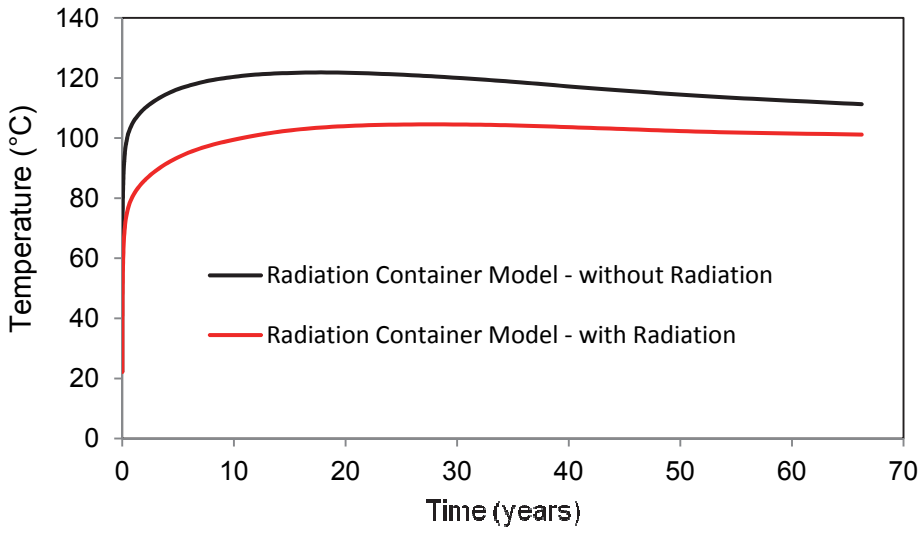

Figure 82: Influence of Radiation Heat Transfer on Container Air Temperature

Due to the greater difference between the temperature on the outside surfaces of the fuel tubes and the temperature on the inside surface of the container for other cases described in this document, the difference induced by considering thermal radiation will be greater than 17°C.

Based on these results, the maximum temperature of the centre air inside a container filled with 30-year-old fuel in a sedimentary repository when accounting for radiation heat transfer is 105°C. Considering the results from the Bundle Model in Figure 42, the corresponding maximum fuel temperature would be 109°C.

4.4.6.2 Influence of Radiation Heat Transfer on Fuel Temperature

To model the influence of radiation heat transfer in the Bundle Model, a one-fourth size Radiation Bundle Model was built as shown in Figure 83. The only difference between this model and the Bundle Model described in Section 3 is that the radiation heat transfer between fuel elements and between fuel elements and the inside surface of the bundle tubes is considered.

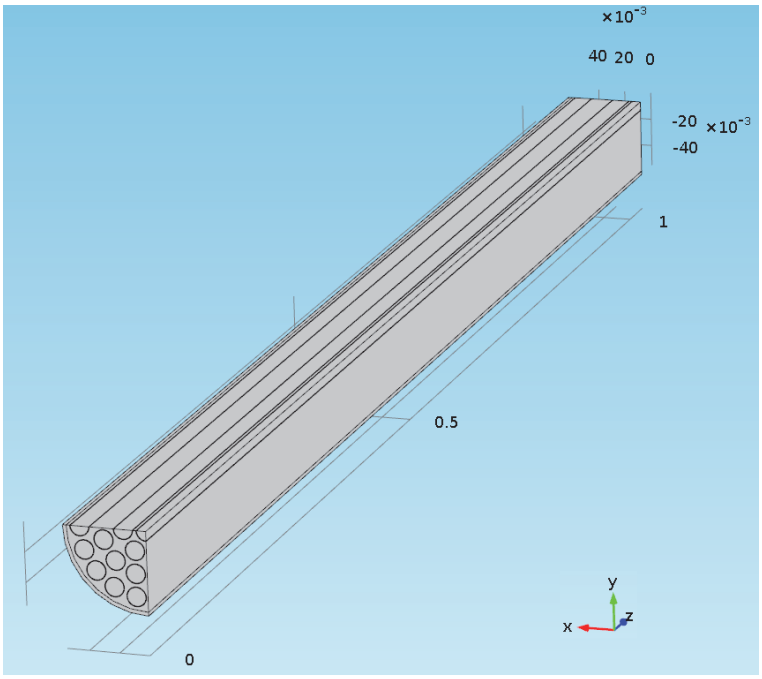

Figure 83: Radiation Bundle Model Geometry

Figure 84 shows the mesh of the Radiation Bundle Model. It includes 194,719 tetrahedral elements and 215,034 nodes.

Figure 85 and Figure 86 show temperatures inside a fuel tube with and without radiation heat transfer at 14.7 years, at which time the fuel centre temperature reaches its peak value. In the sensitivity analyses with radiation heat transfer in the fuel tubes, the outside boundary condition is based on the results of the container model in a sedimentary repository case shown in Figure 42, i.e., without radiation heat transfer inside the container. The maximum temperature of the fuel is 124°C when considering radiation heat transfer and 126°C without considering radiation heat transfer.

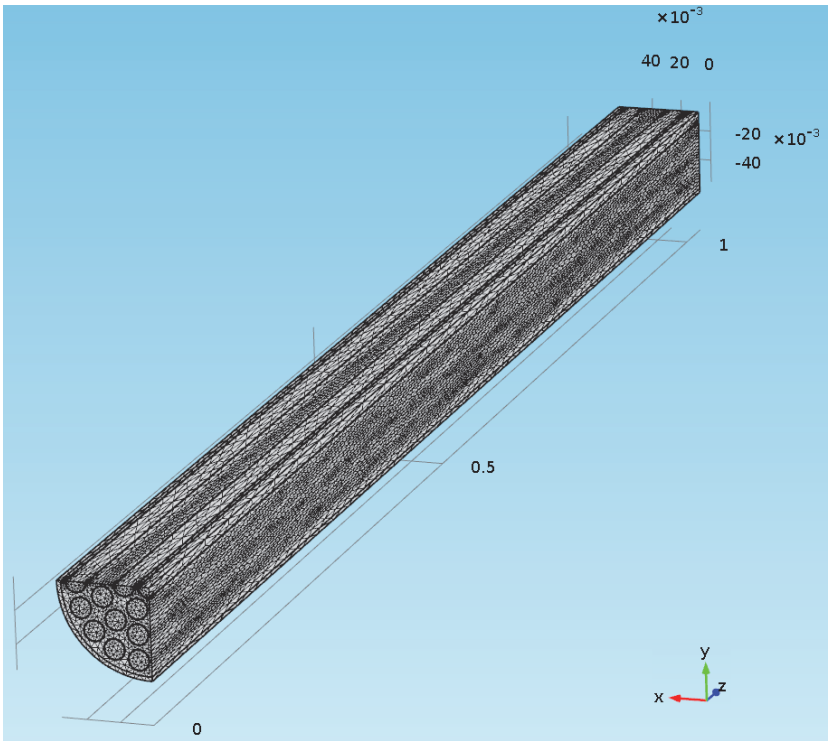

Figure 84: Radiation Bundle Model Mesh

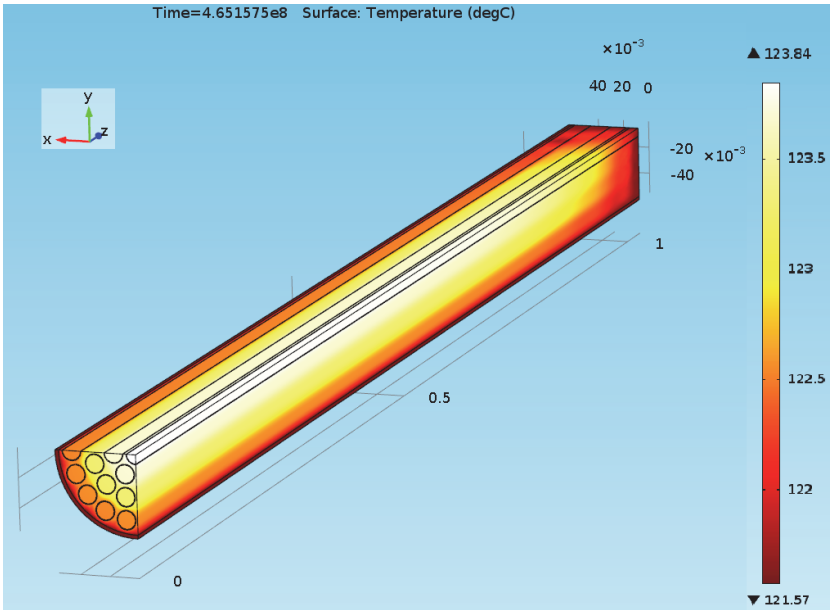

Figure 85: Temperatures in the Radiation Bundle Model

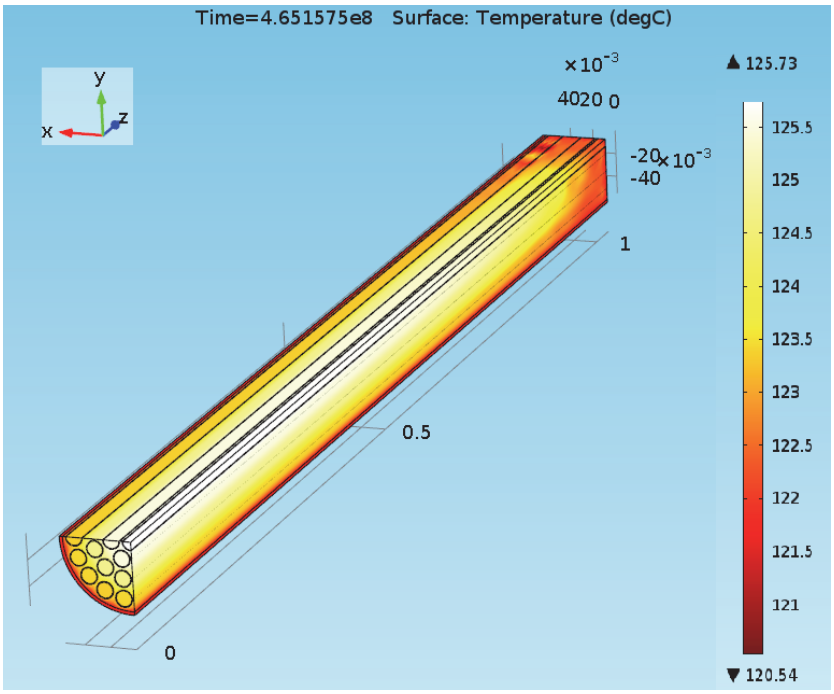

Figure 86: Temperatures in the Bundle Model (radiation not modelled)

Figure 87 shows the time dependence of the maximum fuel temperature both with and without radiation heat transfer. The results show less than 2°C difference, thereby confirming the validity of ignoring radiation heat transfer effects in the Bundle Model described in Section 3.

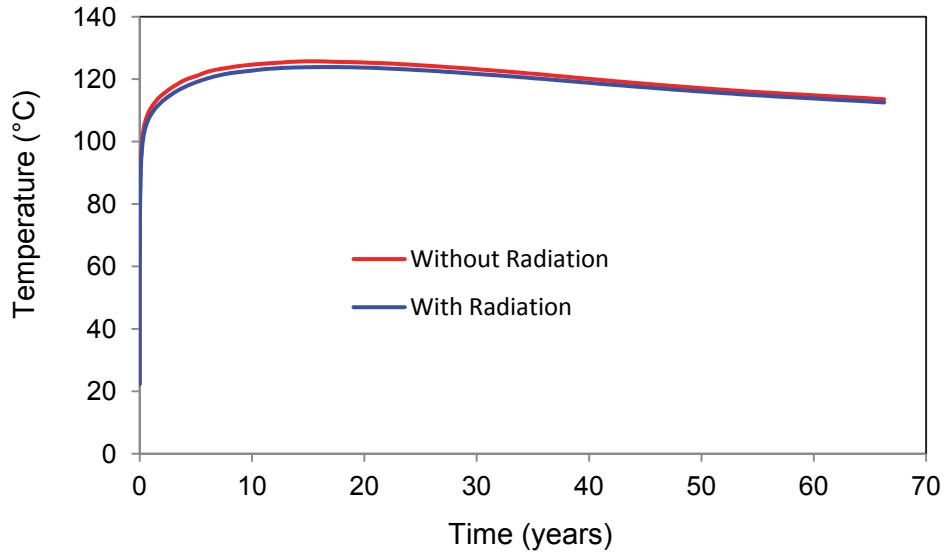

Figure 87: Influence of Radiation in a Fuel Tube on Fuel Central Temperature

4.4.7 Influence of Heat Transfer Coefficient from the Container Surface to Air

Convective heat transfer is difficult to estimate exactly because it depends on the object geometry, fluid properties, the size of the temperature differences, the fluid velocities, the condition of the heating surfaces and so on. This section evaluates the influence of the heat transfer coefficient used to calculate the convective heat transfer from the container surface to the surrounding air. The study is a variant of the Container in Air case.

Figure 88 shows the influence of the convective heat transfer coefficient on the container centre air and container surface temperature. Generally, the container centre air and container surface temperature decreases as the heat transfer coefficient increases. The container centre air temperature is 73°C for a heat transfer coefficient of 5 W/(m^2·°C) and 68°C for a heat transfer coefficient of 15 W/(m^2·°C). The maximum container surface temperature is 28°C for a heat transfer coefficient of 5 W/(m^2·°C) and 22°C for a heat transfer coefficient of 15 W/(m^2·°C). The corresponding fuel temperature would be 79°C for 5 W/(m^2·°C) and 74°C for 15 W/(m^2·°C) considering the difference of 6°C between the fuel centre temperature and the container centre temperature for the Container in Air case.

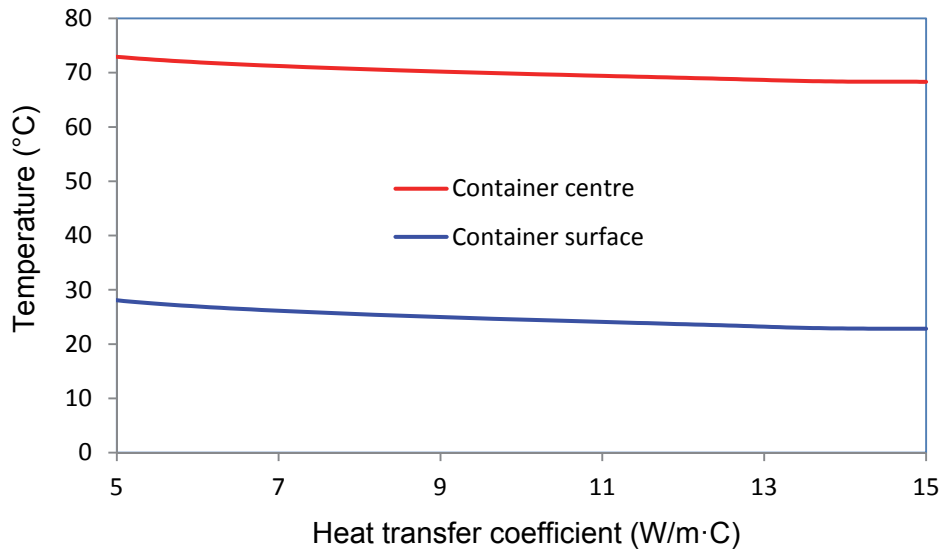

Figure 88: Influence of the Convective Heat Transfer Coefficient on Container Centre Air Temperature

4.4.8 Influence of Higher Burnup

All of the analyses described above assume a fuel burnup of 220 MWh/(kgU). This section evaluates the influence of higher burnup (i.e., 280 MWh/(kgU)) on the fuel temperature.

The analysis uses the Container inside the Buffer Box in the Sedimentary Repository Case with 30-year-old fuel. To meet the constraint that the container surface temperature does not exceed 100°C, the total heat source in a container with 30-year-old 280 MWh/(kgU) burnup bundles must not exceed that in a container filled with 30-year-old 220 MWh/(kgU) burnup bundles.

To meet this constraint, a smaller number of higher burnup bundles are assumed. Because the heat source per bundle with a 280 MWh/(kgU) burnup is about 29% greater than that for a bundle with a 220 MWh/(kgU) burnup, at most thirty-six 30-year-old 280 MWh/(kgU) fuel bundles can be placed inside the container. With this number of bundles, the container outside surface temperature and the container centre temperature will be similar to those shown in Figure 42. The difference between the fuel temperature and the container central air temperature will be 29% higher than that for fuel with a 220 MWh/(kgU) burnup. This means that the fuel temperature would be about 127°C for the higher burnup fuel.

4.5 Summary of the Modelling Results

This document presents fuel, container central air and container outside surface temperatures for the Container in Air Case, the Container inside the Buffer Box in Air Case, the Container inside the Buffer Box in the Sedimentary Rock Repository Case and the Container inside the Buffer Box in the Crystalline Rock Repository Case. The influences of the small space between the container and the bentonite material in the buffer box, the connections between bundle tubes and the container inside surface, water entering the container via an assumed container defect, radiation heat transfer between bundle tubes and between bundle tubes and the container inside surface, and radiation heat transfer between fuel elements and between fuel elements and the bundle tube inside surface are also presented.

Table 2 summarizes the results of the simulations. The table shows the maximum fuel temperature, the maximum container air temperature, the maximum container surface temperature and the times at which the maximums occur.

Table 2: Summary of Maximum Temperature Results

Case	Fuel Age (years)	Maximum Fuel Temperature (°C)	Maximum Container Air Temperature (°C)	Maximum Container Surface Temperature (°C)
Container in Air	30	75 (8.6 days)	69 (8.6 days)	23
Container inside the Buffer Box in Air	30	87 (20 days)	81 (20 days)	37 (20 days)
Container inside the Buffer Box in a Sedimentary Repository	30	126 (14.7 years)	122 (14.7 years)	96 (40 years)
	Mixed Heat Source Model I*	129 (11.9 years)	125 (11.9 years)	96 (28.1 years)
	Mixed Heat Source Model II	133 (7.7 years)	128 (7.7 years)	98 (22.6 years)
	Mixed Heat Source Model III	129 (11.9 years)	125 (11.9 years)	100 (28 years)
	Mixed Heat Source Model IV	137 (7.7 years)	131 (11.9 years)	100 (28 years)
Container inside the Buffer Box in a Crystalline Repository	30	125 (14.7 years)	121 (14.7 years)	94 (34.8 years)

*The number of mixed models can be seen in Section 4.3.

Table 3 summarizes the results of the sensitivity analysis simulations. The table shows the influences of different factors.

Table 3: Summary of Sensitivity Analysis Results

Sensitivity Case	Effect
Separating the buffer box physical system into a Buffer Box Model and a Container Model	No significant influence
Adding a 3-mm-air gap between Container Surface and the Buffer Box	Increases fuel temperature by about 3°C
Adding connections between the bundle tubes and the inside container surface	Reduces fuel temperature up to 28°C
Water filling the container	Reduces the temperature difference between the fuel and the container surface to about 3°C and lowers the peak fuel temperature from 126°C to 99°C
Accounting for radiation heat transfer between bundle tubes and between bundle tubes and the inside container surface	Reduces fuel temperature by about 17°C
Accounting for radiation heat transfer between fuel elements and between fuel elements and the inside surface of bundle tube	Reduce fuel temperature by about 2°C
Variation in the convective heat transfer coefficient	Increases fuel temperature by about 5°C if 5 W/(m^2·°C) is used instead of 15 W/(m^2·°C)
Higher bundle burnup (280 MWh/(kgU) instead of 220 MWh/(kgU))	Increases the fuel temperature less than 2°C if the heat load in the container is the similar in the two cases, i.e., 36 bundles in a container with 280 MWh/kgU burnup fuel and 48 bundles in a container with 220 MWh/kgU burnup fuel.

Based on the analysis results, the anticipated fuel temperature can be determined using the information presented Section 4.2, Section 4.3 and Section 4.4 as follows:

$$T = T_0 + \Delta T_1 + \Delta T_2 + \Delta T_3 \qquad (2)$$

where T_0 is the maximum fuel temperature calculated from the Bundle Models in Sections 4.2 and 4.3;

ΔT_1 is the influence of the air gap between the container and the buffer box. For the Container in Air case, ΔT_1 = 0°C, for the Container inside the Buffer Box case and for the Container in a Repository cases, ΔT_1 = 3°C;

ΔT_2 is the influence of radiation heat transfer between the bundle tubes and between bundle tubes and the inside container surface, for the Container inside the Buffer Box in the Sedimentary Repository case with 30-year-old bundles, ΔT_2 = -17°C; for other cases, the influence of radiation should be grater. Therefore, conservative

results will be obtained by using ΔT_2 = -17°C to modify the results for other cases, and

ΔT_3 is the influence of high burnup fuel, ΔT_3 = 0°C for bundles with a burnup of 220 MWh/(kgU) and ΔT_3 = 2°C for bundles with a burnup of 280 MWh/(kgU).

In the above equation, the overestimation caused by ignoring the connections between the bundle tubes and the inside surface of the container is not considered due to the currently uncertainty associated with the width of the connections.

Application of Equation 2 yields the results shown in Table 4.

Table 4: Summary of Modified Maximum Temperature Results

Case	Fuel Age (years)	Maximum Fuel Temperature* (°C)	
		Burnup of 220 MWh/(kgU)	Burnup of 280 MWh/(kgU)
Container in Air	30	58	60
Container inside the Buffer Box in Air	30	73	75
Container inside the Buffer Box in a Sedimentary Repository	30	112	114
	Mixed Heat Source Model I	115	117
	Mixed Heat Source Model II	119	121
	Mixed Heat Source Model III	115	117
	Mixed Heat Source Model IV	123	125
Container inside the Buffer Box in a Crystalline Repository	30	111	113

*Note that to ensure that heat loads from a container are similar, a container loaded with fuel bundles with a burnup of 220 MWh/(kgU) holds 48 fuel bundles whereas a container loaded with fuel bundles with a burnup of 280 MWh/(kgU) holds 36 fuel bundles

5 CONCLUSIONS

A series of thermal modelling simulations for different conditions has been performed using COMSOL to determine the maximum internal container temperature and the maximum fuel temperature.

In this modelling activity, there are several assumptions which make the modelling results for the fuel temperature conservative. These include:

- In the Container Model, the temperature at the mid-container surface from the Buffer Box Model or from the Repository Model (which is the highest temperature on the container surface), is used as the boundary condition for the outside surface temperature. This results in a conservative temperature in the Container Model,
- Using the centre air temperature in the container as the boundary condition in the Bundle Model,
- Ignoring the connection between the bundle tubes and the inside surface of the container could result in overestimating fuel temperature by up to 28°C, and
- Ignoring radiation heat transfer in the container could result in overestimating fuel temperature by 17°C.

There is only one assumption which may result in calculated temperatures in the container being underestimated. The assumption that there is no air gap between the container and the buffer box may cause an underestimation of the container central air temperature by about 3°C.

The use of higher burnup fuel (280 MWh/(kgU) instead of 220 MWh/(kgU)) results in an increase in fuel temperature of about 2°C, as long as the total heat load from the container remains the similar in both cases. This means that a container loaded with fuel bundles with a burnup of 280 MWh/(kgU) holds 36 fuel bundles whereas as container loaded with fuel bundles with a burnup of 220 MWh/(kgU) holds 48 fuel bundles

Considering the above two kinds of assumptions, the modelling results show the fuel maximum temperature (for the fuel with a burnup of 220 MWh/(kgU)) is less than 58°C during handling of the container, 73°C during handling of the buffer box placement and 123°C after placement in sedimentary or crystalline rock.

REFERENCES

Abdel-Ghany, A. M. and T. Kozai. 2006. On the determination of the overall heat transmission coefficient and soil heat flux for a fog cooled, naturally ventilated greenhouse: Analysis of radiation and convection heat transfer. Energy Conversion and Management. Volume 47, Issues 15-16. pp. 2612–2628.

Baumgartner, P. 2006. Generic thermal- mechanical - hydraulic (THM) data for sealing materials, Volume 1: soil-water relationships. Ontario Power Generation, Nuclear Waste Management Division 06819-REP-01300-10122-R00. Toronto, Canada.

COMSOL. 2013. Heat Transfer Module User's Guide Version 4.3b.

Garamszeghy, M. 2013. Nuclear Fuel Waste Projections in Canada – 2013 Update. Nuclear Waste Management Organization Technical Report NWMO TR-2013-11, Toronto, Canada.

Guo, R. 2010. Coupled Thermal-Mechanical Modelling of a Deep Geological Repository using the Horizontal Tunnel Placement Method in Sedimentary Rock using CODE_BRIGHT. Nuclear Waste Management Organization Technical Report NWMO TR-2010-22, Toronto, Canada.

IAEA. 2006. Thermophysical properties database of materials for light water reactors and heavy water reactors: Final report of a coordinated research project. IAEA-TECDOC-1496.

Lienhard IV, J.H. and J.H. Lienhard V. 2011. A heat transfer textbook (fourth edition). Phlogiston Press. Cambridge Massachusetts. p. 38.

Tait, J.C., H. Roman and C.A. Morrison. 2000. Characteristics and radionuclide inventories of used fuel from OPG Nuclear Generating Stations. Volume 1 - Main report; and Volume 2 – Radionuclide inventory data. Ontario Power Generation Report 06819-REP-01200-10029-R00. Toronto, Canada.